NAVAL POSTGRADUATE SCHOOL

Monterey, California

THESIS

POSSIBLE CONTRIBUTIONS OF LID CONDITIONS DURING EXPLOSIVE CYCLOGENESIS

by

Charles W. Green

December 1988

Thesis Advisor Russell L. Elsberry

Unclassified
security classification of this page

REPORT DOCUMENTATION PAGE

1a Report Security Classification Unclassified	1b Restrictive Markings
2a Security Classification Authority	3 Distribution Availability of Report Approved for public release; distribution is unlimited.
2b Declassification Downgrading Schedule	
4 Performing Organization Report Number(s)	5 Monitoring Organization Report Number(s)
6a Name of Performing Organization Naval Postgraduate School — 6b Office Symbol *(if applicable)* 63	7a Name of Monitoring Organization Naval Postgraduate School
6c Address *(city, state, and ZIP code)* Monterey, CA 93943-5000	7b Address *(city, state, and ZIP code)* Monterey, CA 93943-5000
8a Name of Funding Sponsoring Organization — 8b Office Symbol *(if applicable)*	9 Procurement Instrument Identification Number
8c Address *(city, state, and ZIP code)*	10 Source of Funding Numbers Program Element No / Project No / Task No / Work Unit Accession No

11 Title *(include security classification)* POSSIBLE CONTRIBUTIONS OF LID CONDITIONS DURING EXPLOSIVE CYCLOGENESIS

12 Personal Author(s) Charles W. Green

13a Type of Report	13b Time Covered	14 Date of Report *(year, month, day)*	15 Page Count
Master's Thesis	From To	December 1988	99

16 Supplementary Notation The views expressed in this thesis are those of the author and do not reflect the official policy or position of the Department of Defense or the U.S. Government.

17 Cosati Codes			18 Subject Terms *(continue on reverse if necessary and identify by block number)*
Field	Group	Subgroup	Meteorology,explosive cyclogenesis,upper air sounding,GALE.

19 Abstract *(continue on reverse if necessary and identify by block number)*

Maritime soundings acquired during the Genesis of Atlantic Lows Experiment (GALE) Intensive Observing Periods (IOP's) 6 and 11 are evaluated to determine the presence of mid-tropospheric, dry continental air that forms a capping inversion over cool, moist marine air, which is defined to be a lid. The strength of these lid conditions is evaluated using the Lid Strength Index (LSI) developed by Carlson et al. (1980) for continental thunderstorms. The environmental factors contributing to lid conditions and the lid's possible effects on explosive cyclogenesis are analyzed. During IOP 6, a predominantly zonal flow advects warm, dry continental air over the region upstream of the convective heat release. Consequently, the air-sea fluxes and horizontal advection of moist air into the central region of the low are trapped below the lid. With the superposition of upper-level forcing that lifts and weakens the lid, the IOP 6 low develops explosively. During IOP 11, the mid-tropospheric air flow is more meridional and no-lid conditions occur upstream from the cyclone region. Consequently, the air-sea fluxes and horizontal advection of moisture is not confined to the lower troposphere. Although cyclogenesis occurs in this environment, it is not explosive. The presence of lid conditions during IOP 6 and the absence of lid conditions during IOP 11 are suggested to be one of the factors that differentiated explosive and non-explosive maritime cyclogenesis.

20 Distribution Availability of Abstract ☒ unclassified unlimited ☐ same as report ☐ DTIC users	21 Abstract Security Classification Unclassified	
22a Name of Responsible Individual Russell L. Elsberry	22b Telephone *(include Area code)* (408) 646-2373	22c Office Symbol 63Es

DD FORM 1473,84 MAR — 83 APR edition may be used until exhausted. All other editions are obsolete

security classification of this page
Unclassified

Approved for public release; distribution is unlimited.

Possible Contributions of Lid Conditions During
Explosive Cyclogenesis

by

Charles W. Green
Lieutenant Commander, United States Navy
B.S., University of Washington, 1978

Submitted in partial fulfillment of the
requirements for the degree of

MASTER OF SCIENCE IN METEOROLOGY AND OCEANOGRAPHY

from the

NAVAL POSTGRADUATE SCHOOL
December 1988

Author: 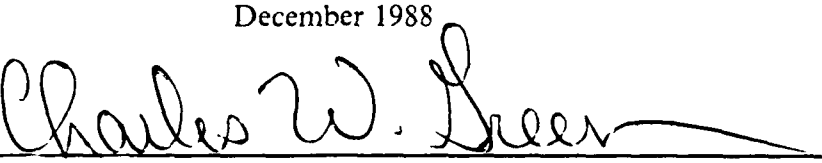

Charles W. Green

Approved by: 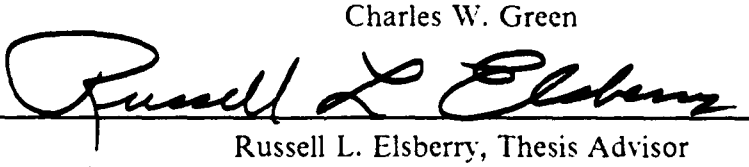

Russell L. Elsberry, Thesis Advisor

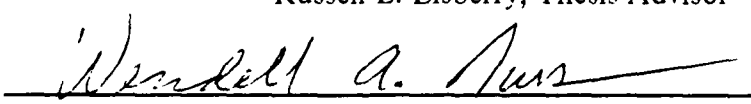

Wendell A. Nuss, Second Reader

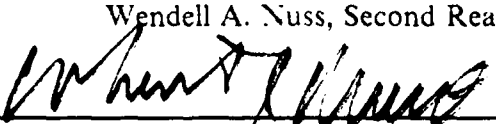

Robert J. Renard, Chairman,
Department of Meteorology

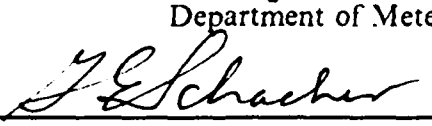

Gordon E. Schacher,
Dean of Science and Engineering

ABSTRACT

Maritime soundings acquired during the Genesis of Atlantic Lows Experiment (GALE) Intensive Observing Periods (IOP's) 6 and 11 are evaluated to determine the presence of mid-tropospheric, dry continental air that forms a capping inversion over cool, moist marine air, which is defined to be a lid. The strength of these lid conditions is evaluated using the Lid Strength Index (LSI) developed by Carlson et al. (1980) for continental thunderstorms. The environmental factors contributing to lid conditions and the lid's possible effects on explosive cyclogenesis are analyzed. During IOP 6, a predominantly zonal flow advects warm, dry continental air over the region upstream of the convective heat release. Consequently, the air-sea fluxes and horizontal advection of moist air into the central region of the low are trapped below the lid. With the superposition of upper-level forcing that lifts and weakens the lid, the IOP 6 low develops explosively. During IOP 11, the mid-tropospheric air flow is more meridional and no-lid conditions occur upstream from the cyclone region. Consequently, the air-sea fluxes and horizontal advection of moisture is not confined to the lower troposphere. Although cyclogenesis occurs in this environment, it is not explosive. The presence of lid conditions during IOP 6 and the absence of lid conditions during IOP 11 are suggested to be one of the factors that differentiated explosive and non-explosive maritime cyclogenesis.

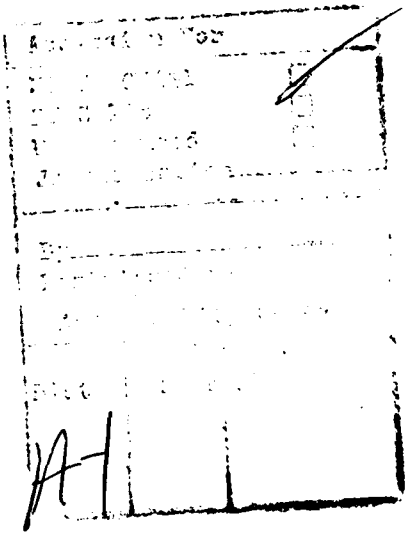

TABLE OF CONTENTS

LIST OF TABLES

LIST OF FIGURES

Acknowledgements

I wish to extend thanks to Mike McDermet and Ben Borelli for their assistance in providing the charts and information necessary to conduct this research, and to Larry Frazier for his help in solving the problems with the NPS GThesis system. I would also like to thank Rolf Langland of NEPRF for supplying the trajectories used in this research. I also thank Stacy Heikkinen for her assistance with the computer programs for the cross-section and skew-T plots as well as supplying the dropwindsonde data. Special thanks goes to Professor W.A. Nuss for his highly professional and in-depth critical review of this document. I am greatly indebted to my thesis advisor Professor R.L. Elsberry for his critical review and constructive criticism of this thesis. This study would not have been completed were it not for his suggestions, knowledgeable insight and direction. Finally, my love and sincere appreciation are extended to my wife, Judy, and my sons for their strong support and patience over the past year.

I. ATLANTIC CYCLOGENESIS

A. INTRODUCTION

Severe storms during the winter season are common along the east coast of the United States. Some of these storms develop slowly and predictably. Other storms deepen at an extremely fast rate and become very intense storms. Miller (1946) studied 208 cyclones and noted that a severe storm could develop and threaten the coastal United States within a 12-h period. These fast-growing storms can cause property damage and effectively shut down the eastern seaboard north of Virginia. Forecasting these fast developing cyclones poses a difficult problem.

Several studies have been conducted to increase the understanding of these fast-growing storms and the physical processes involved. Sanders and Gyakum (1980) studied these explosively deepening storms and credited Tor Bergeron for providing the formal definition of a "rapidly deepening low" as one which has a sea-level pressure decrease exceeding 24 mb in 24 h. The Sanders and Gyakum (1980) study was the first to investigate the physical and statistical properties of explosively deepening cyclones.

The Genesis of Atlantic Lows Experiment (GALE) was a major experiment designed to obtain data on the cyclogenetic environment by studying a wide variety of atmospheric phenomena. A core objective of GALE as listed in the **GALE Experimental Design** (1985) was "to understand the physical mechanism controlling the formation and rapid development of east coast storms". The GALE data collection phase lasted from 15 January through 15 March 1986 and was divided into 13 Intensive Operating Periods (IOPs). In addition to the GALE rawinsonde network, dropwindsondes were used to observe regions of maritime cyclogenesis. A complete discussion of the GALE study and data distribution is available in the **GALE Experimental Design** (1985) and the **GALE Field Program Summary** (1986).

The large number of maritime upper air soundings achieved during GALE allows studies of the precyclogenetic environment. The possible effects of "lid" conditions in these soundings (rawinsondes and dropwindsondes) on explosive cyclogenesis during two IOPs (6 and 11) in GALE are the focus of this study. During IOP 6, a coastal cyclogenesis event occurred with explosive deepening after the storm exited the GALE region. The IOP 11 maritime cyclogenesis was a modest (nonexplosive) deepening event.

This research examines the hypothesis that explosive cyclognensis is favored where "lid" conditions established by advection of a dry, continental air mass with a conditionally unstable lapse rate in mid-tropospheric air streams occurs over a cool, moist maritime surface layer. These conditions are hypothesized to exist in regions upwind of the convective heat release that accompanies rapid cyclogenesis, but do not exist in the same areas of non-rapid cyclogenesis. Maritime lid conditions are recognizable in the environment by the presence of a capping inversion in the sounding. The presence of the lid prevents vertical mixing of the low-level air mass with the overlying dry air. As a result of the lid, surface air is trapped close to the surface while increasing in Convective Available Potential Energy (CAPE) of the system through air-sea fluxes.. Concurrent with the APE increases, a mechanism for overcoming the lid is advected into the area, which lifts the surface air through (or from under) the lid, and thus rapidly converts the potential energy to kinetic energy and provides extra vigor to the storm growth.

B. EXPLOSIVE CYCLOGENESIS STUDIES

1. East coast cyclogenesis

The study by Miller (1946) established a two-part classification scheme for cyclogenesis in the eastern U.S. and the adjacent ocean regions. Type A storms form on the front in a cold outbreak over the ocean, with a high pressure system covering the entire eastern half of the U.S. After cyclogenesis, the storm moves in a northeastern direction. Type B storms generate in coastal regions on a warm front southeast of a weakening low that is normally located west of the Appalachian Mountains in the Great Lakes region. Miller (1946) determined that Type B storms were more numerous from December through April.

Early efforts to determine the physical reasons for cyclogenesis are described in Petterssen (1955) and Petterssen et al. (1955) who proposed that cyclogenesis occurred when positive vorticity advection in the upper troposphere moved over a sea-level baroclinic disturbance. Since then, the effects of positive vorticity advection have been recognized as a prominent factor in cyclogenesis. Petterssen and Smebye (1971) developed a storm classification scheme based on the presence or absence of vorticity advection.

2. Explosive cyclogenesis

The physical mechanisms identified as vorticity advection and jet streak interaction also are found in explosive cyclogenesis. The difficult forecast problem is to establish the degree to which these mechanisms influence explosive cyclogenesis. The classical discussion of explosive cyclogenesis (Sanders and Gyakum, 1980) is a summary of Northern Hemisphere cyclogenesis between September 1976 and May 1979. This type of storm growth is primarily a maritime event with the highest incidence of explosive cyclogenesis occurring in western oceans in regions of high sea-surface temperature (SST) gradients. The Sanders and Gyakum (1980) conclusion that rapid cyclogenesis was linked to PVA has been supported in later studies (Roebber, 1984; Sanders, 1986; MacDonald and Reiter, 1988). Positive vorticity advection was found upstream in all but one of the 46 storms studied by Sanders (1986).

Upper-level jet streak divergence has been shown to enhance cyclone growth. Explosive cyclogenesis was linked to the effect of a polar jet streak (Uccellini et al., 1984; Uccellini et al., 1985) during the Presidents' Day Cyclone (18-19 February 1979). Jet streak divergence is enhanced when the maximum velocity is in the base of the upper-level trough. In this arrangement, the strong divergence in the left exit region of the jet adds to the advection of curvature vorticity downstream of the trough. A correlation between divergence and cyclogenesis was found by Mac Donald and Reiter (1988), who also noted a marked level of nondivergence near the middle troposphere in explosive storm development cases.

3. Latent heat exchange

Sensible and latent heat exchanges have been found to be important in east coast cyclogenesis (Gall and Johnson, 1971; Danard 1964; Bullock and Johnson, 1971; and Petterssen et al., 1962). Danard (1966) concluded that the latent heat released in convection offsets the effects of adiabatic cooling. The difference in availability of surface moisture between continental and oceanic regions should have an impact on storm development. In regions of a large SST gradient, sensible heating of the atmosphere can add extra energy to storm generation (Gall and Johnson, 1971). The effects of a low-level jet streak advecting moisture into coastal region prior to an explosive cyclogenesis event was shown in Uccellini et al. (1987). The effects of latent and sensible heating in the North Atlantic can contribute to the energy for cyclone development in that region.

Latent heating effects in cyclogenesis over the data intensive continental regions is documented better. Case studies of individual storms and the effects of latent heat on storm growth were conducted by Robertson and Smith (1983) and Chang et al. (1984).

Latent heating was found to be a "significant source" of energy for a mid-latitude cyclone over the continental U.S. (Robertson and Smith, 1983). The greatest heating in the middle troposphere (Vincent et al., 1977) is between 700 and 500 mb. Even though the heating is in the upper levels, the largest effect of latent heating is located in the lower troposphere where associated convergence occurs. This low-level effect provides the "catalyst" for a more vigorous storm growth (Chang et al., 1984).

4. Lid concept

Positive vorticity advection, upper-level jet streak divergence and the effects of latent heating can contribute to cyclogenesis. No single process has been shown to be unique in explosive cyclogeneis, as rapid storm development often appears to be a combination of these factors. MacDonald and Reiter's (1988) review of cyclogenesis over the central and eastern U.S. most aptly describes the effects of latent heating:

> We conclude that the developing bombs move into an environment with considerably more moisture in the lower layers than is available in their incipient stage. This aspect of explosive cyclogenesis may be different for marine bombs than it is for continental bombs. Apparently, incipient marine bombs are seen over warm moist air in the lower layers (Sanders and Gyakum 1980; Sanders 1986); however, there are no specific data present to support this notion.

Continental storms must be supplied moisture from low-level advection processes, while maritime regions have an ample supply of moisture. One uncertainty associated with explosive cyclogenesis is whether air-sea fluxes or advection processes cause the increase in moisture in the lower troposphere.

The hypothesis tested here is that the presence of a capping inversion in the middle troposphere could indicate the potential for a very rapid release of latent heat, and consequently the potential for explosive cyclogenesis. Once this lid is established, the effects of evaporative processes and sensible heat exchange are confined to the lower troposphere. The accumulation of moisture adds to the Convective Available Potential Energy and continues while the lid is sufficiently strong to inhibit convection. This energy in the lower troposphere is released when a lifting mechanism pulls the surface air from under the inversion. The cumulative effects of positive vorticity advection and jet streak divergence provide the triggering mechanism to overcome the maritime lid. The saturated surface air parcel then follows the moist pseudoadiabat as it is lifted through the lid into the conditionally unstable air immediately above the inversion. Once above the lid, the moist air becomes unstable and the resulting vertical motion will provide additional vigor to storm growth. The increased vertical motion in the middle

troposphere also causes larger convergence in lower levels, which contributes to the spinup of low-level vorticity during storm growth. This study examines the maritime soundings obtained during GALE for the presence of lid conditions. The comparison of two contrasting storms (one with a lid and one without a lid) will demonstrate the effects of the lid in a cyclogenetic environment and the possible contributions of the lid to explosive cyclogenesis.

II. METHODS AND DATA ANALYSIS

A. LID ANALYSIS

1. Lid Definition

Lid establishment occurs when a layer of dry air with a conditionally unstable lapse rate overlies cool, moist maritime air (Fig. 1). The inversion, or lid, is located near 780 mb and has a sharp temperature increase with height. Coincident with the temperature increase is a rapid moisture decrease. Between 780 and 600 mb, the lapse rate is less than moist adiabatic, which satisfies the lid definition. In this example, moisture is found above 600 mb and below the lid at 780 mb. Later discussion will provide evidence of the continental origin of the dry air mass.

The 18°C surface air would be unstable if lifted moist adiabatically to the700 mb level. However, the relatively dry surface air must first ascend along the dry adiabat until saturation is reached and then ascend moist adiabatically. In this case, the air will be stable when it reaches the inversion, which inhibits deep convection. If a lifting mechanism could provide sufficient lifting to overcome the lid, then convection would continue since the air would be warmer than the surrounding environment.

2. Lid Strength Index

The suppression effects on deep convection by the lid were described by Carlson et al. (1980) in terms of a "Lid Strength Index" (LSI). Originally, the LSI was developed to indicate the potential for severe storms in an inversion-dominated summer environment over the continental U.S. This study will use the LSI to provide an indication of the existence of lid conditions in the marine environment. A correlation of severe storm LSI values discussed in Carlson et al. (1980) is not possible in the winter environment of the GALE study area. However, a general quantitative assesment is discussed later.

The LSI is defined (see Fig. 2) as the difference between a buoyancy term $(\bar{\theta}_w - \bar{\theta}_{sw})$ and an inversion strength term $(\theta_{sw_1} - \bar{\theta}_w)$ or

$$LSI = (\bar{\theta}_w - \bar{\theta}_{SW}) - (\theta_{SW_1} - \bar{\theta}_w). \quad (1)$$

$\bar{\theta}_w$ is the average wet bulb potential temperature of the lower 50 mb of the atmosphere. The buoyancy term $(\bar{\theta}_w - \bar{\theta}_{sw})$ reflects the instability of the surface air parcels when raised

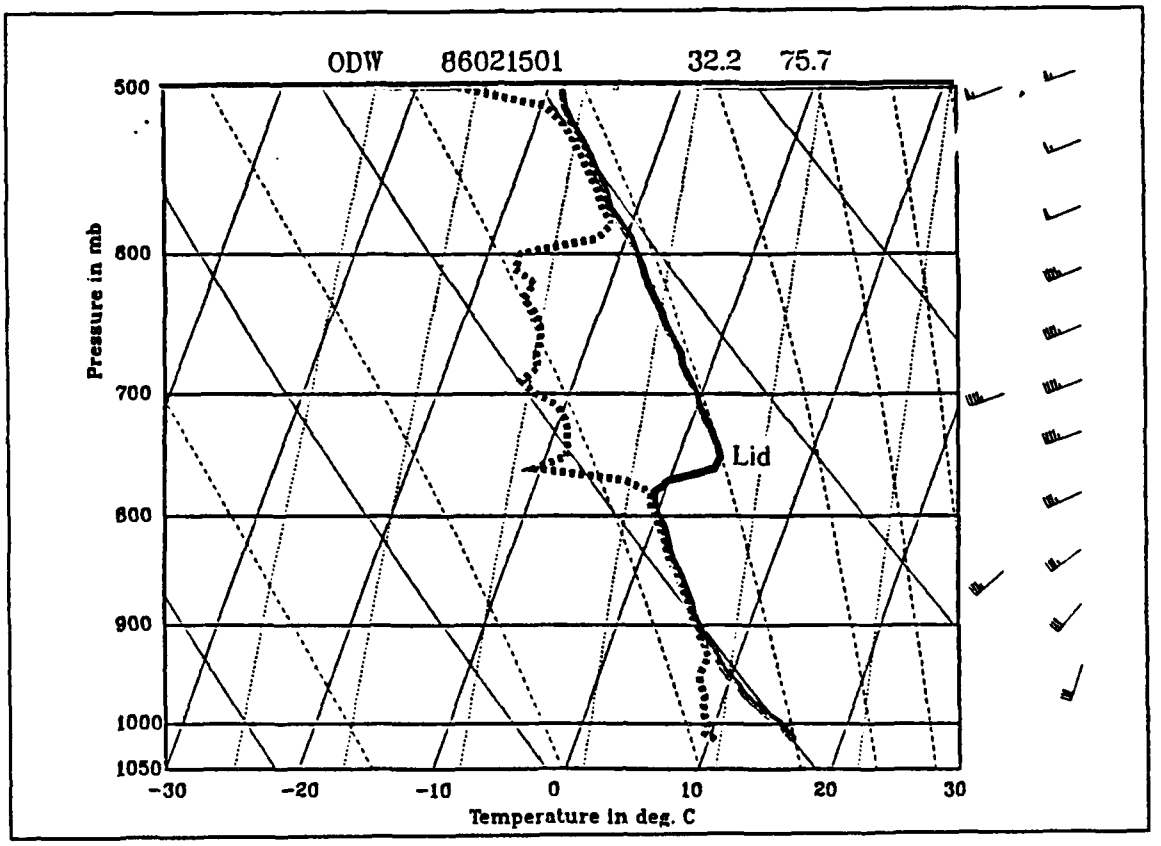

Fig. 1. Sample Lid diagram: Skew-T ln p diagram with station identification across the top as follows: station ID or dropwindsonde type, date and time, latitude and longitude. Dashed lines are moist pseudoadiabats, dotted lines are mixing ratio lines, curved solid lines are the dry adiabats and the straight slanted lines are temperature lines. The temperature sounding is the thick solid line and the dew-point temperature is the thick dashed line. One wind barb equals 5 $m \cdot s^{-1}$.

moist adiabatically to 500 mb. $\overline{\theta}_{sw}$ is the average saturation wet-bulb potential temperature between the base of the lid and the 500 mb level. The difference $(\theta_{sw1}-\overline{\theta}_{w})$ reflects the potential for moist convection of the surface air to 500 mb. If the term is positive, the result would be an unstable air mass since the surface air would be warmer than the surrounding environment (larger $\overline{\theta}_{w}$). A stable air mass would be represented by a negative buoyancy term (larger $\overline{\theta}_{sw}$).

The lid strength term $(\theta_{sw1}-\overline{\theta}_{w})$ reflects the strength of the capping inversion or the lid. θ_{sw1} represents the maximum saturation wet bulb potential temperature in the air column at the lid, which is at 780 mb in Fig. 2. A positive value for the lid strength term indicates that the surface air mass would be colder than the surrounding environment when lifted to the level of θ_{sw1}, which indicates a stable air mass. Even if a mechanism exists to lift the surface air, the lid will suppress upward vertical motion unless the forcing is strong enough to overcome the presence of the lid. A strong inversion will tend to make the LSI more negative, due to the subtraction of the inversion strength term from the buoyancy term in (1).

A program to compute the LSI for individual soundings was developed using logic decisions similar to those of Graziano and Carlson (1987). A step-by-step sequence in the decision process determines first if there is a lid present, and then calculates the LSI. The program uses a rapid moisture decrease of greater than 1 % per mb to define a humidity break. If such a break exists in the sounding, then the program checks for an increase in temperature with height within 100 mb of the humidity break. When both conditions of humidity break and temperature increase are satisfied, a lid condition exists and the LSI is calculated for that sounding.

Although a direct comparison with the LSI values discussed by Carlson et al. (1980) is not possible due to environmental differences, a general correlation of LSI, lid conditions and explosive cyclogenesis can be made. Large negative values of LSI (less than -10 K) will be considered to represent strong lid conditions, and an environment that would suppress convection to below the lid. By contrast, large positive values of LSI would indicate an unstable environment $(\theta_{sw1}-\overline{\theta}_{w})$ having negative or near zero values, thus lifting would cause deep convection. Small negative values of LSI indicate a possible weak lid. The hypothesis suggests that when strong lid conditions exist upwind of the latent heat release areas, explosive development is possible when the moist flow trapped under the lid is allowed to ascend over the low pressure center area.

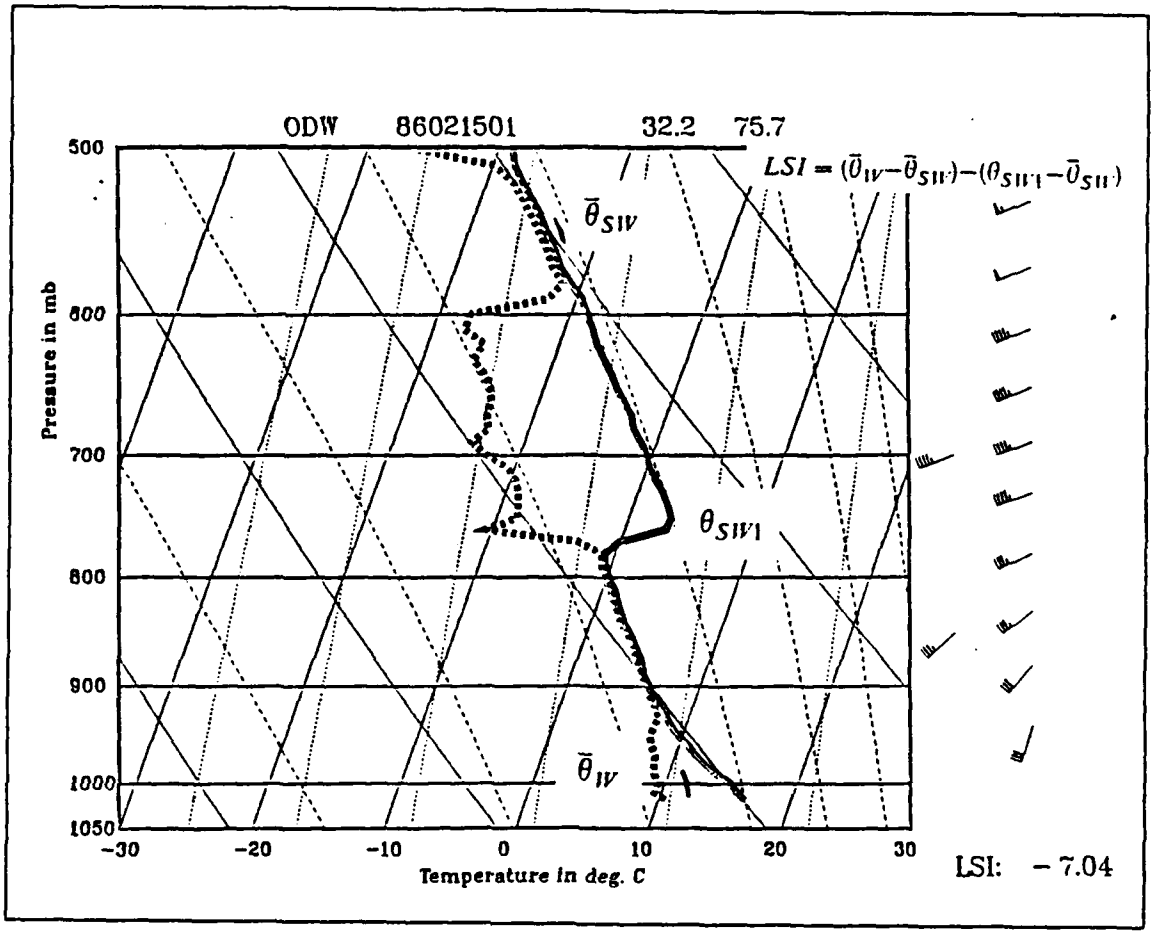

Fig. 2. Example of Lid Strength Index Solution: As in Fig. 1 with the definitions of variables in Eq. (1).

B. DATA ANALYSIS AND PRESENTATION

Cross-section analysis, trajectories and skew-T ln p diagrams have been used for analyzing and for describing the differential advection in the complex marine environment. Cross-sections of isentropes and isotachs provide representation of the atmosphere along the axis, while soundings give details of the vertical moisture and temperature profiles. The trajectories indicate the different source regions of the air in the cyclogenesis region. The identification of the trajectory source region, when combined with the cross-sections and soundings, specifically identify the atmospheric air mass sources.

1. Cross-sections

The cross-section program was available on the Naval Postgraduate School (NPS) mainframe computer. The program incorporates multiple (usually five or six) rawinsonde and/or dropwindsonde profiles. Elevations of the continental stations are corrected and plotted on the cross-section as a blanked area. Vertical pressure levels are calculated logarithmically between 1050 mb and the top of the cross-section. Due to the limitations of the dropwindsondes, the upper level of the cross-section has been limited to 400 mb. The values of potential temperature are calculated in the program for each sounding level, and the data are interpolated into a 50 by 50 matrix (vertical and horizontal). Values on the horizontal axis are interpolated using the actual distance between the stations. Due to the linear horizontal interpolation, an area of baroclinity may not have sufficiently tight gradients or will have a jump discontinuity between stations.

Isotachs displayed in the cross-sections are calculated from the perpendicular wind components. Each of the soundings used in the cross-sections are provided in Appendix A to allow comparison of wind speeds and directions as necessary.

2. Skew-T ln p diagrams

The skew-T ln p diagrams utilized in this study are plotted with the DISSPLA Executive on the NPS mainframe. Values of temperature are plotted directly, and dewpoint temperatures are calculated from relative humidity values using equations in the Smithsonian Meteorological Tables (List, 1949). LSI values are provided in the lower right of the sounding for reference.

3. Trajectories

The trajectories for this study have been provided by Rolf Langland of the Naval Environmental Prediction Research Facility (NEPRF). Wind speed and direction as calculated in the Navy Operational Regional Atmosphere Prediction System (NORAPS) (Hodur, 1982) were used for trajectory calculations. The model was run for a 48-h period ending at the time of the trajectory, and wind fields at 3-h intervals were saved for trajectory determination.

Starting with a position and pressure level, the air mass was then back plotted for each three-hour increment. Each trajectory interval used a constant wind speed and direction for the applicable level. In the event that all past positions cannot be plotted within a reasonable area, only those points that are within bounds of the study area will be plotted. This condition is easily identified by the reduced number of data points in the trajectory for that level.

4. Synoptic maps

The surface synoptic maps for each of the IOP times provide pertinent synoptic information from the National Meteorological Center (NMC) final surface analysis. Maps displayed here are those of the DISSPLA Executive with a selected set of GALE stations identified on the map (Fig. 3 for example). Upper-level height and isotachs charts are direct copies of the NMC analyses. Values of vorticity are those in the Nested Grid Model (NGM) initial analysis. Each of the cross-sections will be identified on the synoptic plots to provide a better physical orientation of the cross-section.

III. EXPLOSIVE CYCLOGENESIS CASE

A system overview is first provided to assist the reader in following the discussion of these synoptic periods and how the formation of a lid contributes to the growth of the storm. Cyclogenesis occurred between 00 and 12 UTC 15 February 1986, about 24 h after a surface cyclone crossed the coast into a favorable oceanic environment established by air-sea interaction within the cold outbreak behind a previous cyclone. Cold, dry air associated with the high pressure system at 12 UTC 14 February 1986 is confined beneath an inversion produced by warm continental air. Over the next 18 h, this low-level air is modified by the oceanic influences with a gradual decrease of the inversion strength. Convergence aloft inhibited development of the low pressure system until Positive Vorticity Advection (PVA) entered the cyclogenetic region and provided the lifting mechanism to overcome the inversion. Meanwhile, the air beneath the lid warms and becomes more moist with time as energy from the ocean is stored under the inversion.

After 00 UTC 15 February 1986, strong PVA (associated with a short wave) passes over the developing low pressure system. A Polar Front Jet streak also translates east of the low-level system, which places the divergent entrance region of the jet above the low. Warm, moist surface air previously held beneath the inversion is lifted sufficiently to overcome the lid. When the convective energy stored below the inversion is injected into the dry, almost neutral layer above the lid, the convection is particularly vigorous and the latent heat release contributes to the explosive deepening. Although the PVA and divergence aloft provide the triggering mechanism, the hypothesis is that rapid release of the latent heat in the region of the surface center produced the extra energy necessary for explosive growth.

A. INITIAL PERIOD (12 UTC 14 FEBRUARY 1986)

1. Synoptic discussion

A high pressure system is located at 34.3°*N*, 76.5°*W* with a central pressure near 1028 mb as shown in Fig. 3. The pressures throughout most of the southeast corridor of the U.S. are within the 1024 mb isobar. During the next 18 h, a low pressure center in Louisiana moves over the Tennessee Valley and weakens significantly. As this system weakens, a Miller (1946) type B cyclogenesis occurs off the coast of North Carolina. An

850 mb ridge (not shown) has moved eastward and is located west of the surface anticyclone position at 12 UTC 14 February 1986. Zonal flow dominates at the upper levels (300 mb) with Polar Front Jet (PFJ) speeds that range from 60 to 90 kt (30 to 45 $m \cdot s^{-1}$).

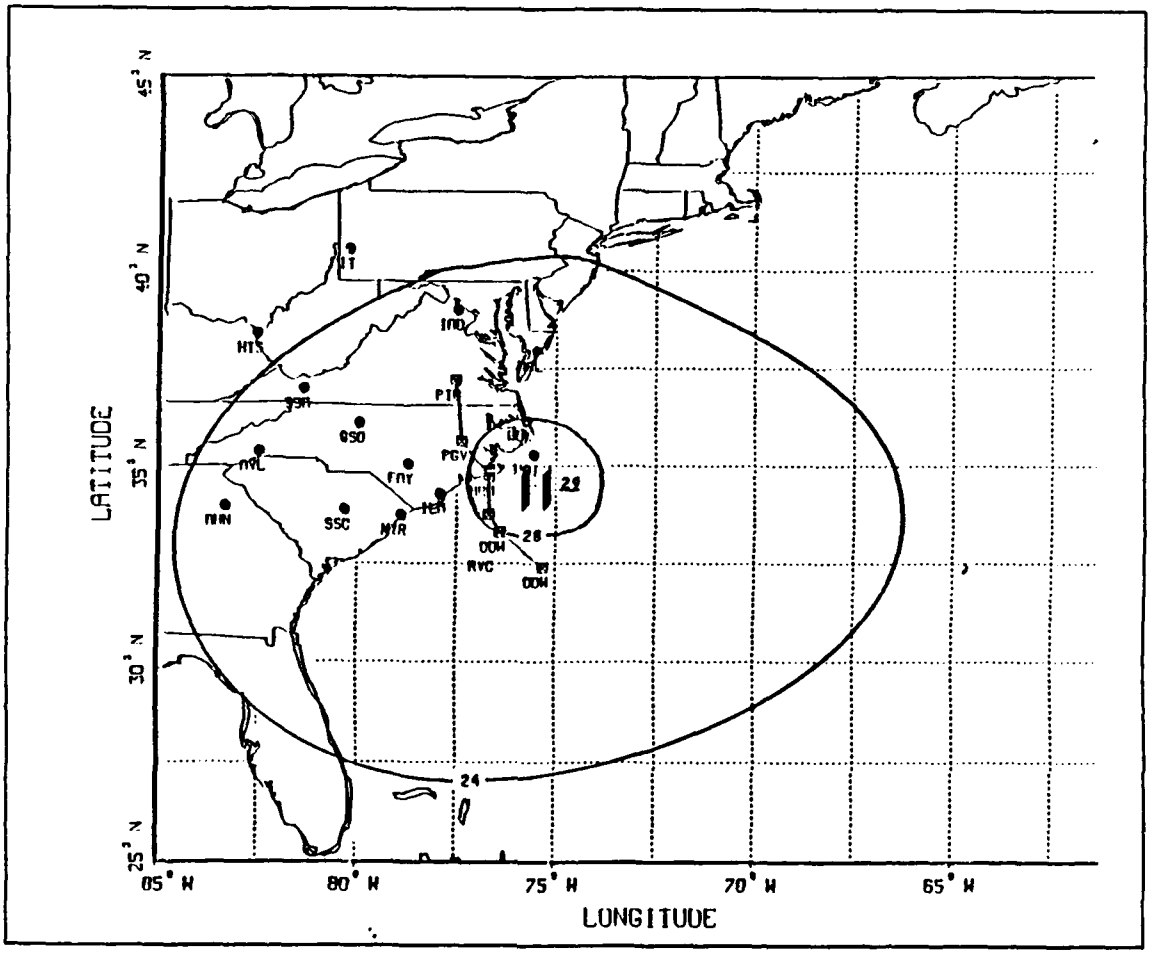

Fig. 3. Synoptic weather pattern, 12 UTC 14 February 1986: Relevant portions of the NMC sea-level analysis for the GALE region. Solid lines represent pressure in mb, "÷" indicate GALE stations and "⊗" represent the stations used in cross-section analysis.

2. Cross-section

The cross-section analysis in Fig. 4 reflects some common characteristics of the high pressure system. Two oceanic dropwindsondes and an oceanic rawinsonde are available to supplement three continental rawinsondes. Subsidence at the center of the

high pressure system is evident by the downward tending isentropes and increasing tropopause height over the R.V. Cape Hatteras (RVC).

A low-level inversion is located between 850 and 900 mb throughout the cross-section, with slightly stronger vertical gradients and a higher base over the ocean. This inversion is providing the cap that limits the depth through which the near-surface air is modified. A weak mid-level inversion is present near the 600 mb level at all locations along the cross-section. South of the anticyclone center, the mid-level inversion is noticeably weaker (cross-section not shown) due to a weaker subsidence regime.

Significant low-level baroclinity exists between Morehead City (MRH), North Carolina and the RVC. This coastal baroclinity is also present on two other cross-sections (not shown) farther north along the coast. This coastal front is probably more concentrated than shown by the interpolated isentropes between the RVC and MRH. Finally, a broad Polar Front Jet with winds in excess of 80 kt (40 $m \cdot s^{-1}$) is centered on the cross-section near the 250 mb level (not shown).

3. Dropwindsonde

The sounding at 33.3°N, 76.4°W taken at 10 UTC 14 February is shown in Fig. 5. The low-level and mid-level inversions are quite marked on the landward dropwindsonde along the cross-section. A large negative Lid Strength Index (LSI) is calculated with the lid at the 850 mb level. Other soundings in the area of the high (not shown) have equally strong lids with LSI values in the -20 to -25 K range. The dropwindsonde that is closest to the center of the high has abundant moisture from just below the lid down to the 950 mb level. Thus, the inversion tends to keep the moisture trapped close to the surface and limits the depth of influence of the ocean energy flux. A dry layer extending to 400 mb is found above the inversion. The near-saturation of the air at 400 mb is in sharp contrast to the dry layers below and above. This upper-level moisture will be shown to come from the inland low pressure system. Other soundings in the area (not shown) have similar moist layers near 400 mb. The role of differential advection between various layers will be examined through parcel trajectories.

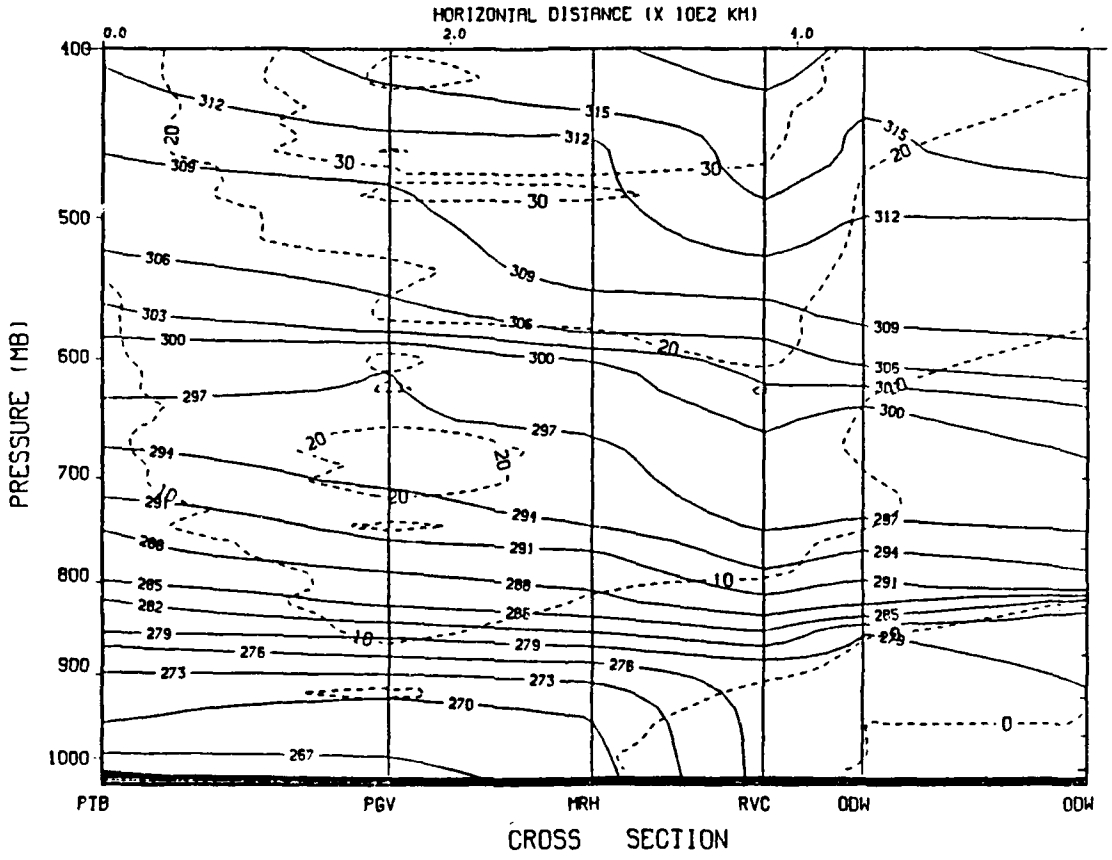

Fig. 4. Cross-section, 12 UTC 14 February 1986: Cross-section analysis of isentropes (solid lines) in K and perpendicular wind isotachs (dashed lines) in $m \cdot s^{-1}$. Station identifiers are located at the bottom of the plot and the orientation of the cross-section is shown in Fig. 3.

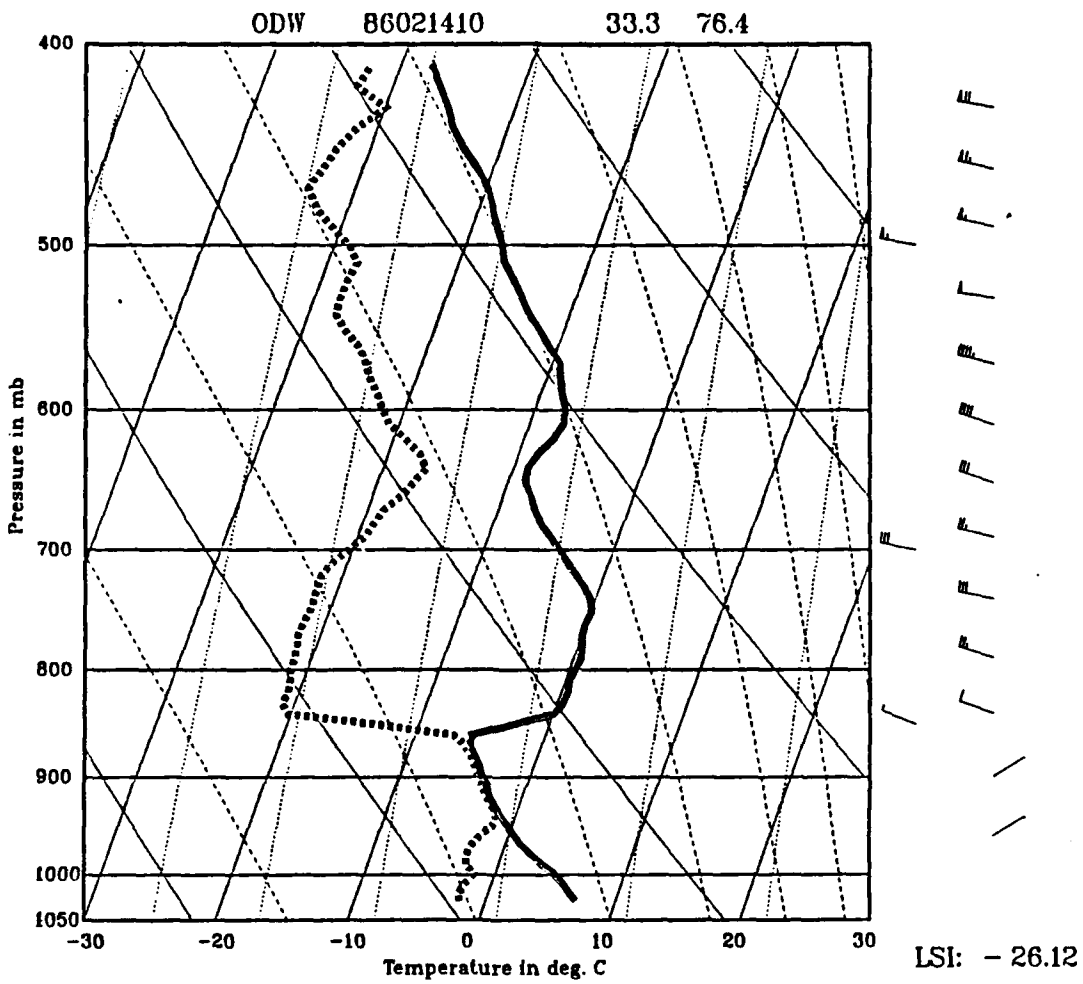

Fig. 5. Dropwindsonde ODW, 10 UTC 14 February 1986: Skew-T ln p diagram with station identification across the top as follows: station ID or dropwindsonde type, date and time, latitude and longitude. Dashed lines are moist pseudoadiabats, dotted lines are mixing ratio lines, curved solid lines are the dry adiabats and the straight slanted lines are temperature lines. The temperature sounding is the thick solid line and the dew-point temperature is the thick dashed line. One wind barb equals 5 $m \cdot s^{-1}$.

4. Trajectories

Trajectories indicate that the source region of the air parcels at 900 mb above the surface high center is from the West Virginia and Pennsylvania area (Fig. 6). The air flows past the Chesapeake Bay with slight anticyclonic curvature, and over the ocean surface to the location of the sounding shown in Fig. 5. Dry continental air subsides from 550 mb to the 850 mb level. This subsiding continental air provides the lid that keeps the moist layer close to the surface. The moist layer near 400 mb in the sounding (Fig. 5) was located over the Midwest U.S. cyclone only 9 h earlier and has been advected by 60 kt winds in the upper-level zonal flow.

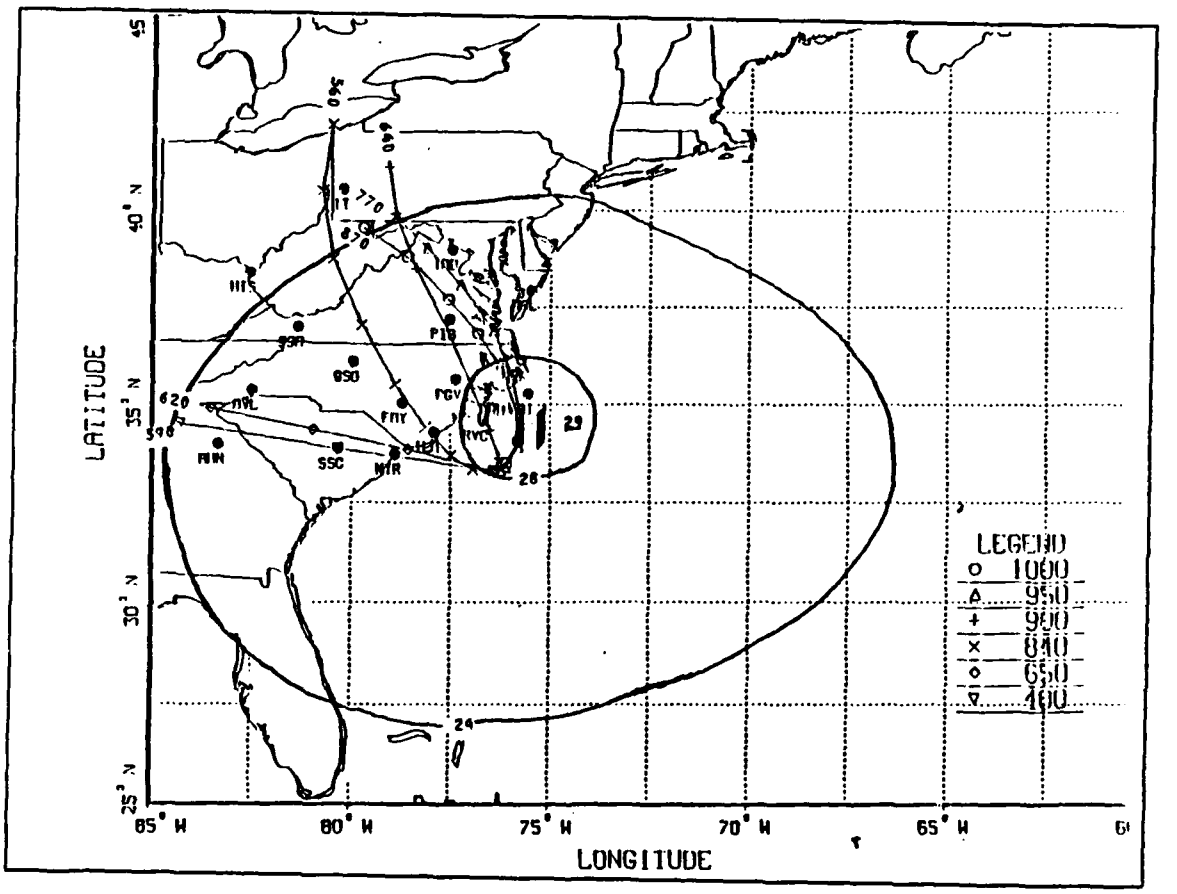

Fig. 6. Trajectories, 12 UTC 14 February 1986: Air parcel trajectories ending at key pressure levels (indicated in legend) in the sounding in Fig. 5. Each marker along the trajectory indicates a 3-h time interval.

5. Summary

In summary, the multi-layered thermal and moisture structure of the air columns in the early pre-cyclogenetic region off the North Carolina coast is produced by differential advection. Although the middle and lower levels of the troposphere are in a subsiding anticyclonic flow, a moist surface layer is trapped below the inversion over the ocean. The flow at upper levels is also from continental regions, but it is moist because it originated from a cyclone area over the Midwest and is advected by much stronger upper-level winds.

B. PRECYCLOGENETIC PERIOD (00 UTC 15 FEBRUARY 1986)

1. Synoptic discussion

The oceanic high has moved eastward into the central North Atlantic (Fig. 7) while the low center that was previously over Louisiana has weakened as it moved over northeastern Tennessee. However, pressures are decreasing throughout the southeastern U.S. with current pressures near 1016 mb. The NMC analysis includes a convoluted stationary front through Tennessee and the Carolinas. The upper-level wave (not shown) has also moved eastward. The axis of the upper-level trough now extends southward from the Great Lakes over the weakening surface low and into the Gulf of Mexico. Zonal flow in the upper levels during the previous period is being replaced by southwesterly winds associated with the deepening trough and the eastward movement of the PFJ. A slight increase (10 kt) in jet speeds occurred over the last 12 h.

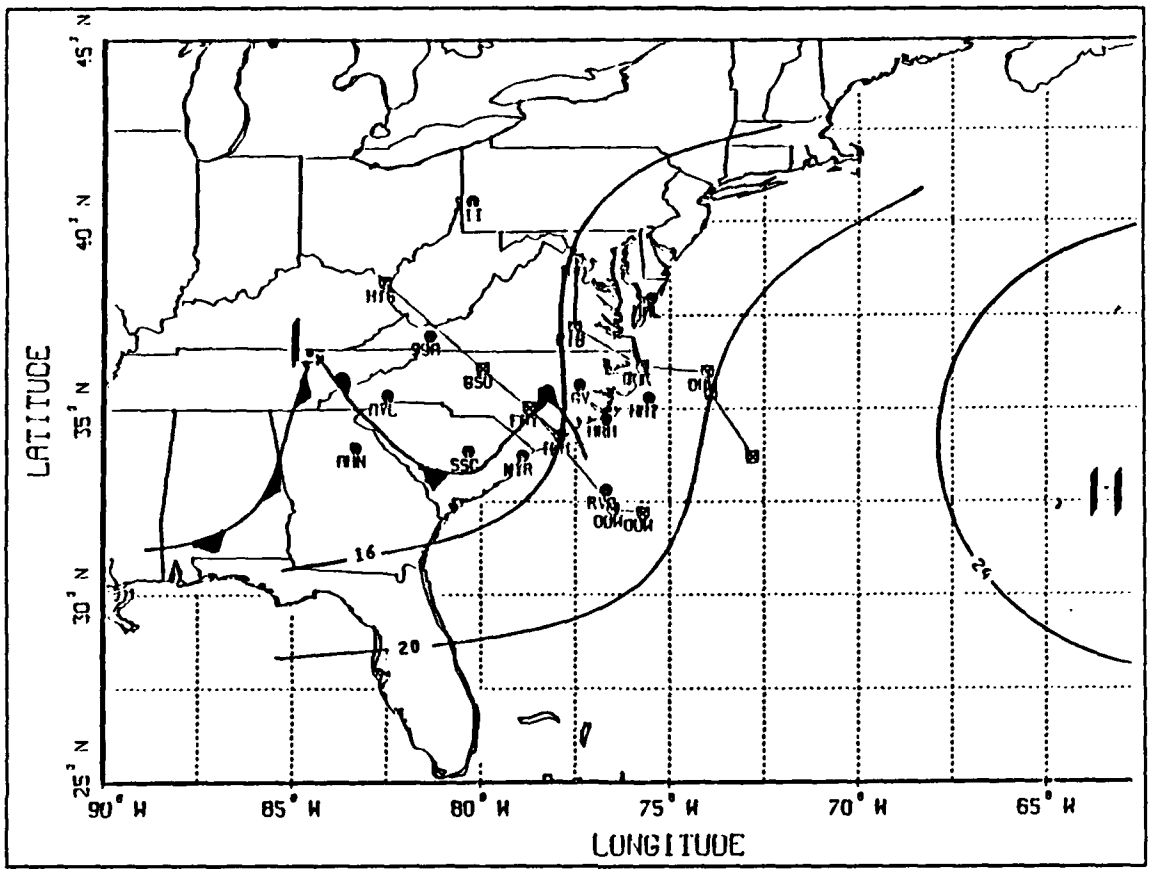

Fig. 7. Synoptic weather pattern, 00 UTC 15 February 1986: As in Fig. 3.

2. Cross-sections

The cross-section (Fig. 8a) chosen to illustrate the precyclogenetic environment is nearly perpendicular to the 700 mb wind field. Three continental rawinsondes, one coastal rawinsonde, and two oceanic dropwindsondes show the changes that have occurred during the previous 12 h. Over the continental stations, the isentropes are becoming nearly horizontal. The continental inversion is becoming weaker with the approach of the trough. The discontinuity near Fayetteville (FAY), North Carolina reflects the convoluted stationary front in an exaggerated manner. The coastal baroclinity that is present between Wilmington (ILM), North Carolina and the offshore dropwindsondes also is exhibited on other cross-sections (not shown) along the east coast.

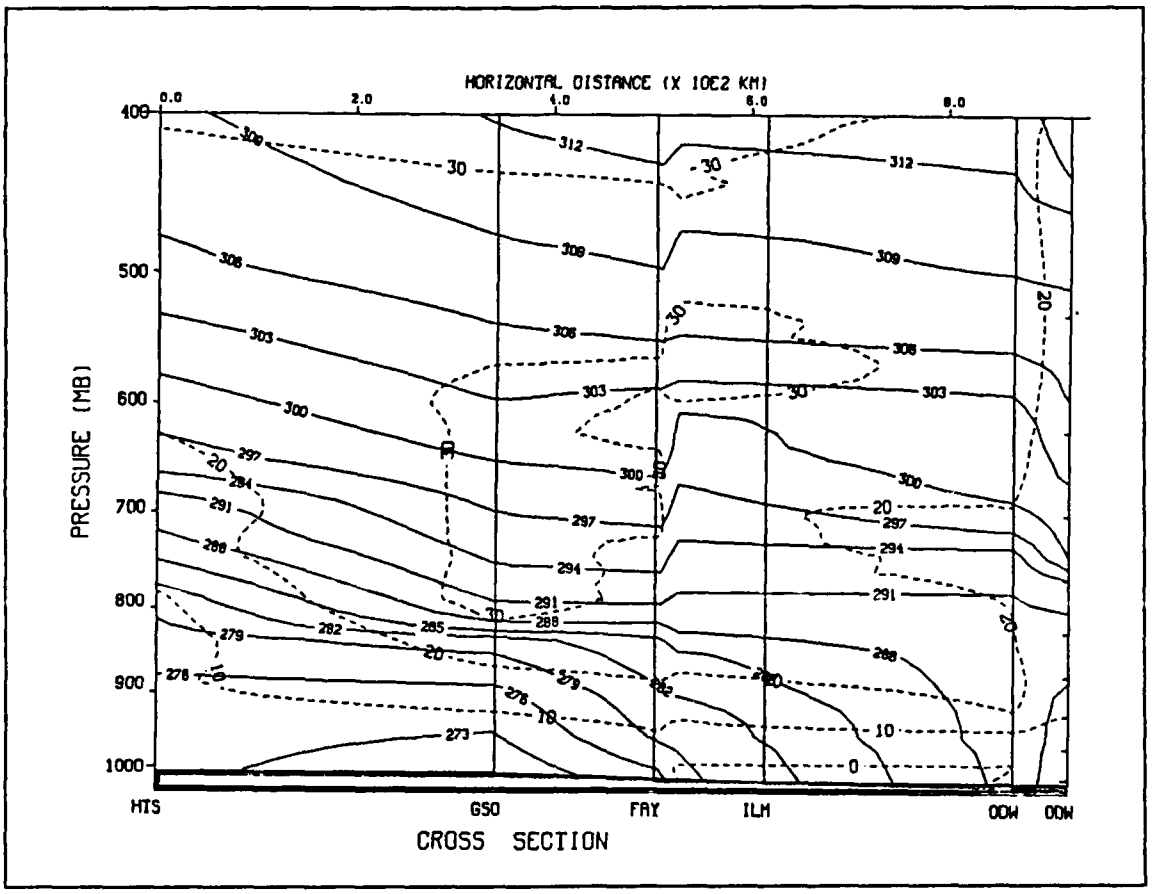

Fig. 8a. Cross-section, 00 UTC 15 February 1986: As in Fig. 4, for the southern cross-section shown in Fig. 7.

A significant new factor is the presence of a southwesterly low-level jet with winds of greater than 60 kt (30 $m \cdot s^{-1}$) between 800 and 600 mb over Greensboro (GSO), North Carolina and FAY. Nearer the coast, the jet is centered around 600 mb. Trajectory analysis will show that dry continental air is being transported by the high winds towards the precyclogenetic region off the Virginia/North Carolina coast. This warm, dry continental air tends to support the lid and (as will be shown later) continues into the formation region of the storm. The PFJ maximum over FAY and ILM has speeds in excess of 100 kt (50 $m \cdot s^{-1}$).

A parallel cross-section (see orientation in Fig. 7) consists of two continental and one coastal rawinsonde and three oceanic dropwindsondes (Fig. 8b). Velocities in the area of the low-level jet are smaller in this section, which indicates that this is in the

exit region of the low-level jet. Lower static stabilities are present in the mid-levels of the dropwindsondes in both cross-sections, which are in the region that experiences cyclogenesis during the next 6 h.

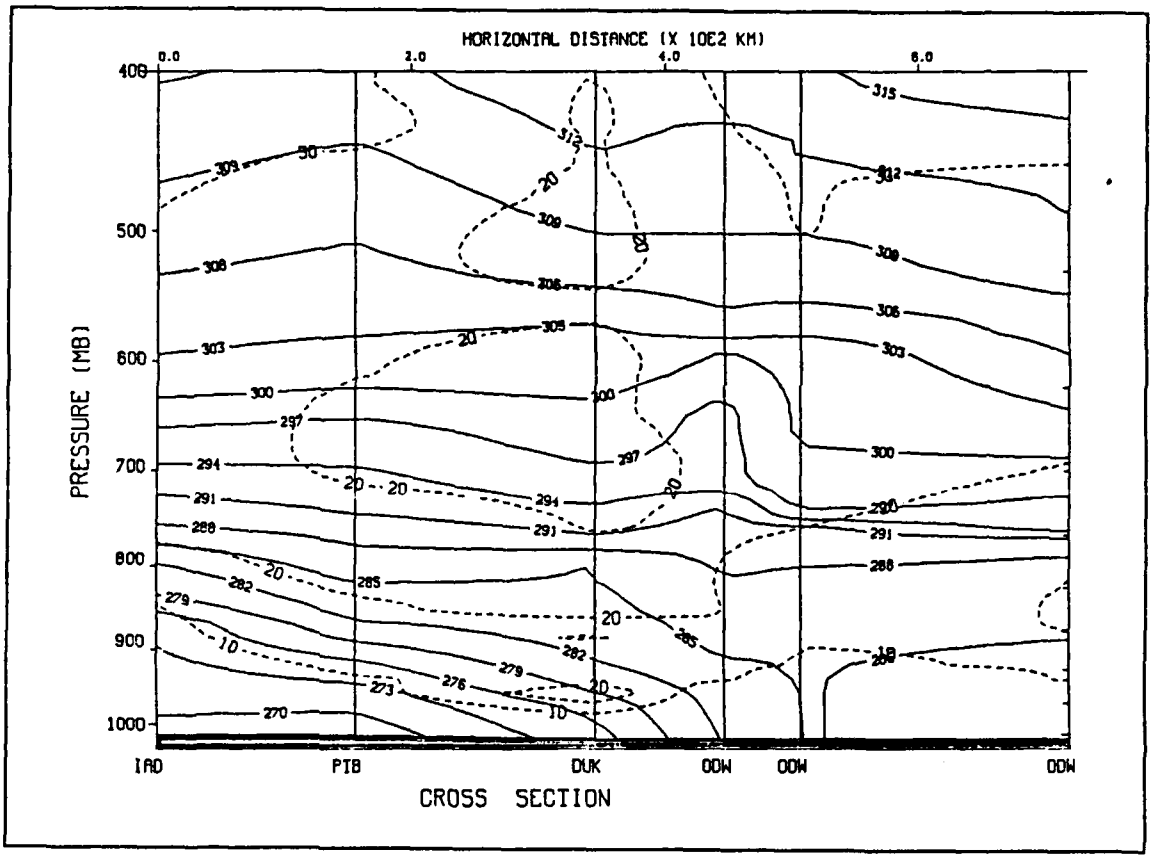

Fig. 8b. Alternate cross-section, 00 UTC 15 February 1986: As in Fig. 4, for the northern cross-section shown in Fig. 7.

3. Dropwindsonde

The sounding at 35.4°*N*, 73.9°*W* taken at 01 UTC 15 February shown in Fig. 9 is located in the area of incipient cyclogenesis. The marine layer below the lid has thickened over the past 12 h, while the surface air has been warmed and moistened. The lid height has increased to 750 mb and the lid strength has decreased to -9.8 K versus -20.0 K previously in the cyclogenetic region. The warming of the surface layer has eroded the lower layers of the lid and resulted in an increase in lid height. However, the lid remains sufficiently strong to suppress free convection while further warming and moistening of the marine layer continues. The top of this marine layer is at or near saturation. Southwesterly winds throughout the sounding are increasing with height to near

65 kt (32 $m \cdot s^{-1}$) at upper levels. Similar conditions exist in all of the oceanic dropwindsondes. Lid values in the other dropwindsondes range from near zero to -15 K as dry conditionally unstable air is above the inversion (between 750 and 600 mb) and warm moist air is below (soundings in Appendix A).

4. Trajectories

The passage of the surface anticyclone across the coast of North Carolina can be clearly seen in the near-surface trajectory of Fig. 10. An anticyclonic curvature in the low-level trajectory 12 h earlier has been changed by the straight southwesterly flow during the last 3 h. The lower layer has been kept close to the surface by the strength of the lid and, as indicated in the dropwindsonde, warming and moistening has occurred. The layer near 800 mb beneath the lid in Fig. 9 evidently has travelled from northern Florida to the current location without much ascent or descent. The dry layer between 790 mb and 600 mb on the sounding has a continental origin. This air is being transported over the oceanic region after crossing the coast 6 h earlier. This warm dry air constitutes the top of the lid. The upper-level wind shift from zonal to southwest flow is apparent in the mid-level trajectories crossing the coast. Above 600 mb, the PFJ continues to transport moisture that has ascended above the continental storm.

5. Summary

In the 12 h prior to 00 UTC 15 February 1986, the high pressure system moved out of the cyclogenetic area and left a shallow layer of moisture held close to the surface by the lid. Dry continental air that forms the lid has been advected into the region by a low-level jet over much of North Carolina. In addition, the deepening upper-level trough and the PFJ are moving eastward over the cyclogenetic region. Thus, favorable conditions of increasing low-level energy are being established under a cap of conditionally unstable (warm, dry) continental air. Furthermore, the potential lifting mechanism of an approaching trough off the coast of North Carolina is also evident. During the next 12 h, the low will develop in this area and move northeastward into the North Atlantic.

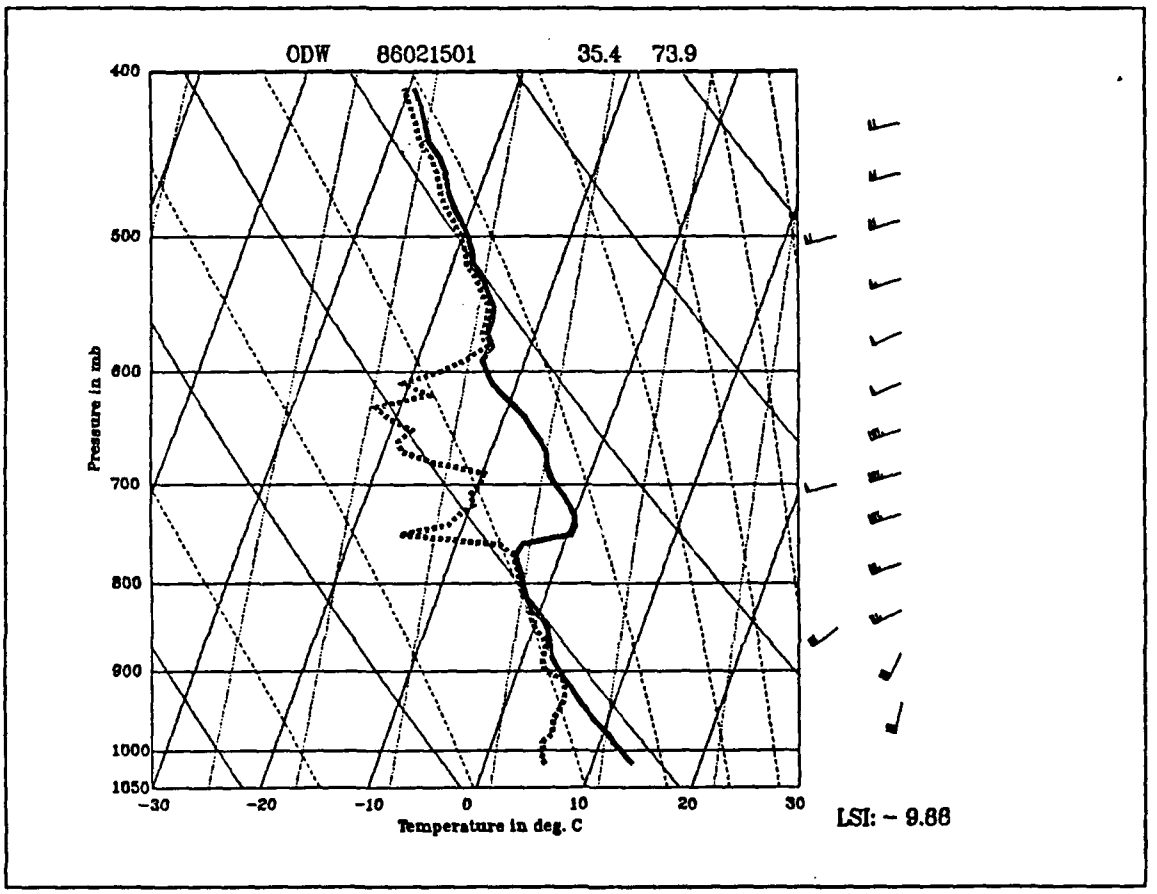

Fig. 9. Dropwindsonde ODW, 01 UTC 15 February 1986: As in Fig. 5.

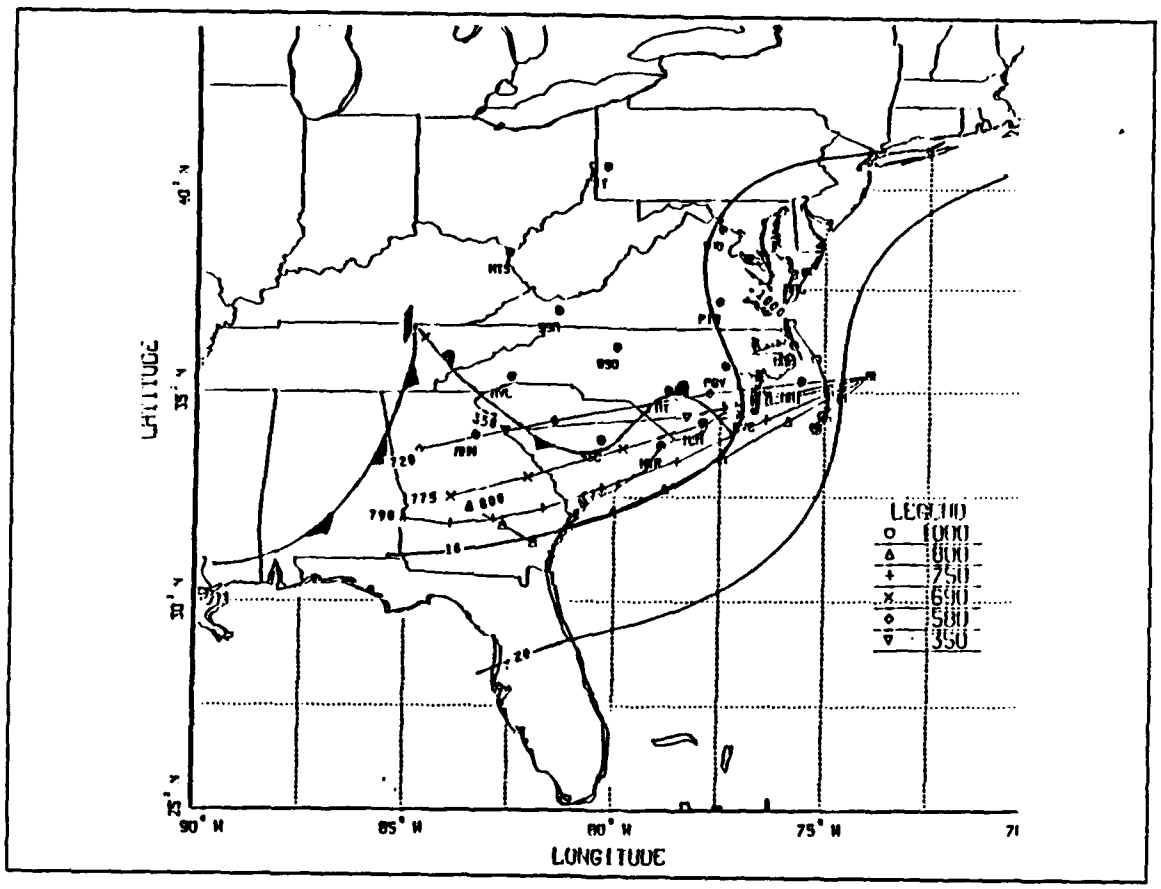

Fig. 10. Trajectories, 00 UTC 15 February 1986: As in Fig. 6, for the sounding in Fig. 9.

C. CYCLOGENESIS (12 UTC 15 FEBRUARY 1986)

1. Synoptic discussion

The intermediate NMC analysis at 06 UTC (not shown) reflects the beginning of a Miller (1946) type B cyclogenesis off the coast of North Carolina with a central pressure of 1010 mb. In the 12 UTC analysis (Fig. 11), the storm center has moved several hundred miles east-northeast. No distinct closed center has been analyzed within the broad area enclosed by the 1008 isobar. Two relative minima at 1005 and 1004 mb are potential centers. A cold front extends from the southern minimum southeastward across northern Florida and into the Gulf of Mexico.

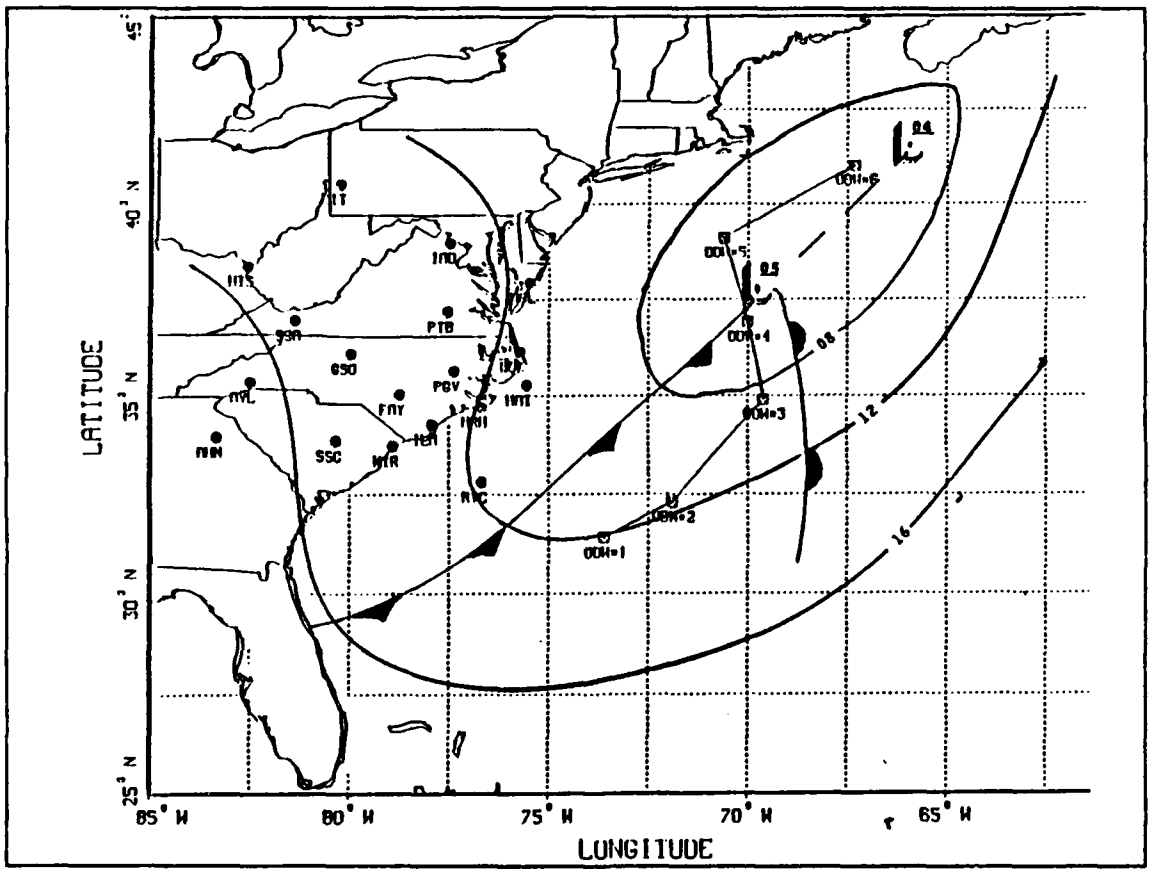

Fig. 11. Synoptic weather pattern, 12 UTC 15 February 1986: As in Fig. 3.

As the upper-layer trough (not shown) moves eastward, an embedded short wave is approaching the trough axis. A large 500 mb vorticity maximum of $18 \times 10^{-5} s^{-1}$ that is associated with this short wave (Fig. 12) is centered over coastal North Carolina. Positive Vorticity Advection (PVA) associated with this trough is now

superposed over the low-level center. This upper-level trough has not deepened during the past 12 h. Jet streak movement (not shown) has continued in a northeastward direction. The low-level center is now located under the left exit region of the PFJ. The combination of PVA associated with the short wave and jet streak divergence is believed to provide the mechanism for rapidly lifting the surface air from under the capping inversion. Satellite imagery (not shown) indicates suppressed convection south of 33° to 35°*N* with higher convective activity north. The southern boundary of the convection moves farther south (later imagery not shown) as the lid appears to be overcome. The potentially large latent heat release from lifting of the moist surface layer appears to contribute to rapid deepening of the surface low.

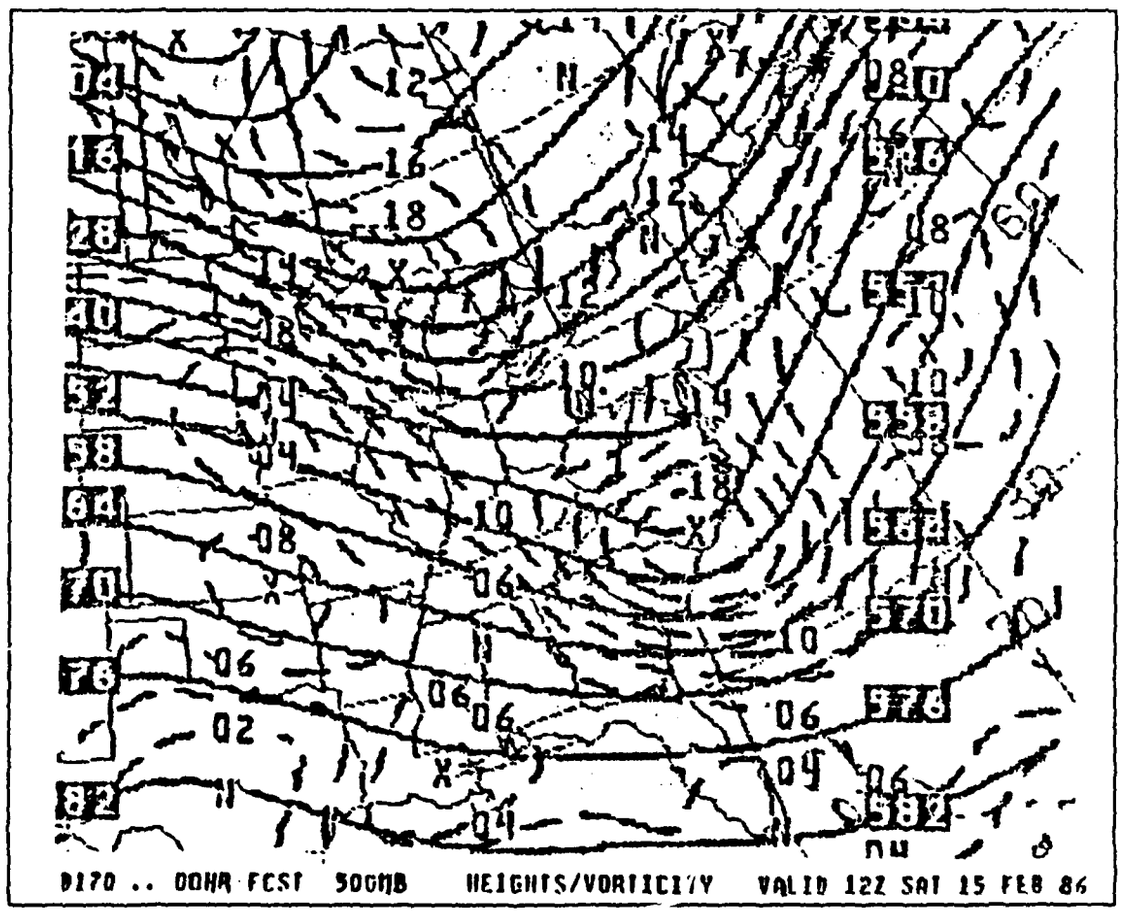

Fig. 12. 500 mb heights/vorticity, 12 UTC 15 February 1986: NMC 500 mb height (solid, values in decameters) and vorticity (dashed, values times $10^{-5}s^{-1}$) from the Nested Grid Model (NGM) analysis.

2. Cross-section

The system structure along the north-south axis of the storm is illustrated in Fig. 13. This cross-section is comprised of four Air Weather Service (AWS) dropwindsondes in the warm sector and two AWS dropwindsondes north of the storm (see locations in Fig. 11). An almost homogeneous layer exists below 800 mb in the warm sector. This air is slowly moving upward along the isentropes in the area south of the low (between soundings no.4 and no. 5). This pattern is consistent with the establishment of the warm conveyor belt (Carlson, 1980) that supplies moisture to the developing low. A weak inversion appears to be present above the marine layer that is deepening as the air moves north. This lid keeps the air close to the surface of the ocean. A layer of weakly stable air between 750 and 650 mb also is increasing in height from the southern station to 600 and 500 mb at the storm location (station no. 5). The upward sloping isentropes north of sounding no. 4 in the cross-section indicates the upward motion of the air that is expected above a developing center. The frontal system is located between soundings no. 4 and no. 5. Although the graphics routine indicates equal spacing between these two stations, the actual spacing is probably much tighter than shown. Moist air travelling along the warm conveyor belt is capped by the lid inversion until it encounters the frontal boundary. As indicated previously, upper-level support is available for rapid lifting of the air in this region.

3. Dropwindsondes

The sounding (Fig. 14a) at 34.9°*N*, 69.6°*W* at 09 UTC 15 February is located about 120 n mi due south of the analyzed storm position. In the lower levels (below 730 mb) of the sounding, the air is at or near saturation. The top of this layer increased from 780 mb 12 h previously and 850 mb 24 h previously. Meanwhile, the lid has weakened as the Lid Strength Index has decreased from -20 to -25 K values 24 h ago, to -10 to -15 K values 12 h previously, to -5 to 0 K at this time. In the dry conditionally unstable layer from 730 to 600 mb, the lapse rate is nearly dry adiabatic. Another layer of moist air exists from 600 mb to the upper limit of the sounding. Winds throughout the sounding are consistently from the southwest with speeds increasing to nearly 70 kt (35 $m \cdot s^{-1}$) at 500 mb.

The adjacent dropwindsonde (Fig. 14b) at 34.9°*N*, 70.0°*W* on 10 UTC 15 February 86 is located in the immediate vicinity of the developing low. This sounding presents quite a contrast to the sounding in Fig. 14a. The air is saturated throughout the sounding and no lid is present. Note also that the lapse rate above 800 mb is moist neutral. Another significant factor is that the winds are from the same direction with

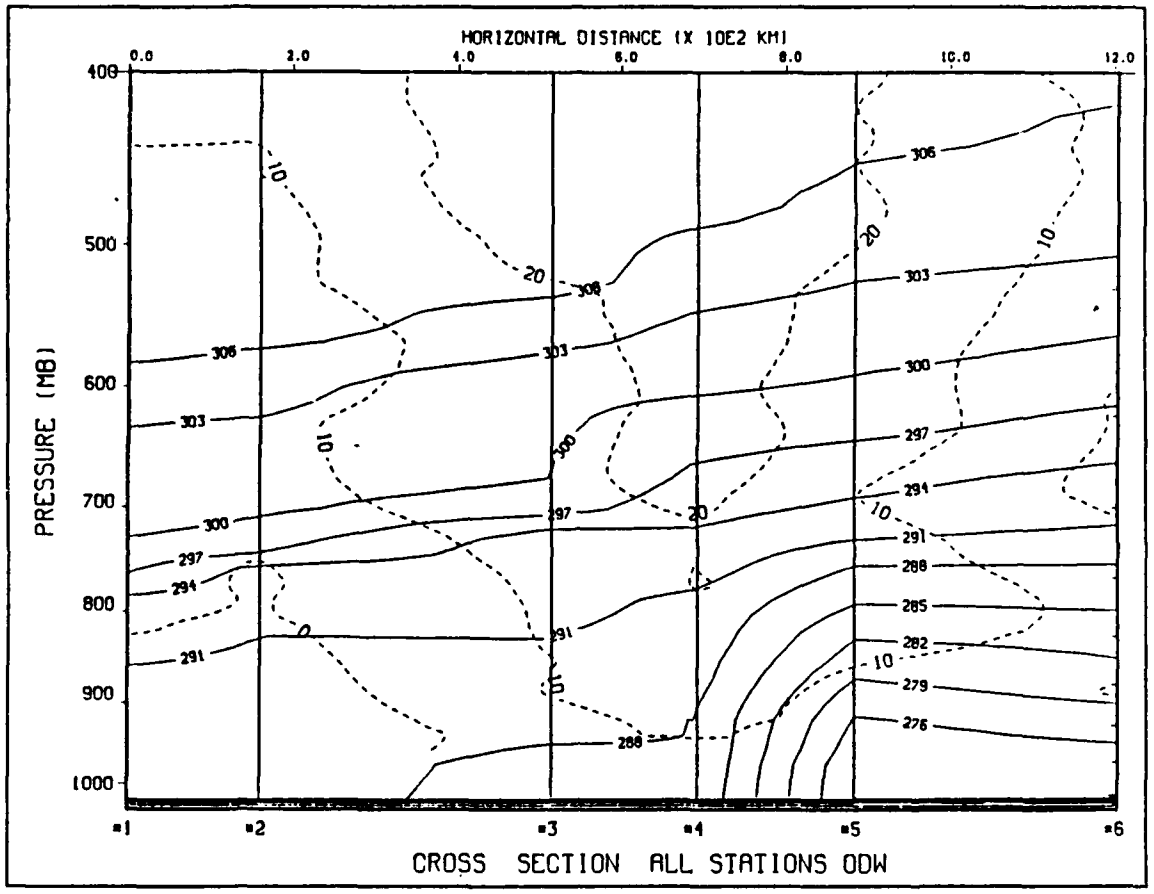

Fig. 13. Cross-section, 12 UTC 15 February 1986: As in Fig. 4.

only a slight increase in speed of 5 to 10 $m \cdot s^{-1}$ in the lower levels. This provides indications that the air parcels from the south in the warm conveyor belt have been modified to such an extent that the lid has been overcome.

4. Trajectories

All of the mid-level and upper-level trajectories (Fig. 15) reflect the southwesterly winds of the sounding. The early portions of the near-surface trajectories reflect the passage of the anticyclone 12 to 24 h previously. Dry continental air near 650 mb has moved from the southern U.S. with very slow ascent during the past 24 h. This air has provided the lid that restricted the release of instability in lower levels prior to storm formation.

A set of trajectories (not shown) terminating at the storm location shows that this air has been flowing parallel to the cold front. This ascending air is consistent with

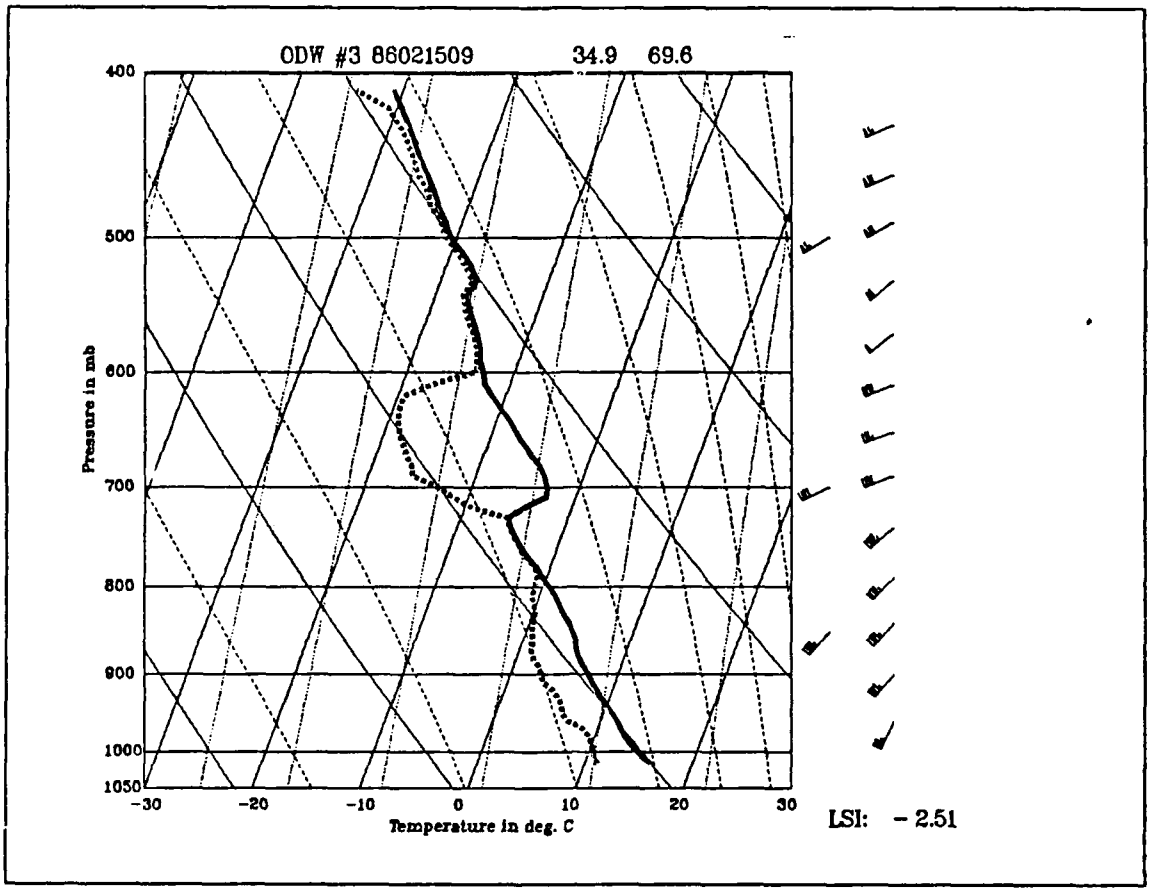

Fig. 14a. Dropwindsonde ODW #3, 09 UTC 15 February 1986: As in Fig. 5.

the establishment of the warm conveyor belt (Carlson, 1980) described in the cross-section (Fig. 13).

5. Summary

Several favorable circumstances have been established for storm intensification. A source of low-level moisture is available via the warm conveyor belt that has developed over the past 12 h. Overlying this surface air is a layer of dry continental air that serves as a lid until the storm center is approached. Divergence associated with upper-level PVA and the PFJ is in place by 12 UTC 15 Feb 86. This provides the lifting mechanism of sufficient strength to pull the surface moisture through (or from under) the lid. Large release of latent heat would then contribute to the explosive development of the low. The subsidence in the region at 12 UTC 14 February (Fig. 4) was slowly replaced by lid conditions with reduced static stability in the cyclogenetic area over the

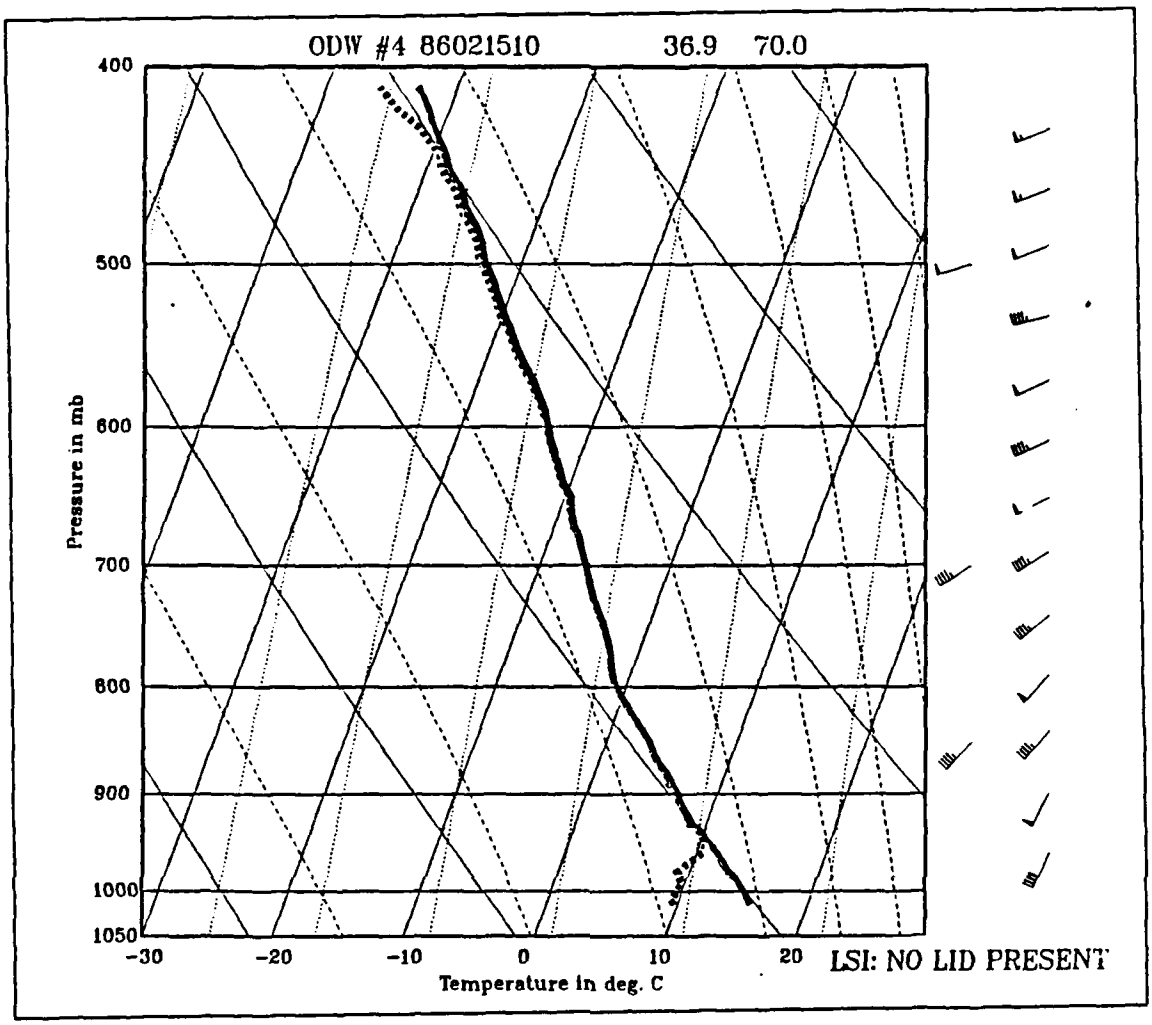

Fig. 14b. Dropwindsonde ODW #4, 10 UTC 15 February 1986: As in Fig. 5.

next 12 h (Fig. 8a and b). Proper superposition of these various components thus changes a suppressed convection situation of only a few hours previously to a convective regime along the warm front to the east of the low center. After cyclogenesis, the isentropes of Fig. 13 reflect the vertical motion of the convective regime.

D. DISCUSSION

1. Synopsis

At the initial times, cold and dry continental air near the surface moves southeastward ahead of a high pressure system located near Cape Hatteras, North Carolina. From the trajectories (Figs. 6, 10 and 15) this surface air mass remains over

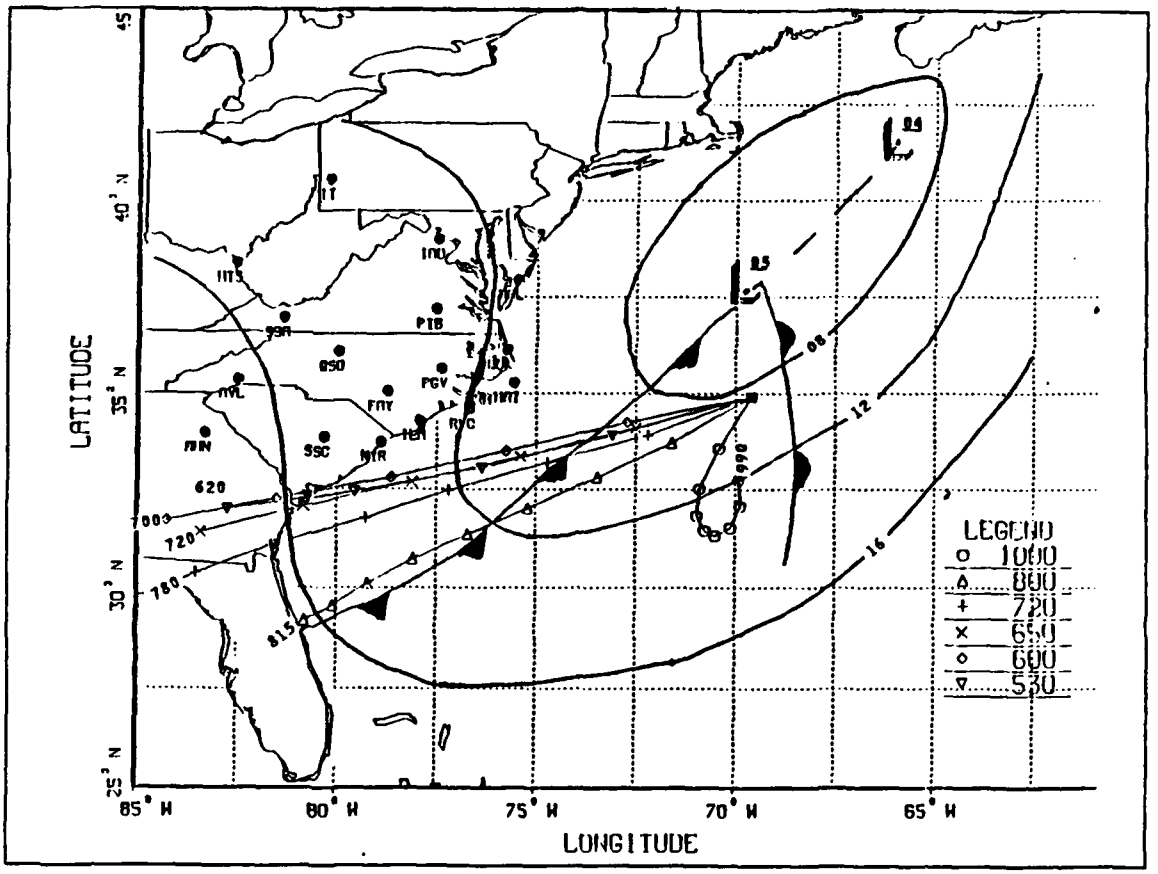

Fig. 15. Trajectories, 12 UTC 15 February 1986: As in Fig. 6 for the sounding in Fig. 14a.

the ocean as it passes in an anticyclonic path into the storm formation region. After crossing the coastline about 00 UTC 14 February, the continental air is modified in the oceanic environment until it enters the developing storm. Concurrently, warm and dry continental air from the southern U.S. is transported in the lower troposphere by a low-level jet. This warm, dry air constitutes the capping inversion (or lid) that very effectively prevents the cold surface air from developing into deep convection as it is warmed at the air-ocean interface. Although the air parcels in the marine layer are sufficiently moistened and warmed by the surface fluxes to become positively buoyant, the parcels only rise until the base of the lid is reached. The lid, which is very strong early in the process (LSI of -26.1 K for the sounding shown in Fig. 5), confines the air to near the surface and results in the absence of free convection above the lid. Over the next 24 h, the lid progressively weakens and slowly increases in height as air from below is

mixed into the lower layers of the dry continental air mass. The upper-level lifting mechanisms discussed earlier then pulls the air from below the lid and triggers free convection over a deep layer, which contributes to the cyclogenesis.

The weakening trend of the lid with time or in space in a northeast direction, along the warm conveyor belt is shown in Table 1. Lower values (-8.9 and -9.9 K) of lid strength are found in the dropwindsondes near 36°*N*, 74°*W*, which is in the vicinity of impending cyclogenesis. Decreasing Lid Strength Index values with time at a single station can be seen from the Research Vessel Cape Hatteras (RVC) soundings in Table 1. Notice that the RVC sounding has no lid at the cyclogenesis time of 06 UTC 15 February. With the northeastward storm motion, the lid is restored by the flow of dry continental air behind the low. The effects of the lid on low-level temprerature (Fig. 16) is to increase the temperature in the air mass trapped under the inversion and increase total moisture.

After the establishment of the warm conveyor (discussed earlier), the dry continental air provides the cap above the surface layer. This warm conveyor belt is depicted well in Fig. 13. As this air is moved northward and warmed, it erodes the lower sections of the lid. However, the lid allows the warm conveyor belt to transport more energy into the center of the low, instead of releasing the energy prior to approaching the low center. Notice from Table 1 that no lid is found near and north of the low. With the lid acting to increase the latent heat accumulation in the lower layers along the warm conveyor, and the strong lifting necessary to overcome the lid, this potentially large release of latent heat may provide the necessary vigor for explosive growth of the storm. Although the explosive growth phase occurred outside the GALE data network, it appears from the available soundings that the necessary conditions leading to explosive growth were very effectively provided.

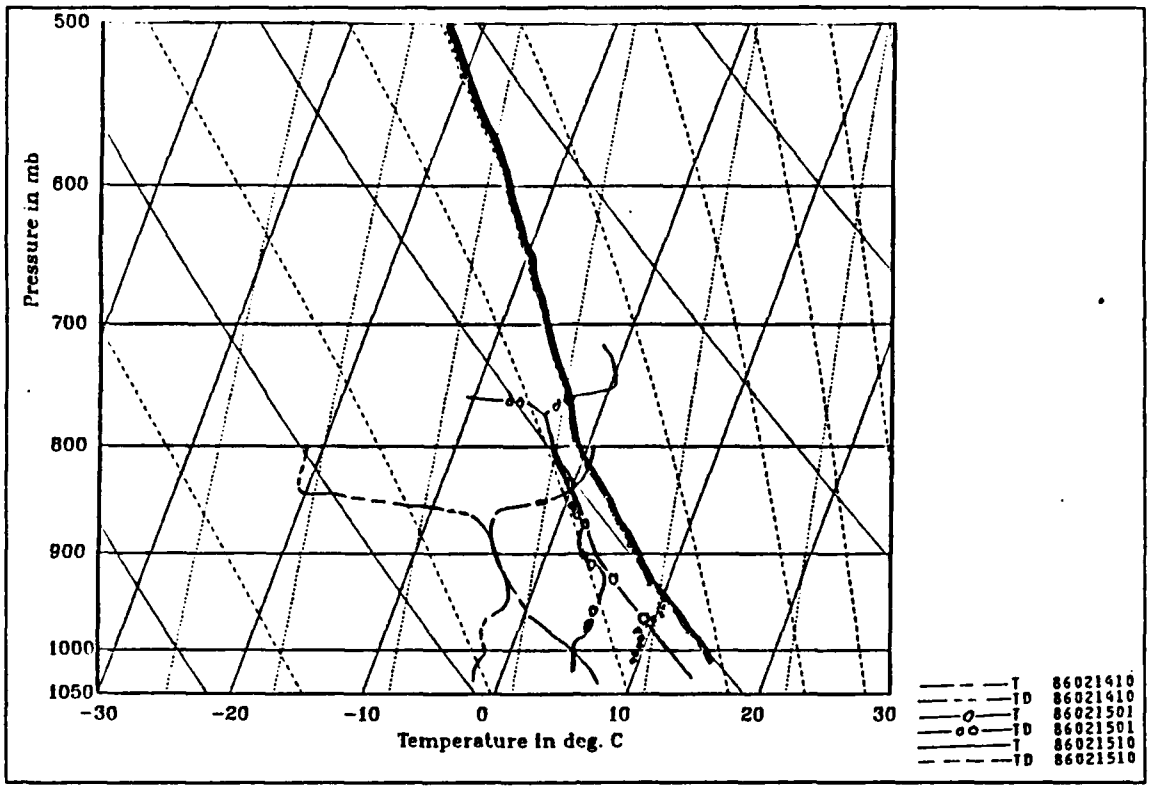

Fig. 16. Air mass modifications: Comparison of three maritime soundings near 35 °N, 72.5 °W. Times of soundings are indicated in the legend.

2. Forecast analysis

The 36 h forecasts from the Navy Operational Global Atmospheric Prediction System (NOGAPS), the NMC Nested Grid Model (NGM) and the NMC man-machine forecast all underestimated the storm intensity and growth. The NOGAPS sea-level pressure error analysis (Fig. 17) for 12 UTC 15 February indicates an underforecast of the intensity of the storm by eight mb. By this time, the warm conveyor belt is established and this surface air is being held down by the lid. Over the next 12 h, the storm grows explosively and the 00 UTC 16 February error analysis (Fig. 18) has errors as high as 12 mb. The subsequent 12 UTC error analysis (not shown) has less error, with only an area of eight mb errors south of the storm location. Although other explanations are possible, it is hypothesized that these errors during the explosive growth reflect the inability of the model to resolve the suppression of the convection when the lid is present, and the vigor of the latent heat release when the lid is removed.

Table 1. LID STRENGTH INDEX (IOP 6): Over ocean Lid Strength Index values for 14-15 February. Note the LSI values in the region of cyclogenesis near 34°N, 75°W at 06 UTC 15 February. Soundings from the cross-section in Fig. 13 are numbered 1 through 6 for convenience.

Station	Time YYMMDDHH	Lat ° N	Long ° W	LSI (K)	Lid Height mb
Temporal Variations for LSI values in precyclogenetic environment.					
ODW	86021410	33.30	76.40	-26.1	760
ODW	86021410	32.40	75.30	-23.9	810
ODW	86021500	36.00	74.00	-8.9	730
ODW	86021501	35.40	73.90	-9.9	750
ODW	86021501	33.70	72.80	-17.34	690
ODW	86021501	32.30	76.50	-0.9	740
ODW	86021501	32.20	75.70	-7.0	760
Spatial variation of LSI along frontal system in cross-section.					
ODW #1	86021509	31.40	73.60	-2.5	790
ODW #2	86021509	32.30	71.90	-1.1	760
ODW #3	86021509	34.90	69.60	-2.5	720
ODW #4	86021510	36.90	70.00	no lid	n/a
ODW #5	86021510	39.10	70.60	no lid	n/a
ODW #6	86021512	31.00	67.30	no lid	n/a
Temporal variation of LSI at R.V. Cape Hatteras					
RVC	86021401	34.57	76.68	-33.0	860
RVC	86021410	33.75	76.67	-31.6	900
RVC	86021413	33.75	76.67	-26.8	900
RVC	86021418	33.75	76.67	-23.7	860
RVC	86021500	33.95	76.93	-8.9	790
RVC	86021503	34.00	77.00	-2.4	820
RVC	86021506	34.13	77.22	no lid	n/a
RVC	86021509	34.13	77.22	-6.4	660
RVC	86021512	34.18	77.20	-9.9	730

The two products from NMC also did not properly forecast the storm growth. During the explosively deepening phase, the errors are four mb at 12 UTC 15 February, six mb at 00 UTC 16 February and eight mb at 12 UTC 16 February for the man-machine product. The NGM failed to indicate cyclogenesis at 12 UTC 15 February and

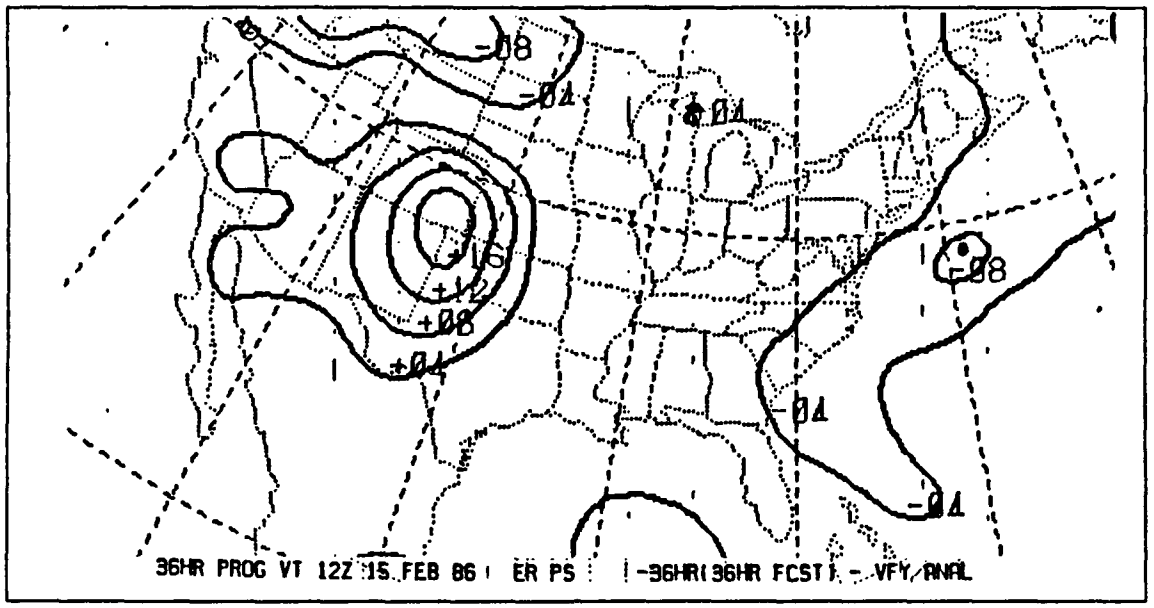

Fig. 17. Forecast errors, 12 UTC 15 February 1986: Forecast sea-level pressure minus verifying pressure (mb) after 36 h for NOGAPS model. Negative (positive) numbers indicate surface pressures verified as lower (higher) than forecast. Storm location at 12 UTC 15 February marked by "• ".

underforecast the 00 UTC 16 February storm central pressure by nearly eight mb. Potentially, these errors could be due to the failure of the model to properly incorporate the effects of latent heat release. Although the NGM forecast the positive vorticity advection and the jet streak divergence, the predicted deepening of the storm was at a nonexplosive rate of less than 20 mb in 24 hours.

Earlier in the storm development, the models had smaller forecast errors. Once the warm conveyor belt is established with the lid holding down the near-surface air until it reaches the vicinity of the storm, extra vigor is available to aid storm growth. It will be shown in the next section that the numerical forecasts more accurately predict storm growth when no lid is present and without the presence of a mid-level jet transporting dry air into the storm region.

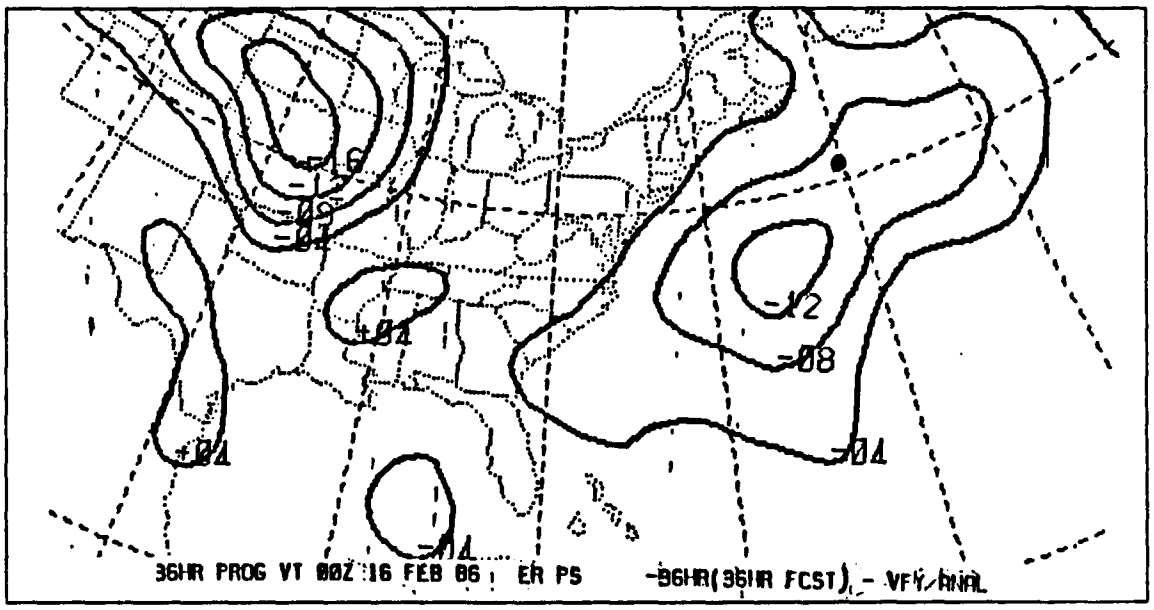

Fig. 18. Forecast errors, 00 UTC 16 February 1986: As Fig. 17.

IV. NONEXPLOSIVE CYCLOGENESIS CASE

The weather pattern early in this period is dominated by cold advection into the eastern half of the U.S. This cold outbreak occurred behind a storm that passed up the east coast of the U.S. on 27-28 February 1986. A very large upper-level trough at 00 UTC 1 March 1986 extends from the low in the Baffin Bay through the central U.S. and into the Gulf of Mexico. This trough deepens over the next 36 h and short waves passing through the trough increasing the PVA ahead of the trough by 12 UTC 1 March 1986. In combination with jet streak divergence aloft, these conditions support the cyclogenesis that occurs well offshore of North Carolina.

Several key differences occur in this storm development period relative to the explosive cyclogenesis event discussed earlier. It will be shown that one major difference is that the middle tropospheric flow is nearly meridional with a long over-ocean component rather than the zonal off-continent flow in the earlier storm. Although cyclogenesis occurs in the same general area, this storm is a Miller (1946) type A cyclogenesis, rather than type B. It will be shown that this storm does not have the lid structure that apparently contributed to explosive growth in the previous case.

A. INITIAL PERIOD (00 UTC 01 MARCH 1986)

1. Synoptic discussion

The surface synoptic conditions during this initial period are dominated by a wide area of nearly constant pressure. As shown in Fig. 19, a 1010 mb low is analyzed within the 1012 mb isobar. A minor surface trough lies across the Florida Panhandle through Georgia and across the coast of South Carolina. Cold air is being advected into the southeast coastal region in the wake of an offshore low pressure center. The upper levels are dominated by the deep trough over the central U.S. (Fig. 20). A jet streak with winds near 100 kt (50 $m \cdot s^{-1}$) is just to the west of the coastal trough at the surface. Notice that mid-level air leaving the continent first passes over the Gulf of Mexico and the Caribbean Sea before moving into the cyclogenetic region. It will be shown that this lengthy trajectory over water prevents any potential lid formation.

2. Cross section

As no dropwindsondes were reported for this time period, no acceptable cross-sections could be developed.

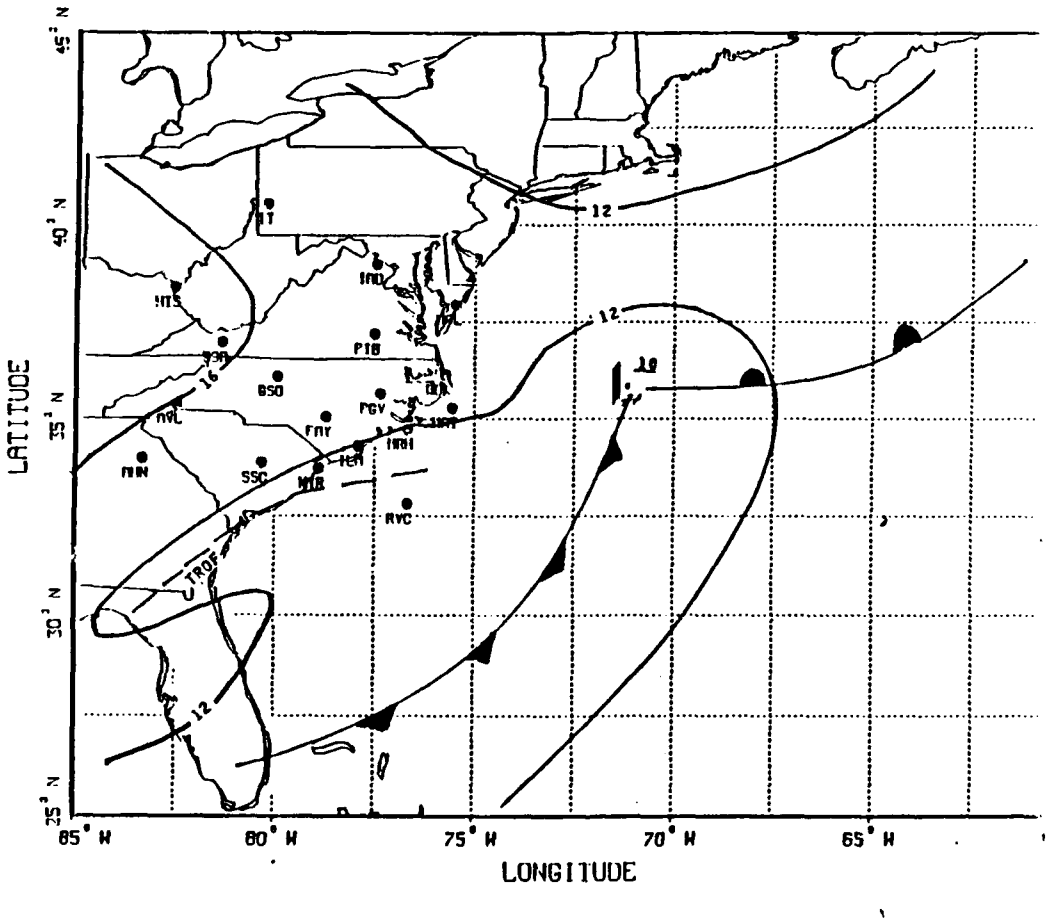

Fig. 19. Synoptic weather pattern, 00 UTC 1 March 1986: As in Fig. 3.

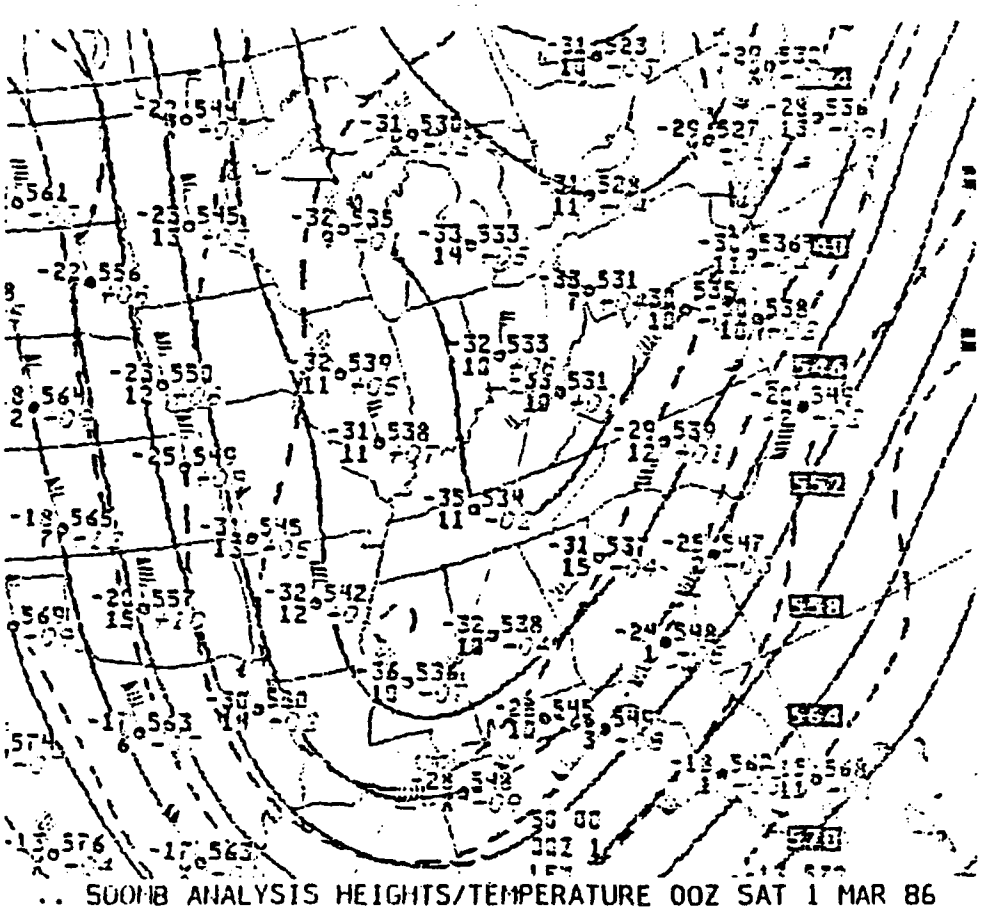

Fig. 20. 500 mb heights/temperature, 00 UTC 1 March 1986: NMC 500 mb heights (solid, values in decameters) and temperatures (dashed, values in ° C) from the Limited Fine Mesh (LFM) analysis.

3. Soundings

Satellite imagery (not shown) suggest considerable moisture in a deep layer is available west of the front analyzed in Fig. 19, although dry air is indicated east of the front. Soundings from RVC (Fig. 21a) and Kindley Air Force Base (XKF), Bermuda (Fig. 21b) effectively illustrate the moisture differences. The RVC sounding has moisture throughout the column, except for a shallow dry layer at 700 mb. Conversely, the XKF sounding has decreasing moisture from the surface to 900 mb, and the air is exceptionally dry above 900 mb. The LSI at XKF is only -0.74 K because the very warm surface temperatures (greater than 20°C) minimize the inversion strength term and the result is effectively no lid. There is also no lid present at RVC. The trajectory analysis is necessary to indicate which type of air is being advected into the region of potential cyclogenesis.

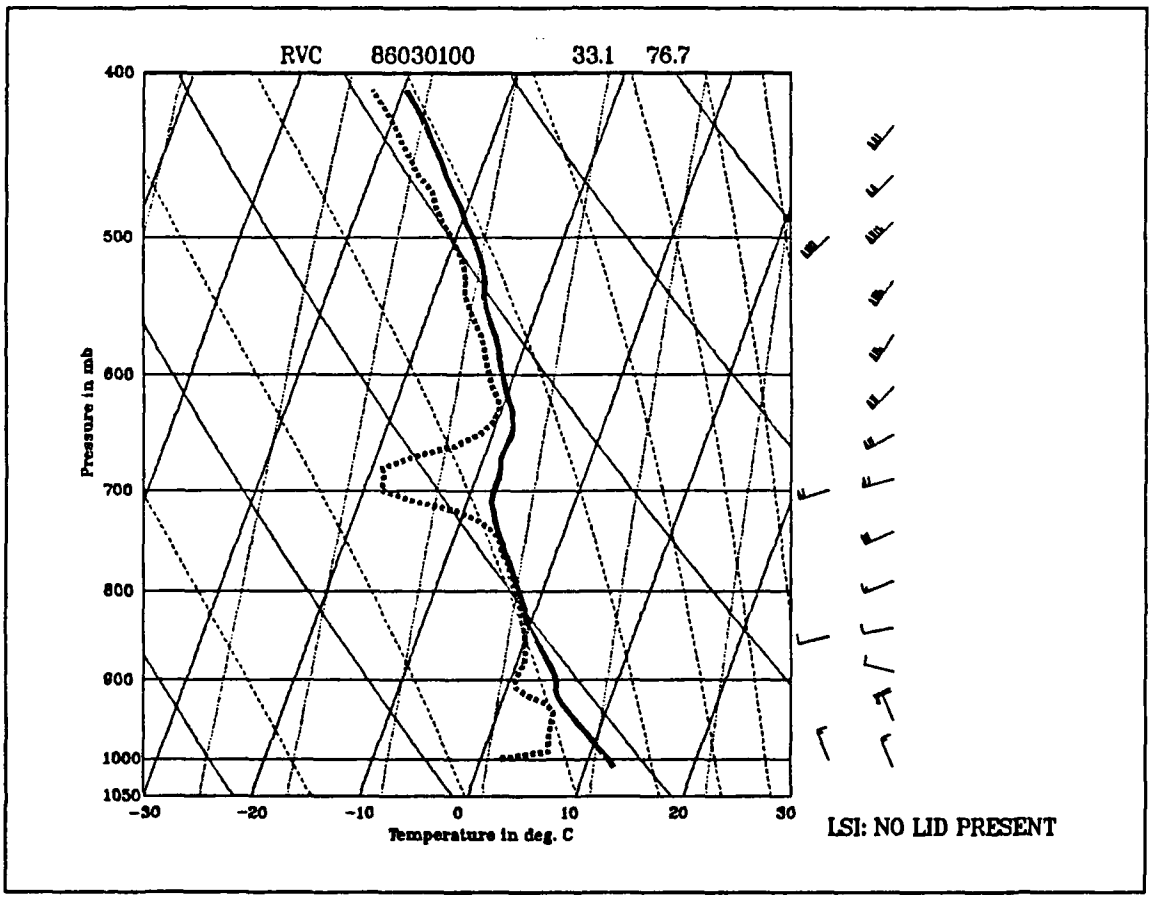

Fig. 21a. Rawinsonde RVC, 00 UTC 1 March 1986: As in Fig. 5.

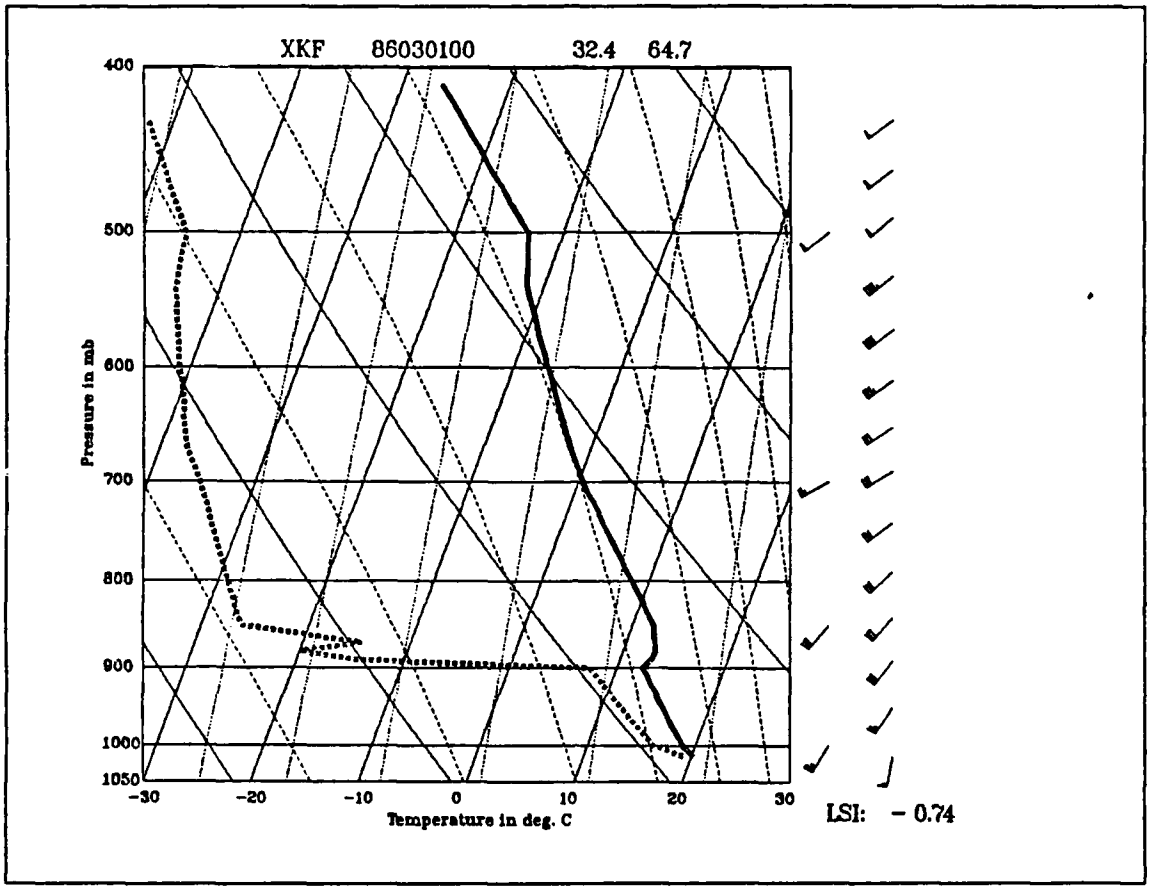

Fig. 21b. Rawinsonde XKF, 00 UTC 1 March 1986: As in Fig. 5.

4. Trajectories

Since no marine dropwindsondes are available in this period, the trajectories are shown (Fig. 22) for -24 h to -12 h positions of a trajectory terminating at 34.6°*N*, 69.2°*W* on 12 UTC 01 March. The trajectories demonstrate an important difference from the explosive cyclogenesis case discussed above. Instead of zonal flow from the continent, these trajectories have left the continent far to the west and approach the cyclogenensis area with a pronounced northward component. One exception is that of the surface trajectory, which has only small displacements from the southwest and the south. The upper-level trajectories reflect the northward motion to the east of the deep upper-level trough (Fig. 20).

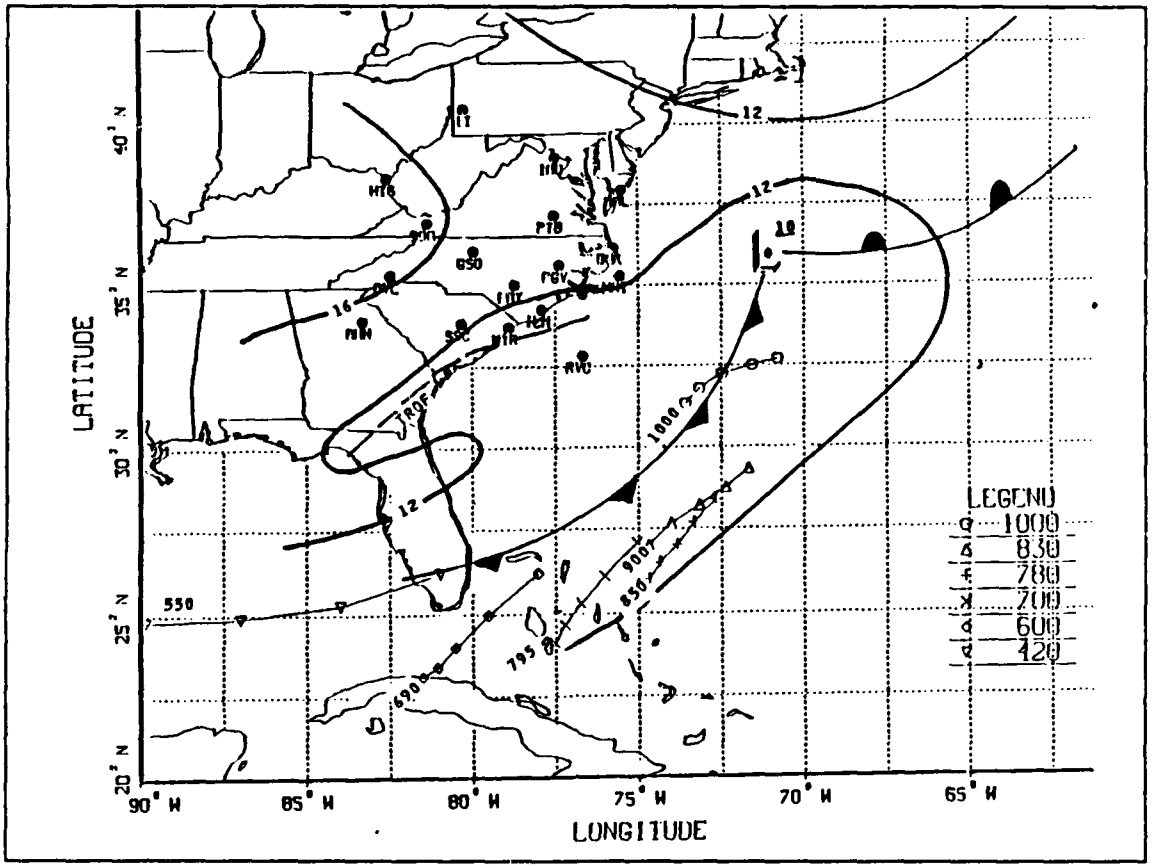

Fig. 22. Trajectories, 00 UTC 1 March 1986: As in Fig. 6 for the -24 to -12 h position of trajectories ending at 34.6°*N*, 69.2°*W* on 12 UTC 1 March 1986 (see sounding in Fig. 27).

5. Summary

During this period, a deep upper-level trough is the dominant feature of the air flow along the eastern seaboard. As a result, the air flow has a greater meridional component than in the explosive growth example. A weak region of frontal activity extends across the precyclogenetic region. A Miller (1946) type A cyclogenesis will occur along the front in about 18 h. A large moisture contrast exists with moist air above the front to the west and dry air to the east. Cyclogenesis occurs in the moist region with the airflow from the southwest (shown in Fig. 22) advecting a deep layer of moist air into the region of the developing low.

B. PRECYCLOGENETIC PERIOD (12 UTC 1 MARCH 1986)

1. Synoptic discussion

The boundaries of the 1012 mb isobar have remained nearly the same during the last 12 h. The coastal surface trough of 12 h earlier is no longer present. Surface pressures have slowly decreased along the front during the past 12 h with a large area below 1008 mb (Fig. 23). Two low pressure centers of 1007 and 1005 mb have been analyzed along the frontal trough.

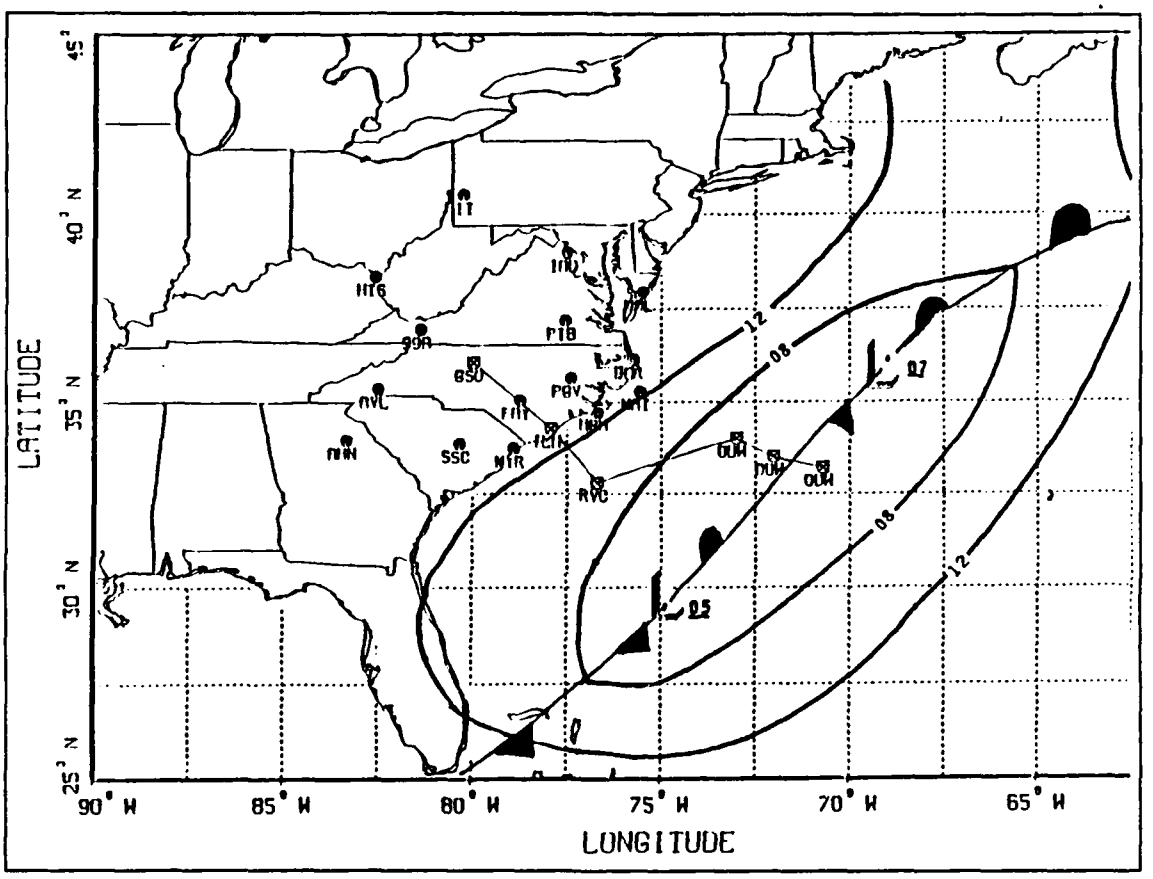

Fig. 23. Synoptic weather pattern, 12 UTC 1 March 1986: As in Fig. 3.

An interesting feature of this case is the snowfall in southern Georgia and northern Florida as an area of PVA crosses the coast and moves over the ocean (Fig. 24). The vorticity maximum of $22 \times 10^{-5} s^{-1}$ is higher than the previous IOP. The resulting vorticity advection that produced snowfall in Florida might be expected to produce a stronger cyclogenetic event over the western North Atlantic. A closed circulation is analyzed at 500 mb over Asheville (AVL), North Carolina. The axis of this cold

trough is now through central Georgia. The upper-level trough continues to deepen and move eastward as a short wave approaches the base of the trough. It is the increased PVA and upward vertical motion (not shown) that are contributing to the severe weather in coastal regions of Georgia.

A jet streak at 300 mb also is passing the bottom of the trough region (not shown). This jet streak will move through the trough and provide upper-level support for cyclogenesis offshore.

2. Cross-section

This cross-section is comprised of two continental rawinsondes (GSO and ILM), a rawinsonde (RVC) located just off the coast and three oceanic dropwindsondes along the line shown in Fig. 23. Sloping isentropes in the cross-section (Fig. 25) reflect the approaching trough with the higher isentropes in the western regions. In this cross-section, the coastal baroclinity probably has much tighter gradients than shown.

Near-surface winds at RVC and the ODW to the east are reported as light and variable (Appendix A). Consequently, the zero isotach has a quite complex pattern near the center of the cross-section. In the upper levels above ILM and RVC, a jet streak is present with wind speeds in excess of 100 kt (50 $m \cdot s^{-1}$). This jet streak is advancing northeastward ahead of the base of the trough. The winds over the ocean regions between the surface and 500 mb do not reflect any low-level westerly jet as in the explosive cyclogenesis case. Only over the most seaward ODW are the winds in the mid-levels over 20 kt (10 $m \cdot s^{-1}$) perpendicular to the cross-section. Another important feature is the absence of any appreciable inversion in the oceanic soundings. There is a large area between RVC and the adjacent oceanic dropwindsonde that is nearly homogeneous with potential temperatures between 288 K and 285 K below 800 mb. This large homogeneous area exists in the absence of the lid condition. Although dry air is present farther to the east (see XKF sounding in Fig. 21b), the large-scale environment in the cyclogenetic region is quite different from the explosive cyclogenesis case. All the oceanic soundings in this cross-section are nearly saturated below 500 mb. That is, a deep moist layer is present, rather than a moist layer trapped below a lid as in the previous case.

3. Dropwindsonde

The sounding (Fig. 26) at 34.6° N, 69.2° W taken at 10 UTC 1 March is located about 60 n mi south of the 1007 mb low. A shallow dry layer is located between 700 and 800 mb. This dry unstable air seems to be below an inversion, so a lid is present. Lid conditions do not exist toward the southwest in the vicinity of the cross-section (Fig. 25). This dry air possibly is the result of some mixing of the dry and moist air

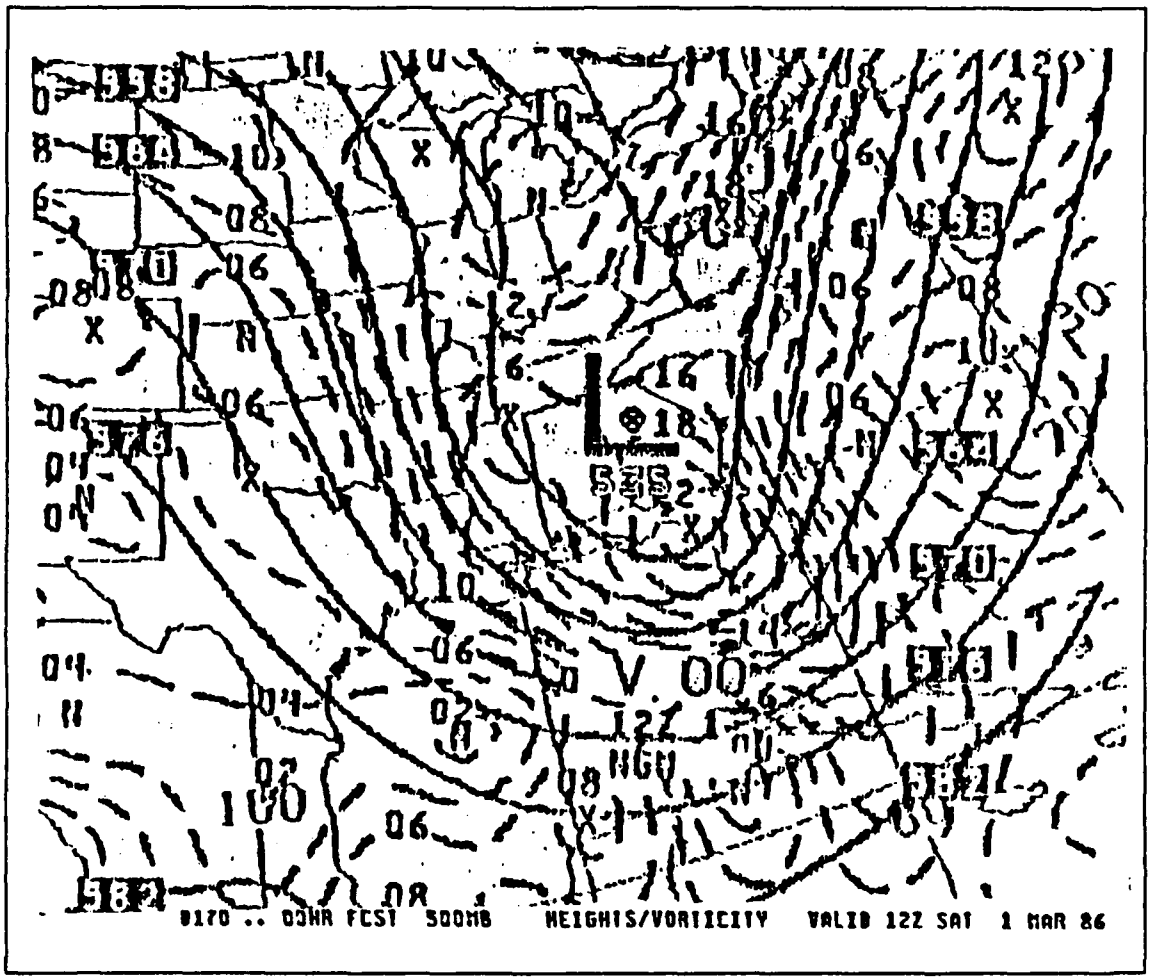

Fig. 24. 500 mb heights/vorticity, 12 UTC 1 March 1986: As in Fig. 12.

masses discussed earlier. The remainder of this sounding both above and below the dry layer is saturated. These moist layers are stable because the lapse rate is less steep than the moist pseudoadiabat. Winds throughout this sounding are from the southwest with little vertical wind shear between 900 mb and the top of the sounding (400 mb).

4. Trajectories

The trajectories discussed previously (Fig. 22) are advanced 12 h to the current time as shown in Fig. 27. Several concurrent processes are occurring that prevent lid conditions as the air parcels approach the sounding at 34.6°*N*, 69.2°*W* . The dry mid-level air from 700 to 800 mb (Fig. 26) has a source region south-southwest of the final destination, and these parcels are the most southerly in the trajectories. All of these

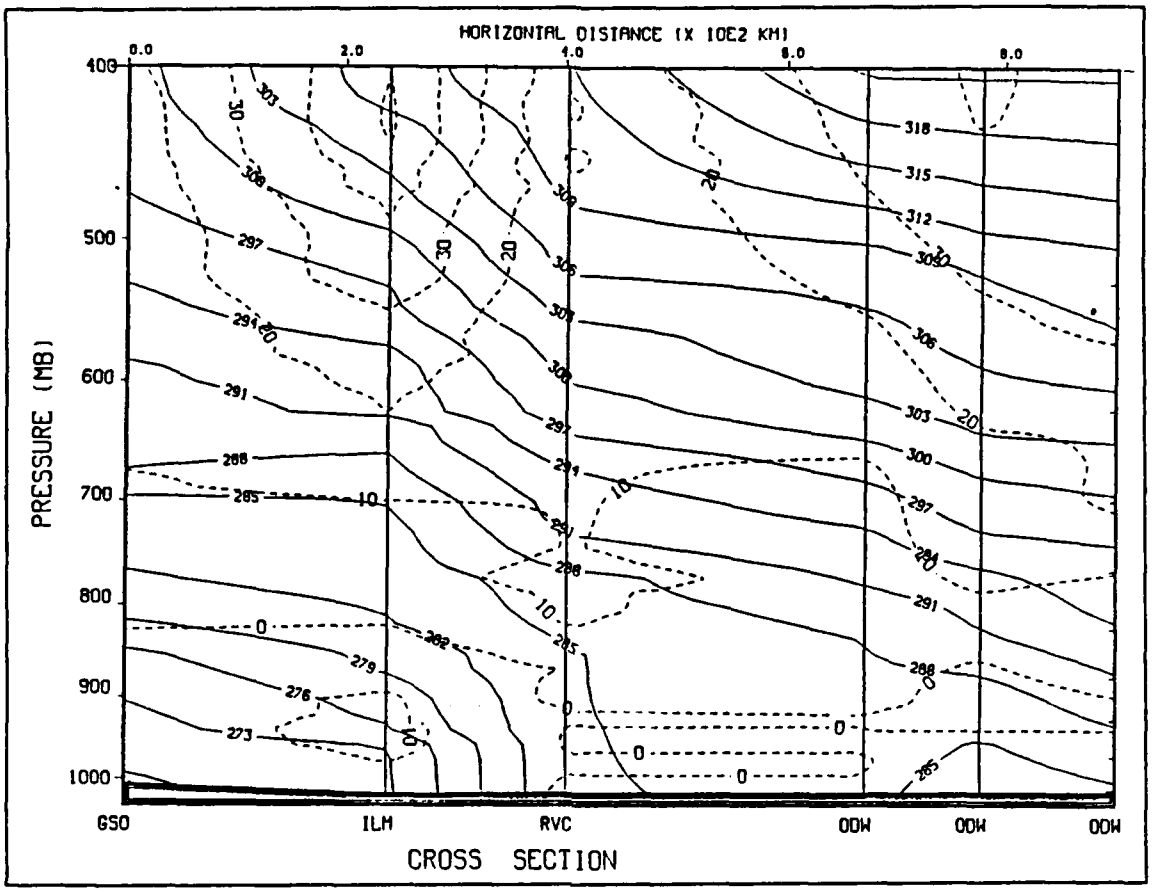

Fig. 25. Cross-section, 12 UTC 1 March 1986: As in Fig. 4.

trajectories have been over water for at least 24 h. Other trajectories in this nonexplosive cyclogenetic area (not shown) also have paths towards the northeast with a significant time period over the water. Any lid effects of dry continental air that would tend to suppress convection have been eroded by entrainment mixing and horizontal advection of moist air. In contrast, the explosive cyclogenesis case had a low-level westerly jet advecting warm, dry continental air into the region upstream of the cyclone center.

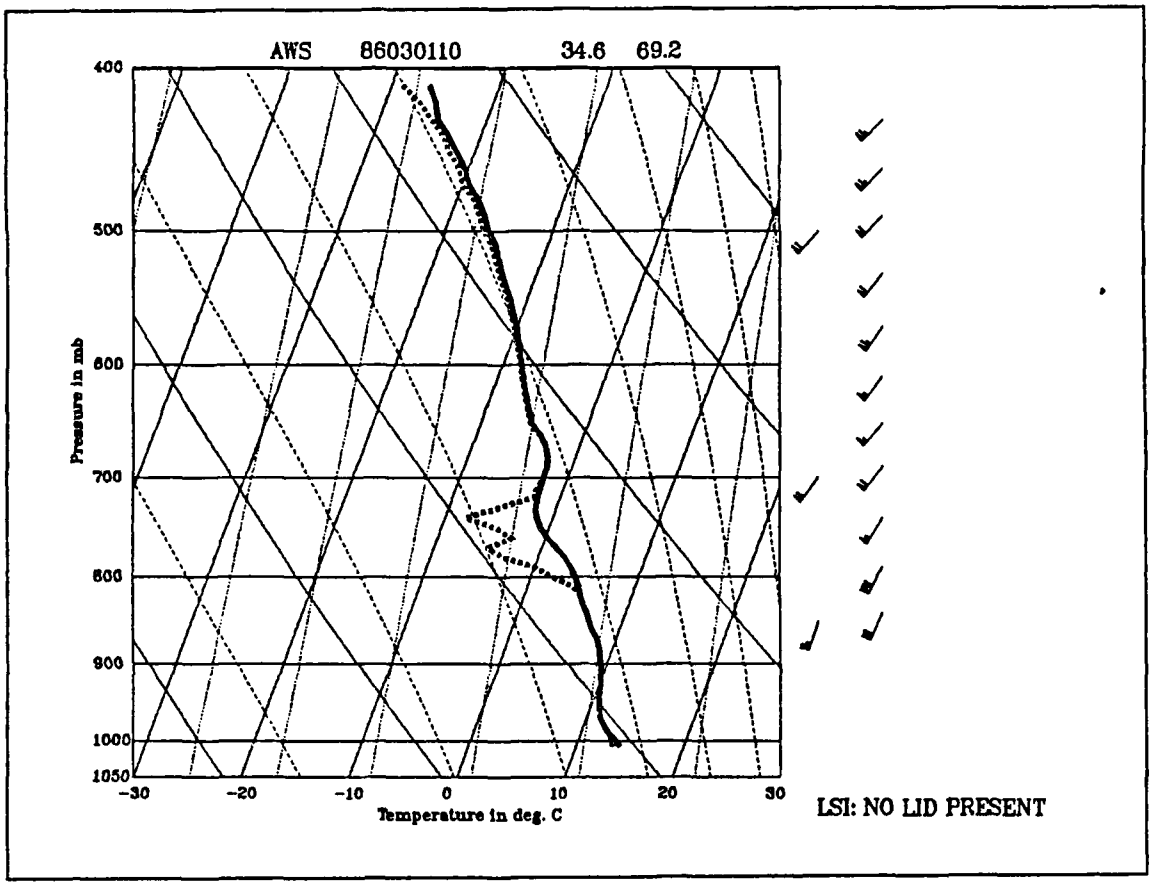

Fig. 26. **Dropwindsonde AWS, 10 UTC 1 March 1986:** As in Fig. 5.

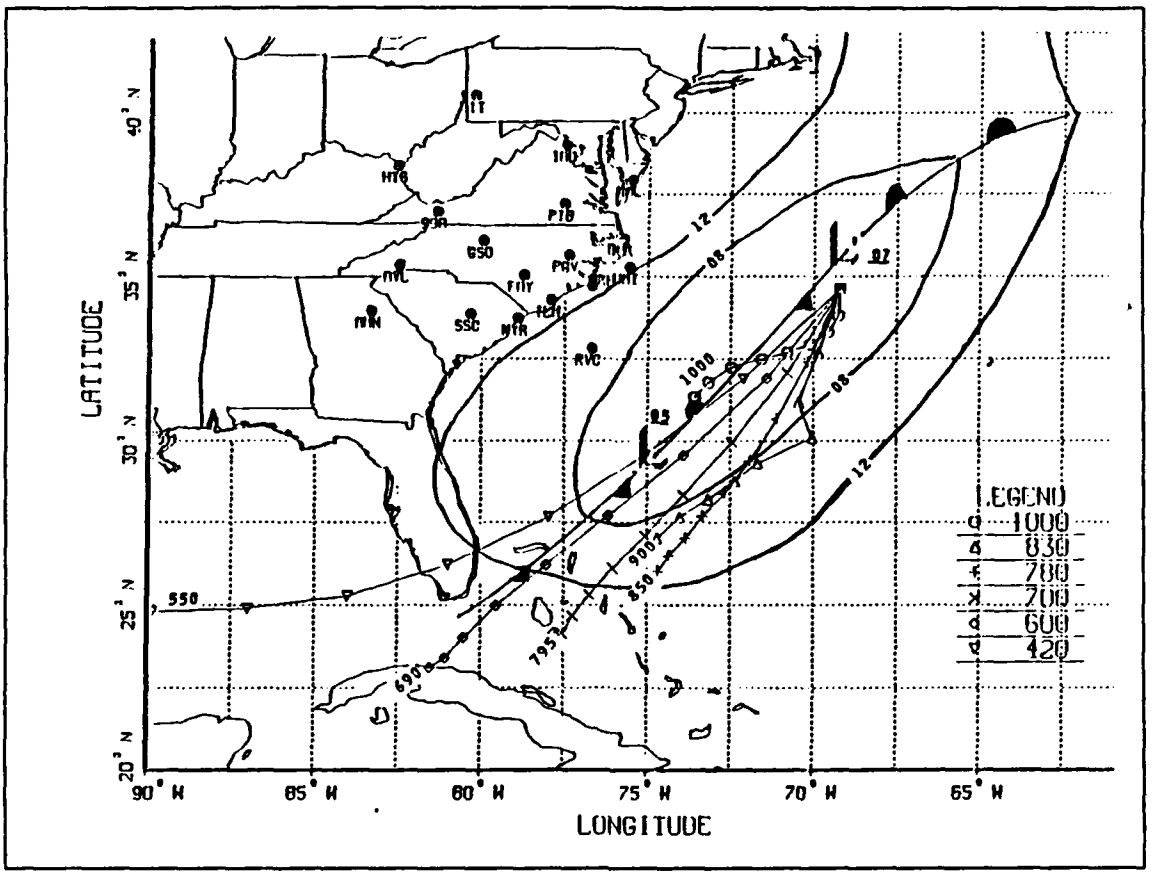

Fig. 27. **Trajectories, 12 UTC 1 March 1986:** As in Fig. 6 except that the trajectories of Fig. 22 are continued 12 h.

5. Summary

The precyclogenetic environment is dominated by the upper-level trough over the entire eastern half of the U.S. Dry continental air is advected over the Gulf of Mexico around the base of the trough. However, no capping inversion is present over the downstream cyclogenetic area after a long over-water trajectory. There is an absence of any lid except in the dry air mass that is well to the east of the formation region. Significant PVA associated with the upper-level trough and jet streak appears to be approaching the area of cyclogenesis. Although cyclogenesis occurs, the development is of a nonexplosive nature. In this case, there can not be a rapid release of latent heat in association with deep convection from below a capping inversion. Rather, the air in the cyclogenetic area appears to be moist neutral.

C. CYCLOGENESIS AND POST CYCLOGENESIS (00-12 UTC 2 MARCH 1986)

1. Synoptic discussion

The intermediate NMC analysis at 18 UTC (Fig. 28) has a Miller (1946) type A cyclogenesis at sea with a central pressure of 996 mb. During the next 6 h, the storm deepens only two mb while moving to 34° N, 69° W (Fig. 29). Cyclogenesis occurred far enough out to sea that the northerly winds behind the storm will bring cold advection near the surface over the east coast of the U.S.

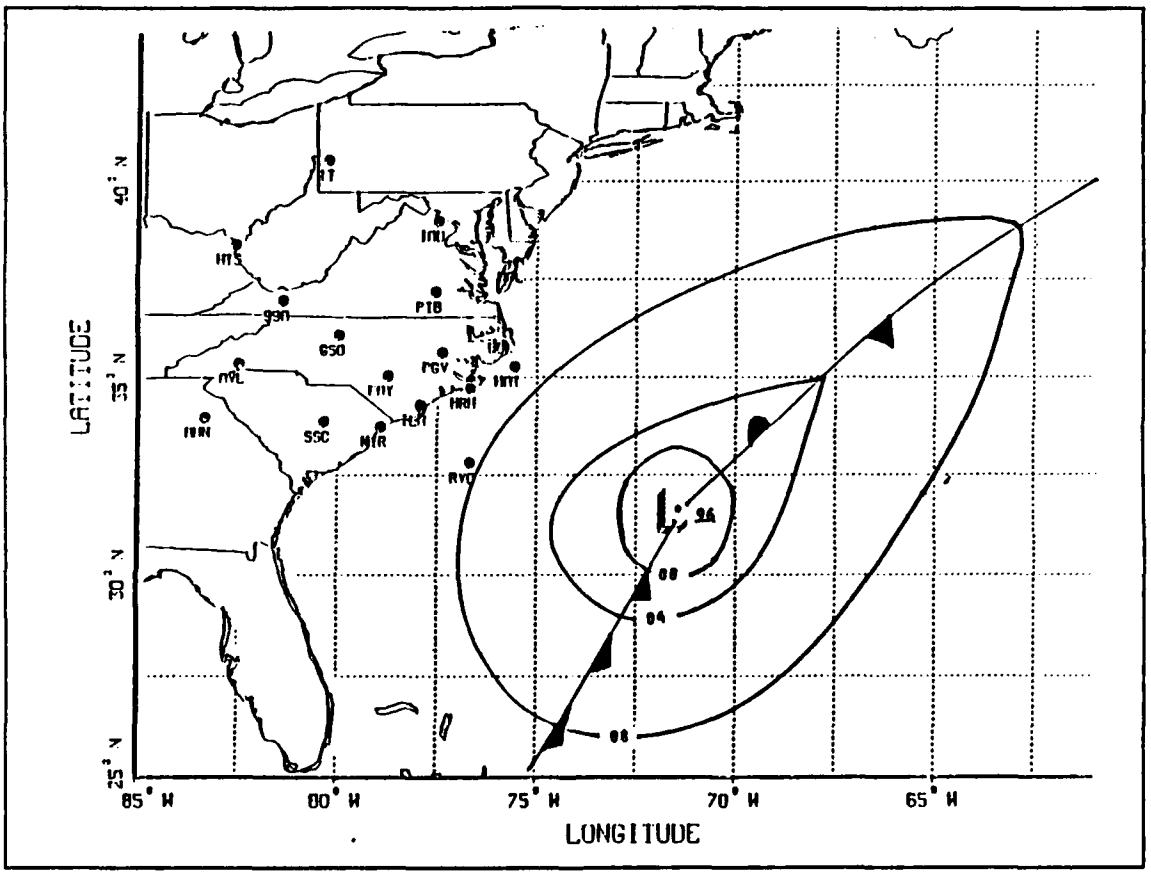

Fig. 28. Synoptic weather pattern, 18 UTC 1 March 1986: As in Fig. 3.

The upper-level trough has moved eastward. The 500 mb trough has crossed the coast near Myrtle Beach (MYR), South Carolina (Fig. 30). The 300 mb trough (not shown) is almost directly above that of 500 mb. The jet streak maximum (speeds of 150 kt or 75 $m \cdot s^{-1}$) has moved through the bottom of the trough with the entrance region over Florida and the exit region off the North Carolina coast.

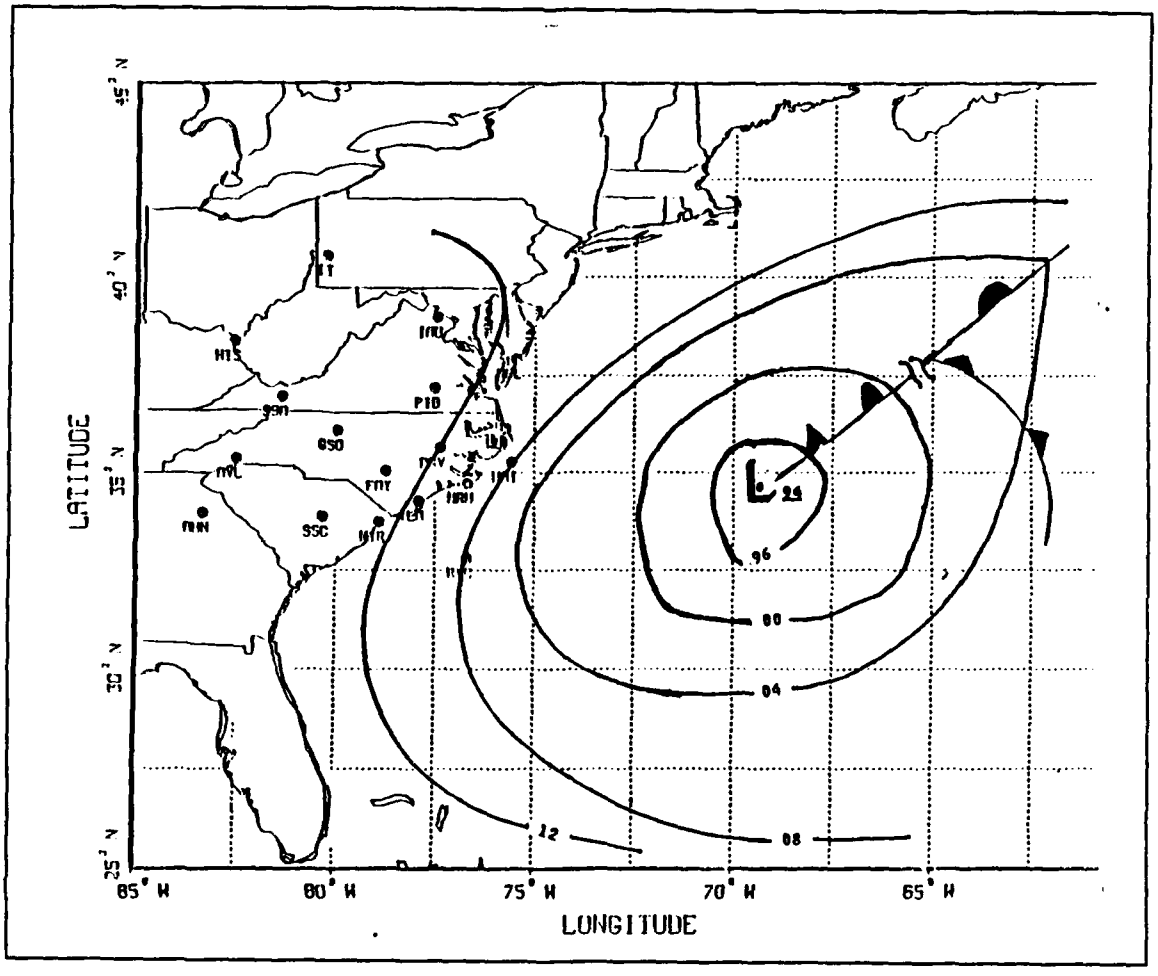

Fig. 29. Synoptic weather pattern, 00 UTC 2 March 1986: As in Fig. 3.

At the 850 mb level, a closed circulation is analyzed almost above the surface low. It will be shown that a lid does not form, and that growth of the storm occurs at a relatively modest rate of four mb during the next 12 h.

2. Satellite imagery

No research or reconnaissance flights into the region occurred during this phase of the storm. Thus, no physical evidence exists for the presence or absence of a lid. Nevertheless, strong implications for the absence of the lid are present in the enhanced IR imagery from the Geosynchronous Observing Environmental Satellite (GOES). The low-level flow off the east coast brings cold, dry air over the ocean. An area of enhanced convection is seen (Fig. 31) in the region off the coast of North Carolina, Virginia in the vicinity of the Gulf Stream. The area of convection is southwest of the analyzed position

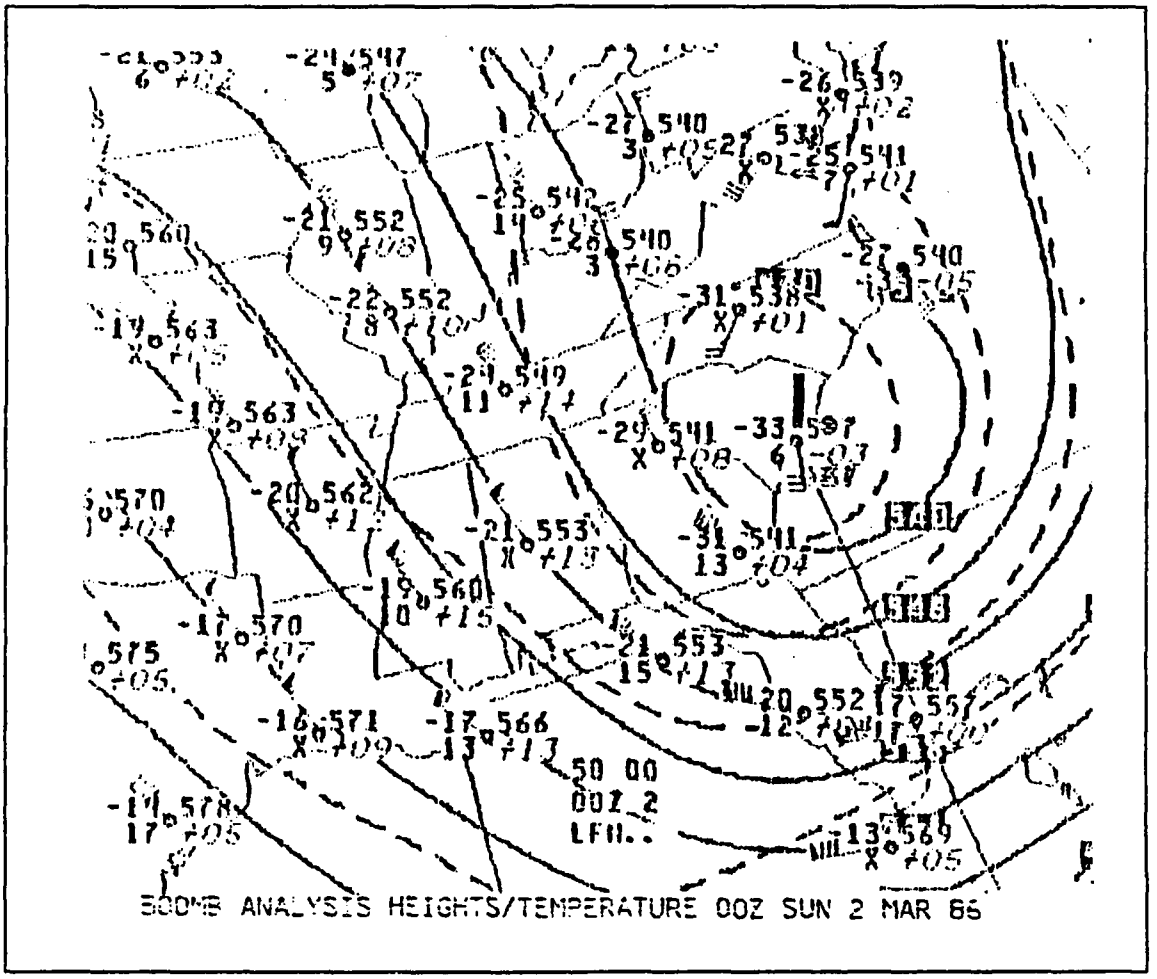

Fig. 30. 500 mb heights/temperature, 00 UTC 2 March 1986: As in Fig. 20.

of the storm at 06 UTC 2 March (Fig. 32). If an established lid existed in this area, no enhanced convection would be present behind the storm. The convection continues over the Gulf Stream (Fig. 33) as the low continues moving towards the northeast.

3. Summary

Cyclogenesis occurred about 18 UTC 1 March in the North Atlantic well off the coast of North Carolina. No low-level processes seem to be available to enhance storm growth, and only slow growth of the storm is observed. Near-surface moisture fluxes are transported into the middle troposphere by convection over the waters south of the Gulf Stream, which eliminates any potential lid effects.

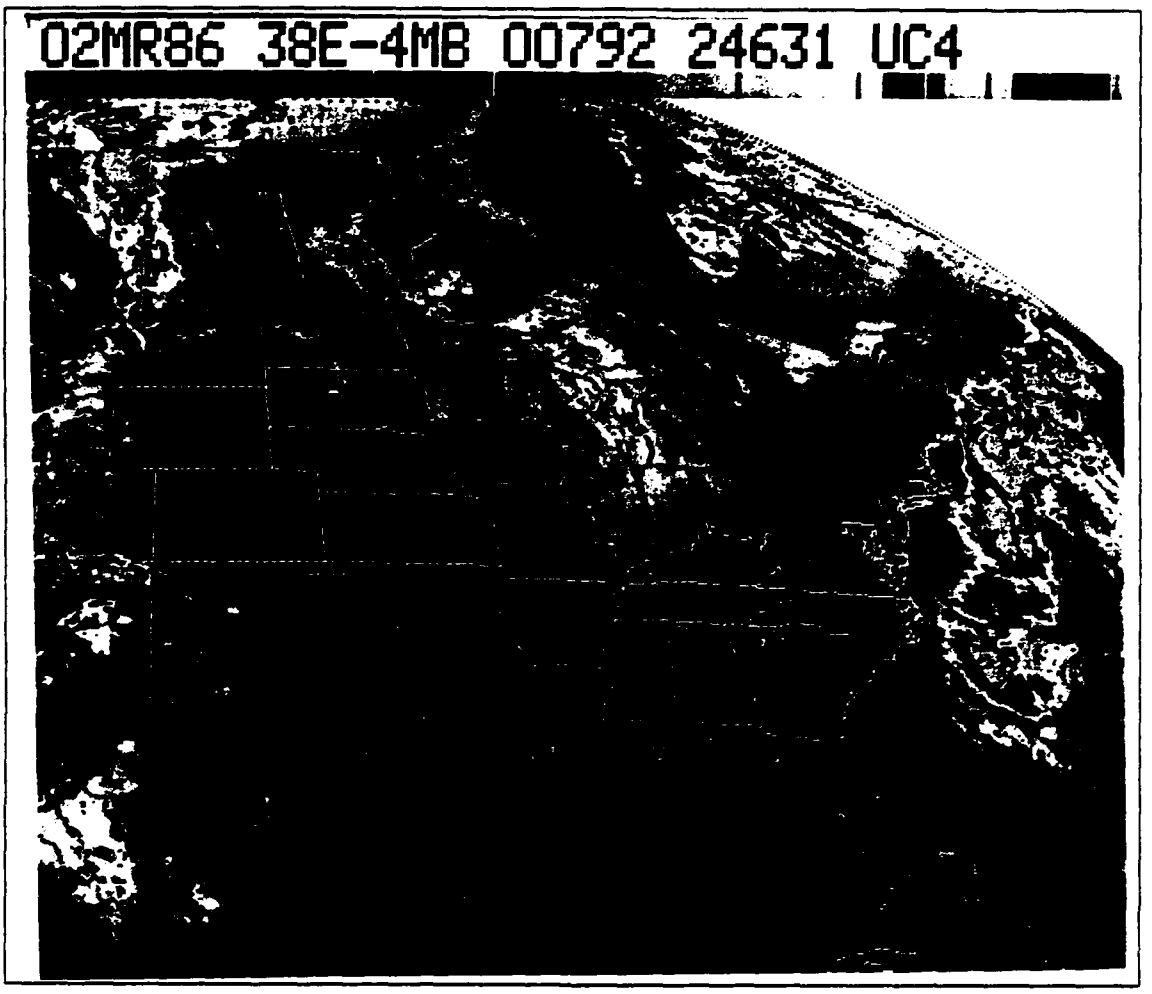

Fig. 31. GOES image, 0931 UTC 2 March 1986: Enhanced IR image (enhancement code MB from Clark,1983).

D. DISCUSSION

1. Synopsis

Cyclogenesis and storm intensification for the 1-2 March storm is different from the 14-16 February storm. The nonexplosive low has quite different environmental support that results in only modest storm growth. Winds in the troposphere have a greater southerly component than in the explosive growth example. The deepening trough in the upper levels is the driving force behind the southerly winds. Furthermore, the lengthy over-water trajectory exposes the air mass to air-sea interaction processes that eliminate any potential capping inversions. Table 2 provides LSI values for the marine soundings

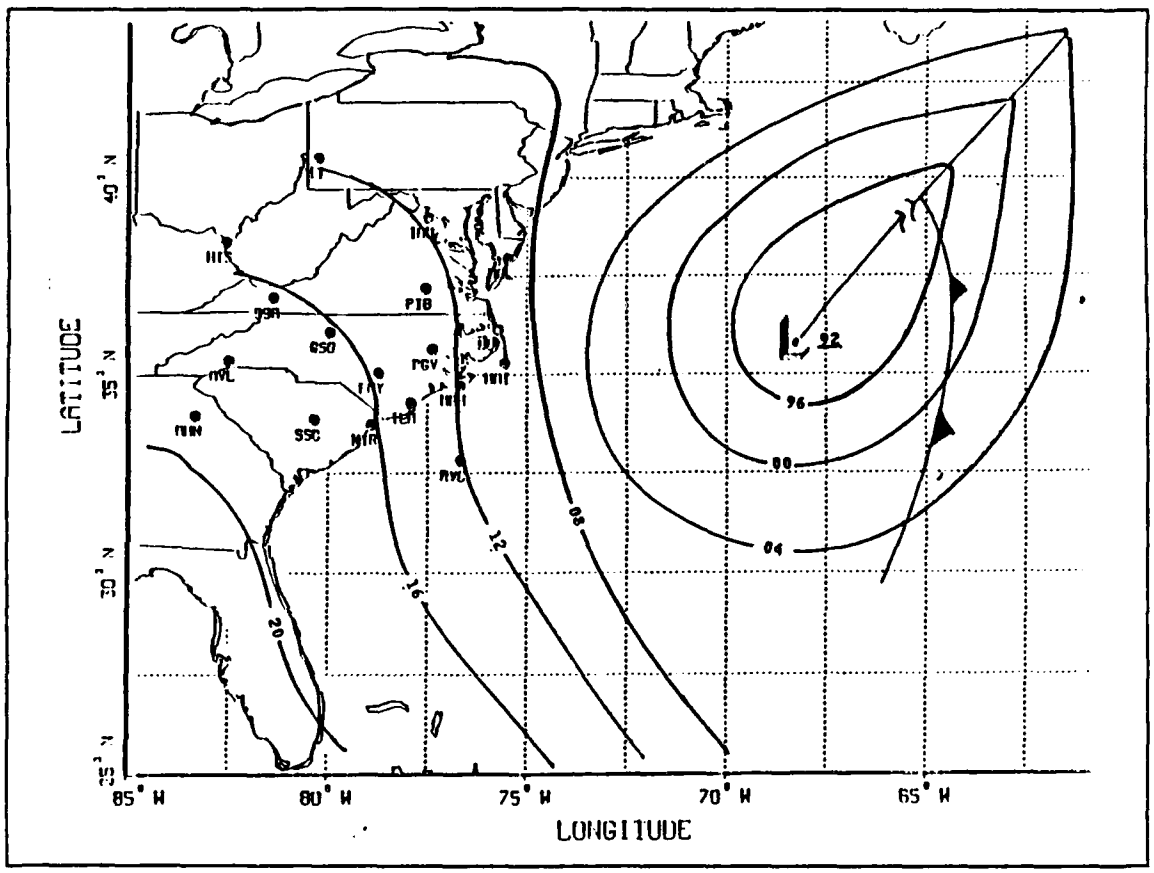

Fig. 32. Synoptic weather pattern, 06 UTC 2 March 1986: As in Fig. 3.

during this period. Although other synoptic features in this case are also different, the purpose here is to show that the absence of any lids differs markedly from the explosive case. Upper-level forcing (vorticity advection) for the IOP 11 storm appears to be stronger, which might suggest that the second storm should be stronger.

In the explosive growth case, a low-level jet streak advected warm, dry continental air into the storm region. A similar low-level jet was present in the nonexplosive storm case. Any potential jet streaks in the lower troposphere were from the south and the air advected into the area of the cyclone was near saturation.

During the cyclogenesis, a potential exists for cold, dry surface air to be advected into the storm. This could provide a large flux of latent heat into the storm from low-level processes under a capping inversion. However, satellite imagery showed enhanced convection southwest of the storm that would not have been possible in the presence of a lid. Such convection was not observed in the explosively deepening storm,

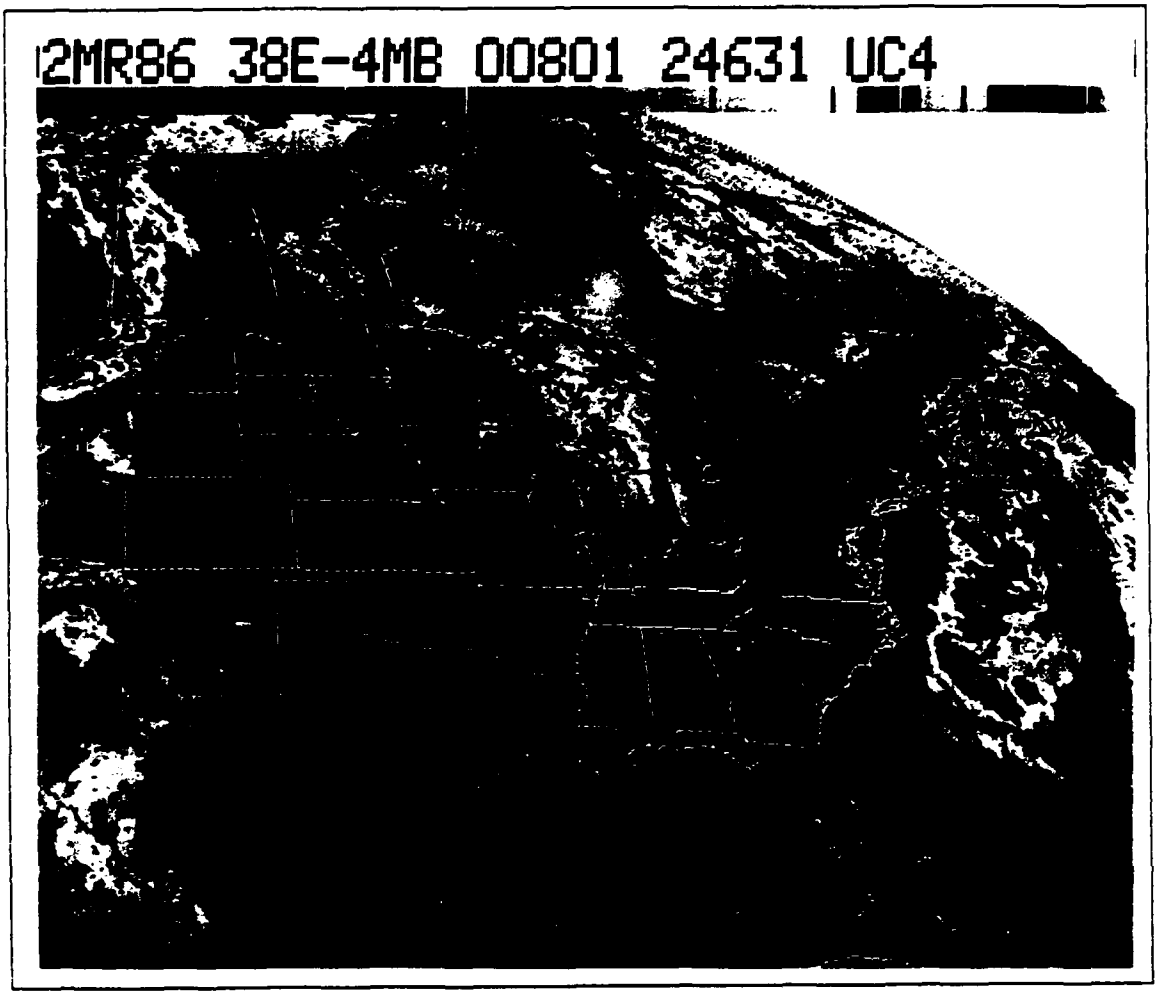

Fig. 33. GOES image, 1101 UTC 2 March 1986: As in Fig. 31.

with all the soundings and cross-sections providing evidence that convection was restricted to the layer underneath the lid. Once the surface air had been advected into the region of cyclone center, the effects of the lid were overcome and the ensuing latent heat release apparently provided the extra energy for storm deepening.

2. Forecast analysis

The NOGAPS sea-level pressure error analysis (Fig. 34) for 00 UTC 2 March indicates an underforecast of the intensity of the storm by 4 mb. The 12 UTC 2 March analysis (Fig. 35) indicates a very accurate forecast with no error in the region of the storm.

Table 2. LID STRENGTH INDEX (IOP 11): Over-ocean Lid Strength Index values for 1-2 March. Note the LSI values in the region of cyclogenesis near 32°N, 72°W at 18 UTC 1 March. Soundings used in the cross-section in Fig. 25 are numbered RVC 1 and ODW 2 through 4 for convenience.

Station	Time YYMMDDHH	Lat ° N	Long ° W	LSI (K)	Lid Height mb
AWS	86030110	34.60	69.20	no lid	710
ODW #2	86030110	34.00	73.00	no lid	n/a
ODW #3	86030110	33.50	72.00	no lid	n/a
ODW #4	86030112	33.20	70.70	no lid	n/a
ODW	86030116	36.10	69.10	no lid	n/a
ODW	86030116	36.50	69.50	no lid	n/a
ODW	86030116	36.50	70.50	no lid	n/a
ODW	86030116	36.50	71.50	no lid	n/a
ODW	86030118	38.10	70.40	-18.2	830
ODW	86030118	38.10	67.30	no lid	n/a
ODW	86030118	38.00	69.00	-14.6	650
ODW	86030118	39.00	67.30	no lid	n/a
XKF	86030100	32.37	64.68	-0.7	890
XKF	86030106	32.37	64.68	-3.0	650
XKF	86030112	32.37	64.68	0.90	650
RVC	86030100	33.09	76.67	no lid	n/a
RVC	86030106	32.80	76.68	-14.7	810
RVC #1	86030112	32.80	76.68	-11.3	770
RVC	86030118	32.83	76.65	-10.4	650

The two products from NMC produced similar results. Both the man-machine interface and the NGM accurately predicted storm development. The NGM forecast (00 UTC 2 March) pressure was within two mb of the actual storm pressure with a positional error of less than 100 n mi to the northeast of storm location. The man-machine product for 12 UTC 2 March accurately forecast the storm location and position.

When there is no capping inversion, all three models provide accurate forecasting of the storm intensity and position. The accuracy of the forecasts in this nonexplosive case indirectly supports the hypothesis of the inability of the models to forecast explosive cases with vigorous latent heat release. The hypothesis is that the models do

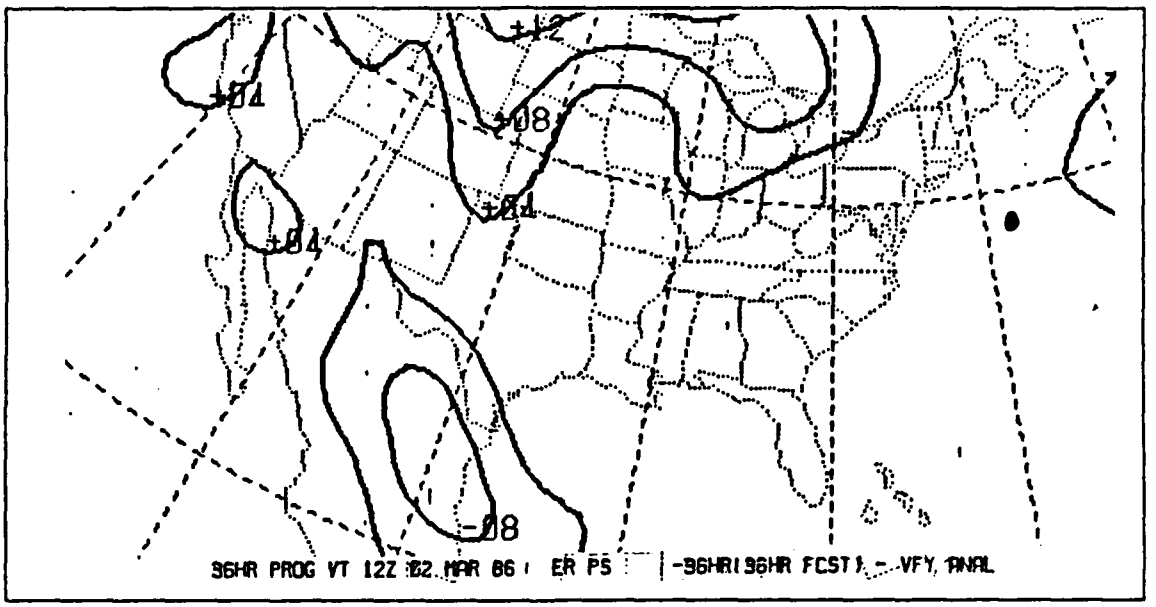

Fig. 34. Forecast errors, 00 UTC 2 March 1986: As in Fig. 17 for the NOGAPS model 36 h forecast.

not accurately reflect storm growth in the presence of a capping inversion. Due to the coarse vertical resolution of the models, such inversions cannot be represented. Consequently, no mechanism is available in the model to restrict vertical overturning as heat and moisture are added in the region of the lid along the warm conveyor belt. With different cyclone environments, one with a lid and one without a lid, the similar performance of the models is noteworthy. The failure of all three models in forecasting explosive cyclogenesis imply a common error in how the models calculate cyclone formation and growth. The investigation into the different cases suggests that one potential difference in the storms is the prevention of the latent heat release in a deep layer upwind of the explosive deepening center, whereas the absence of an upstream lid would not restrict convection upwind of the nonexplosively deepening center. Thus, the incorrect representation of the vigor of the latent heat release in the models is suggested as the most probable reason for forecast error in the explosive cyclone growth.

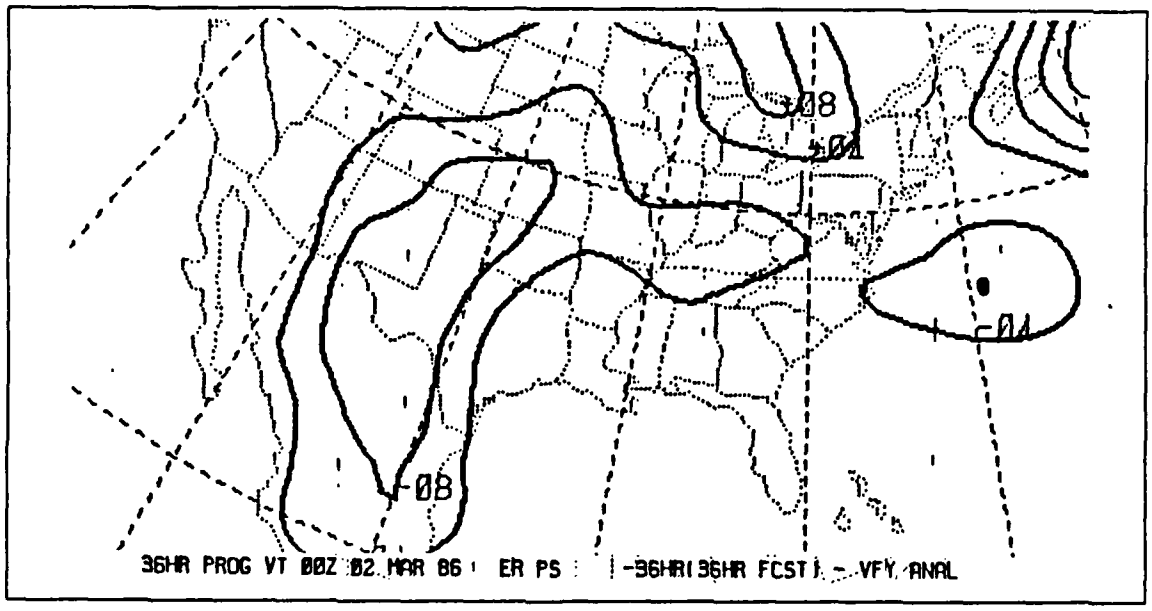

Fig. 35. **Forecast errors, 12 UTC 2 March 1986:** As in Fig. 17 for the NOGAPS model 36 h forecast.

V. CONCLUSIONS AND RECOMMENDATIONS

A. CONCLUSIONS

The hypothesis tested for this study is that explosive cyclogenesis is favored in lid conditions established by advection of a dry, continental air mass with a conditionally unstable lapse rate in mid-tropospheric air stream over a cool, moist layer. These conditions would exist upwind of the region of convective heat release that accompanies rapid cyclogenesis, but would not exist in the same areas of non-rapid cyclogenesis. Since only the GALE IOP 6 and IOP 11 cyclones are studied in this investigation, any conclusions must be regarded as very tentative.

Lid conditions did exist for the Miller (1946) type B cyclogenesis in IOP 6. The advection of warm and dry continental air in the middle troposphere provided lid conditions that trapped the moist layer near the surface. Suppression of deep convection allowed the warming and moistening due to surface fluxes and horizontal advection in the warm conveyor belt in advance of the cold front. In the vicinity of cyclogenesis, the lid is overcome as shown by the RVC LSI at 06 UTC 15 February 1986 (sounding in Appendix A). The environment along the cold front in the cross-section (Fig. 13) and the soundings (Appendix A) in that cross-section verify the lid conditions upwind of the area of convection in the low. Rapid deepening of the cyclone follows from these initial conditions. The explosive phase is apparently associated with the upper-level advection of positive vorticity and the enhanced latent heat release, a result of the lid conditions.

Environmental conditions were different during cyclogenesis for the IOP 11 storm. A deepening trough in the middle and upper troposphere provided support for a Miller (1946) type A cyclogenesis. There was an absence of lid conditions in the area upstream of cyclogenesis. The southerly wind component and the resulting long over-water trajectories prevent the establishment of lid conditions. Although the approaching vorticity maximum is larger for the IOP 11 storm, only modest growth is observed.

Explosive cyclogenesis occurred with the presence of the lid, while non-explosive cyclogenesis did not have these conditions. These two storm cases provide tentative support for the hypothesis. Based on such a limited data set, this should be considered as only a preliminary test of the hypothesis. Other IOP storms were examined in terms of the surface pressure and associated lid conditions (Appendix B). Lid conditions prior

to IOP 2 and 9 preceded explosive cyclogenesis and may have contributed to the explosive growth. High surface temperatures and weak lid conditions were present in the vicinity of nonexplosive cyclogenetic events of IOP's 4 and 5. Although this information comes from a less detailed investigation into the individual storm environments, there is some support for the hypothesis.

B. RECOMMENDATIONS

Because many factors may contribute to explosive cyclogenesis, continued investigation of these mechanisms is clearly required to provide a statistically valid conclusion. The different environments for Miller (1946) type A and B cyclogenesis may provide an important stratification of the data. A simple study is recommended to compare the frequencies of explosive versus non-explosive cyclones for each of the Miller storm types. More detailed studies of differences in the cyclogenetic environment should be possible from the Experiment on Rapidly Intensifying Cyclones over the Atlantic (ERICA) during December 1988-February 1989.

Two techniques appear promising for detecting potential lid conditions. First, mid-tropospheric air flow at 700 and 850 mb may indicate these conditions. Lid conditions are found in IOP 6 with zonal flow off the continental U.S., whereas lid conditions are not found in the more meridional flow of IOP 11. A more direct technique is to use the Visible Infrared Spin Scan Radiometer (VISSR) Atmospheric Sounder (VAS) on the Geosynchronous Observing Earth Satellite (GOES). Channel 9 (water vapor) centered at 600 mb would provide evidence of a dry mid-tropospheric air mass between 800 and 500 mb. Unfortunately, this channel will not detect the dry layer if there are overlying clouds.

Both of the methods above could be used by forecasters to detect potential lid conditions in the precyclogenetic environment. If these lid conditions are suspected, then soundings could be acquired from the coastline and across the Gulf Stream. The source of the soundings might be the NMC/Air Weather Service Winter Storms program to regularly obtain dropwindsondes in zones of potential offshore cyclogenesis. The area where the lid weakens would then be considered likely for explosive cyclogenesis.

Another recommendation is to consult trajectories as used in this study from the operational forecast models. These trajectories could assist in determining the source region of the air masses in the cyclogenetic environment. Lid conditions due to the advection of dry continental air masses over the ocean could alert a forecaster to the

potential for increased energy, and possible underestimation of storm development predicted in the model. Any progress in determining which environment will or will not produce explosive cyclogenesis would be considered an important advance in the present capability to forecast these dangerous maritime storms.

APPENDIX A. SKEW-T LOG P DIAGRAMS

Skew-T log p diagrams used in this research are presented here for additional information and reference. Diagrams used as figures in the main text have been repeated in this Appendix to provide side-by-side comparison of soundings in cross-sections. To present a complete set, skew-T diagrams are arranged in chronological order. Skew-T log p diagrams have station identification across the top as follows: station ID or dropwindsonde type, date and time, latitude and longitude. Dashed lines are moist pseudoadiabats, dotted lines are mixing ratio lines, curved solid lines are the dry adiabats and the straight slanted lines are temperature lines. The temperature sounding is the thick solid line and the dew-point temperature is the thick dashed line. One wind barb equals 5 $m \cdot s^{-1}$.

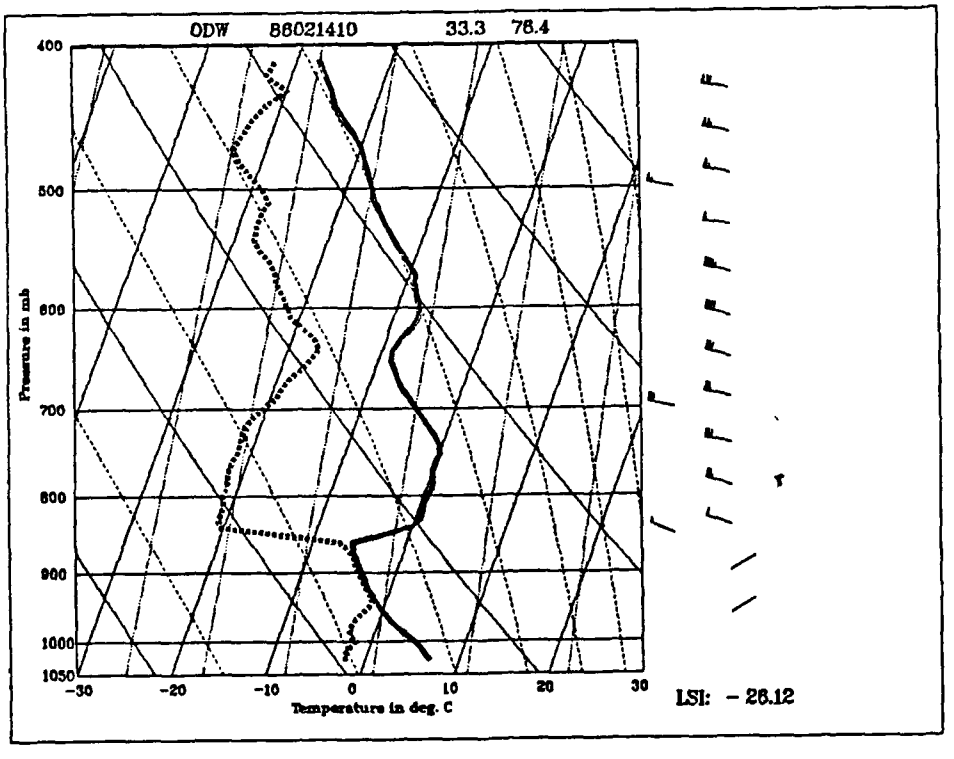

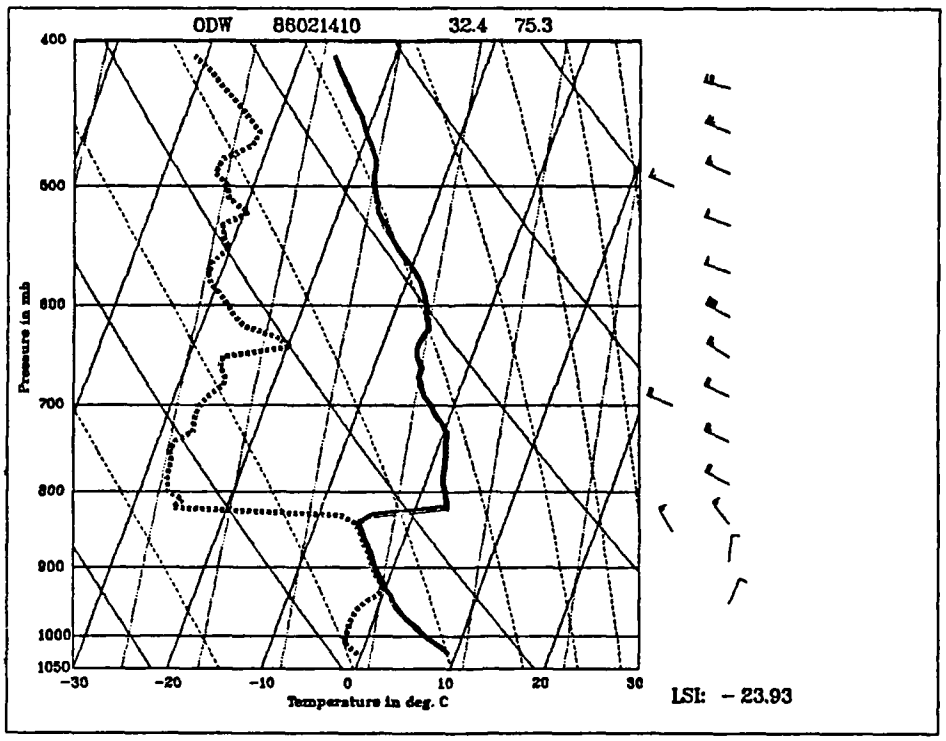
ODW 86021410 32.4 75.3
Pressure in mb
400
500
600
700
800
900
1000
1050
-30
-20
-10
0
10
20
30
Temperature in deg. C
LSI: -23.93

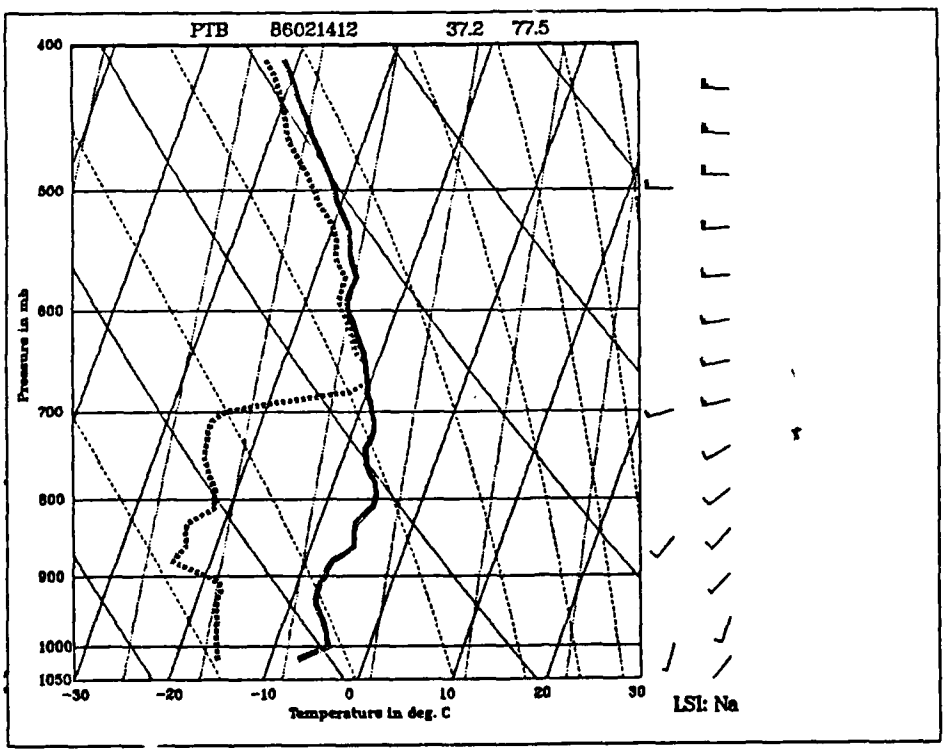
PTB 86021412 37.2 77.5
Pressure in mb
400
500
600
700
800
900
1000
1050
-30
-20
-10
0
10
20
30
Temperature in deg. C
LSI: Na

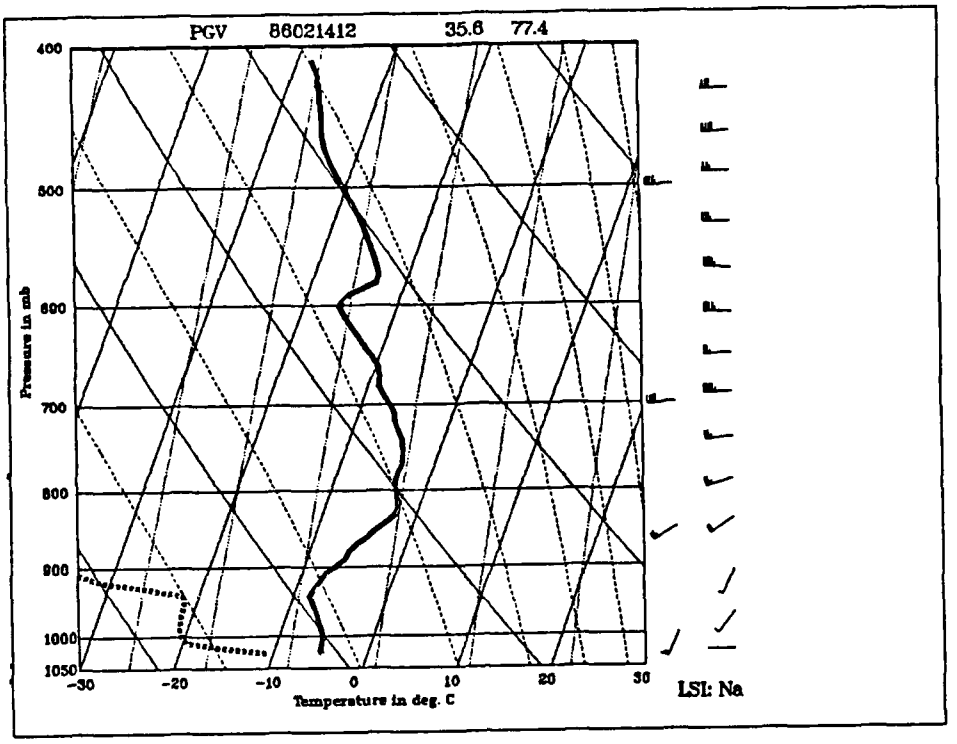
PGV 86021412 35.6 77.4
Pressure in mb
400
500
600
700
800
900
1000
1050
-30
-20
-10
0
10
20
30
Temperature in deg. C
LSI: Na

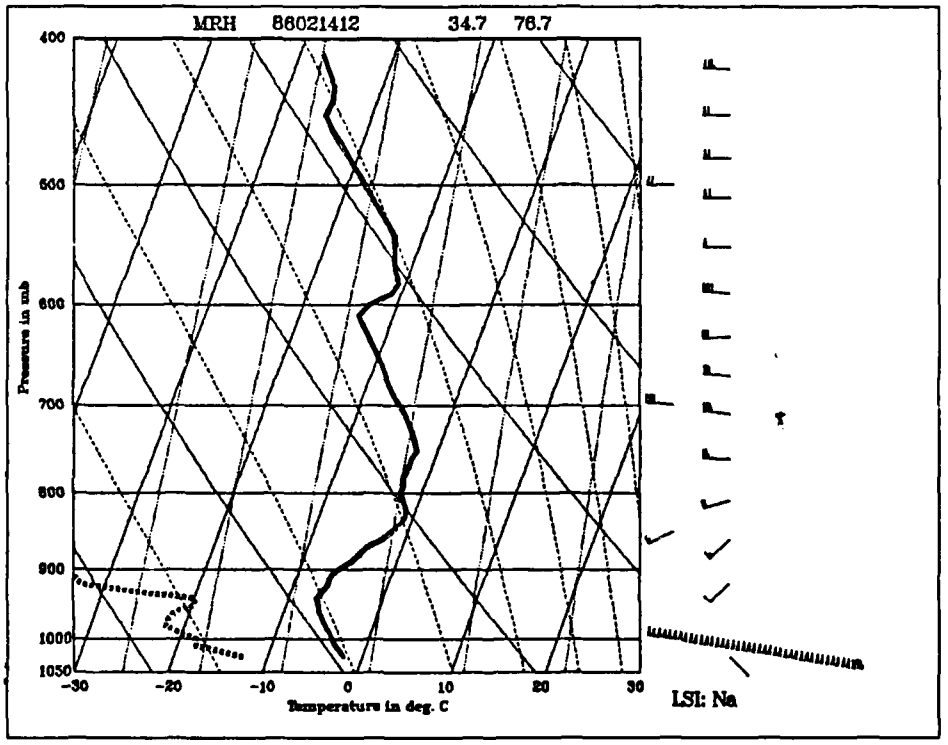
MRH 86021412 34.7 76.7
Pressure in mb
400
500
600
700
800
900
1000
1050
-30
-20
-10
0
10
20
30
Temperature in deg. C
LSI: Na

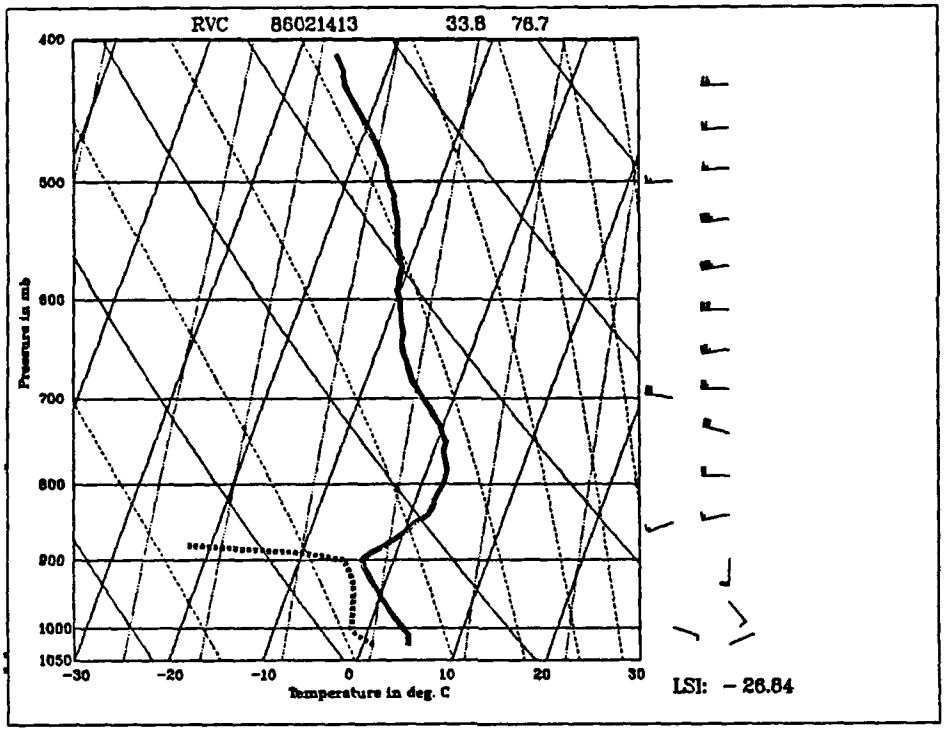
RVC 86021413 33.8 76.7
400
500
600
700
800
900
1000
1050
Pressure in mb
-30 -20 -10 0 10 20 30
Temperature in deg. C
LSI: -26.84

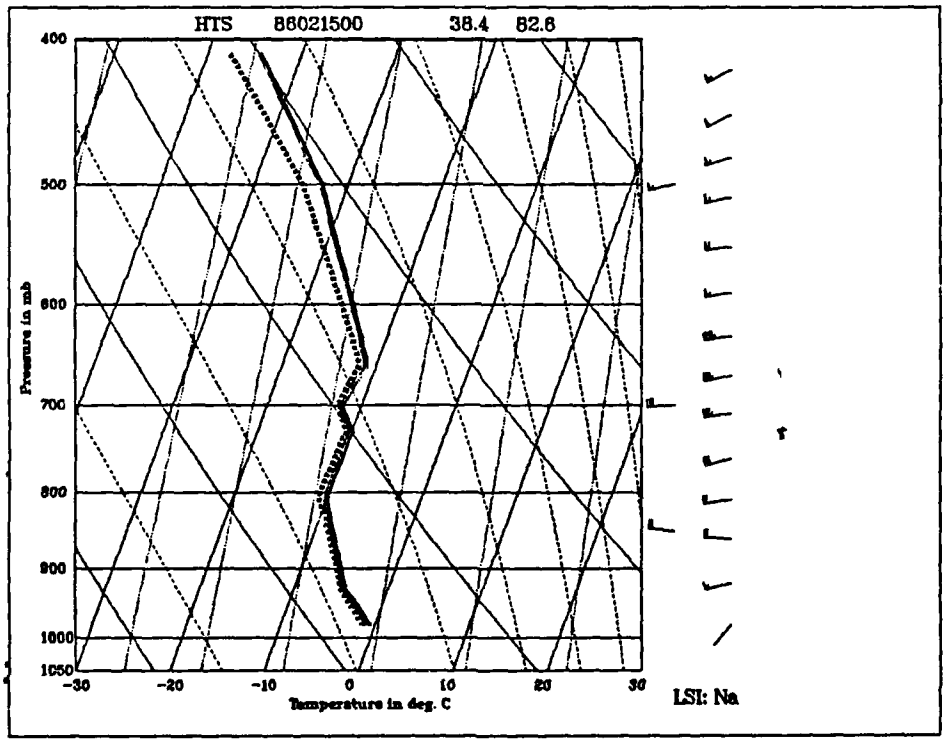
HTS 86021500 38.4 82.6
400
500
600
700
800
900
1000
1050
Pressure in mb
-30 -20 -10 0 10 20 30
Temperature in deg. C
LSI: Na

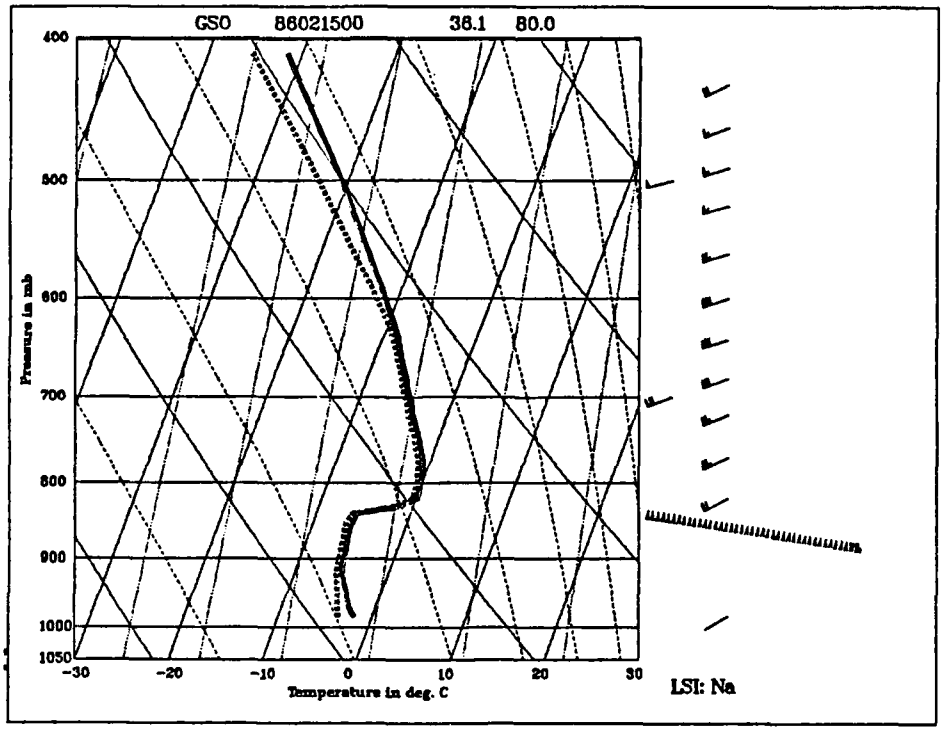
GSO 86021500 36.1 80.0
400
500
600
700
800
900
1000
1050
Pressure in mb
-30
-20
-10
0
10
20
30
Temperature in deg. C
LSI: Na

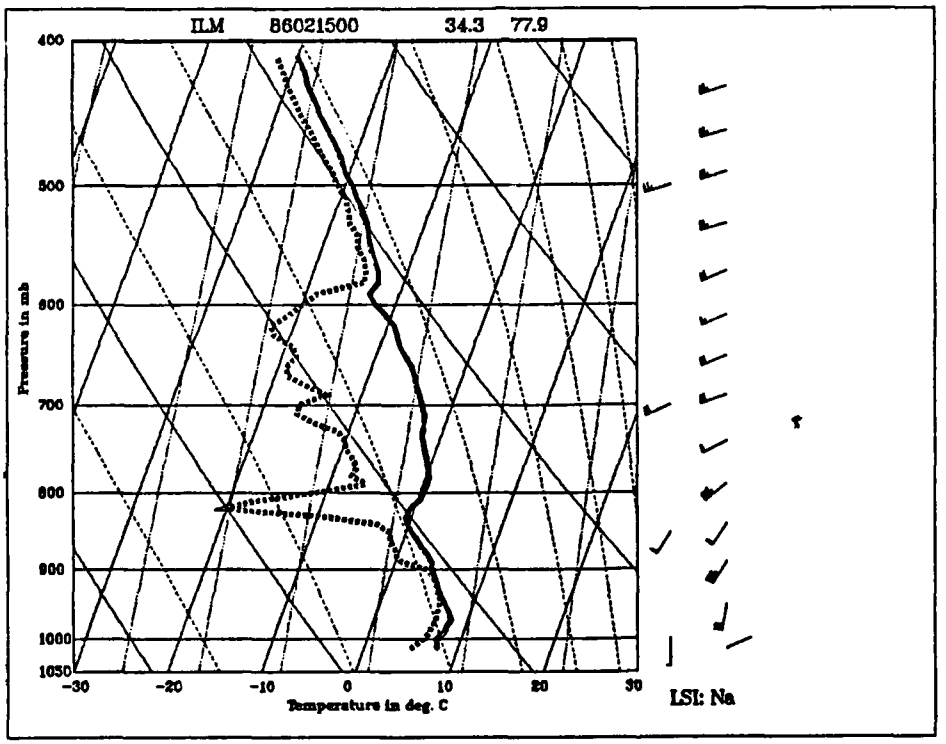
ILM 86021500 34.3 77.9
400
500
600
700
800
900
1000
1050
Pressure in mb
-30
-20
-10
0
10
20
30
Temperature in deg. C
LSI: Na

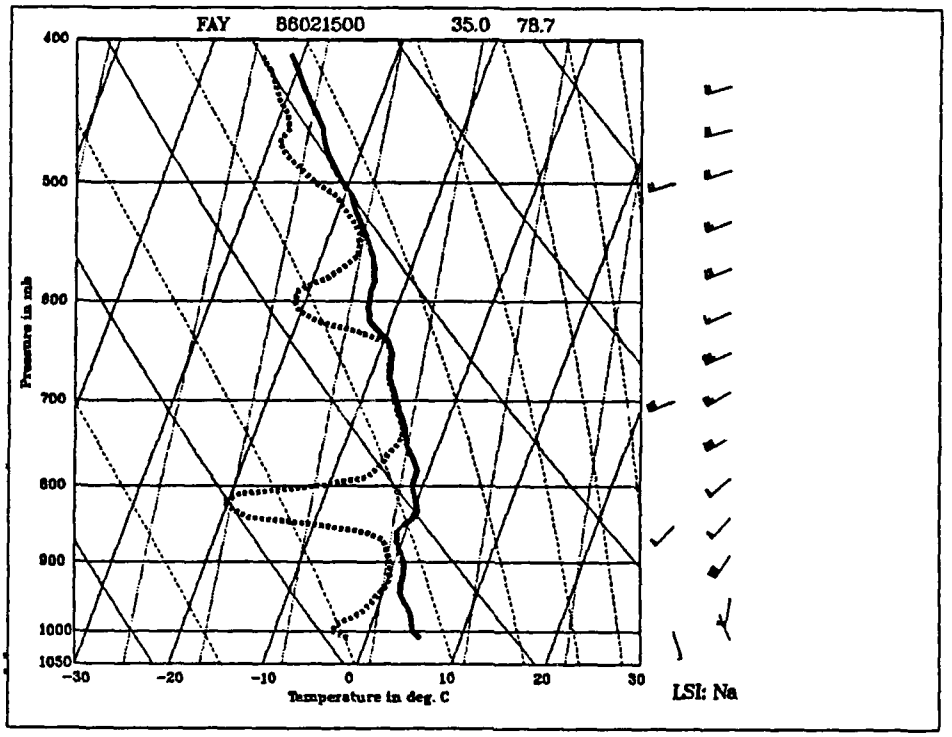
FAY 86021500 35.0 78.7
400
500
600
700
800
900
1000
1050
Pressure in mb
-30 -20 -10 0 10 20 30
Temperature in deg. C
LSI: Na

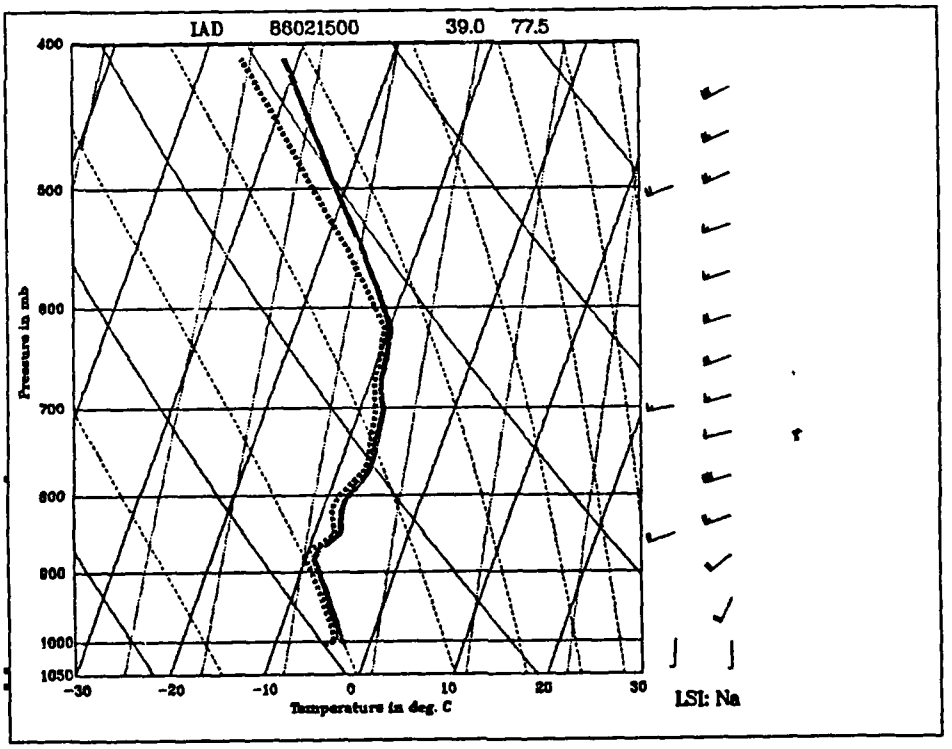
IAD 86021500 39.0 77.5
400
500
600
700
800
900
1000
1050
Pressure in mb
-30 -20 -10 0 10 20 30
Temperature in deg. C
LSI: Na

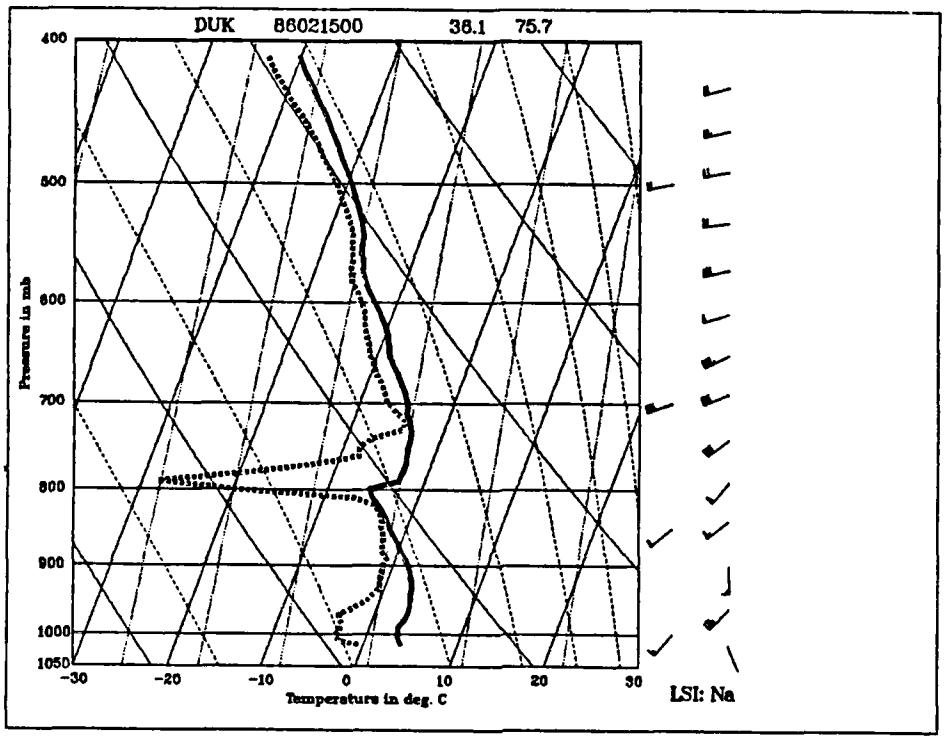
DUK 86021500 36.1 75.7
Pressure in mb
400
500
600
700
800
900
1000
1050
-30
-20
-10
0
10
20
30
Temperature in deg. C
LSI: Na

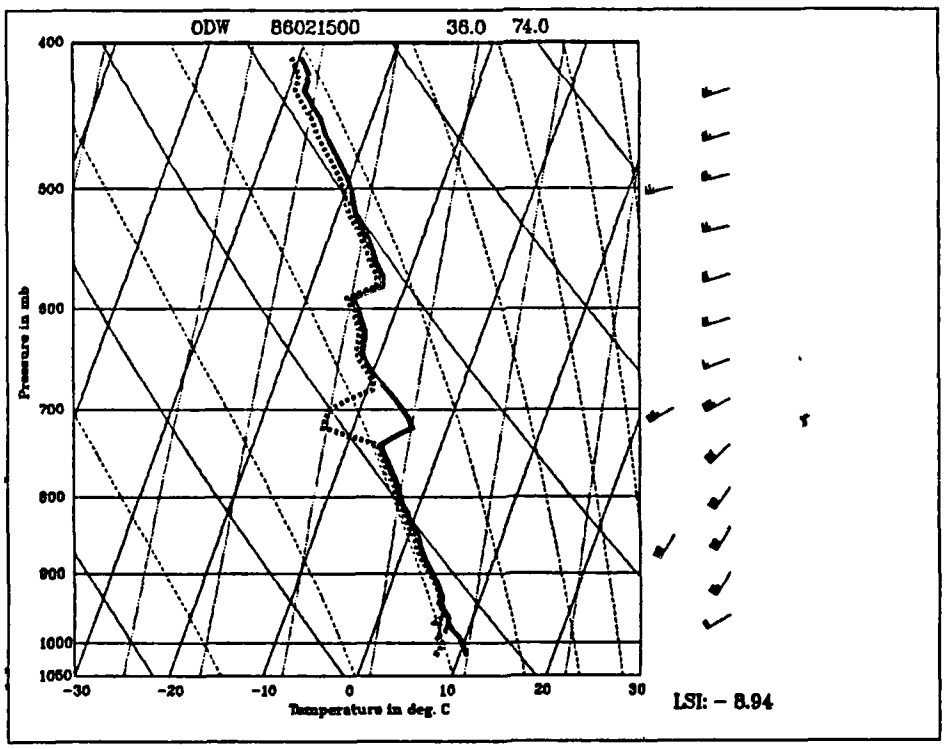
ODW 86021500 36.0 74.0
Pressure in mb
400
500
600
700
800
900
1000
1050
-30
-20
-10
0
10
20
30
Temperature in deg. C
LSI: - 8.94

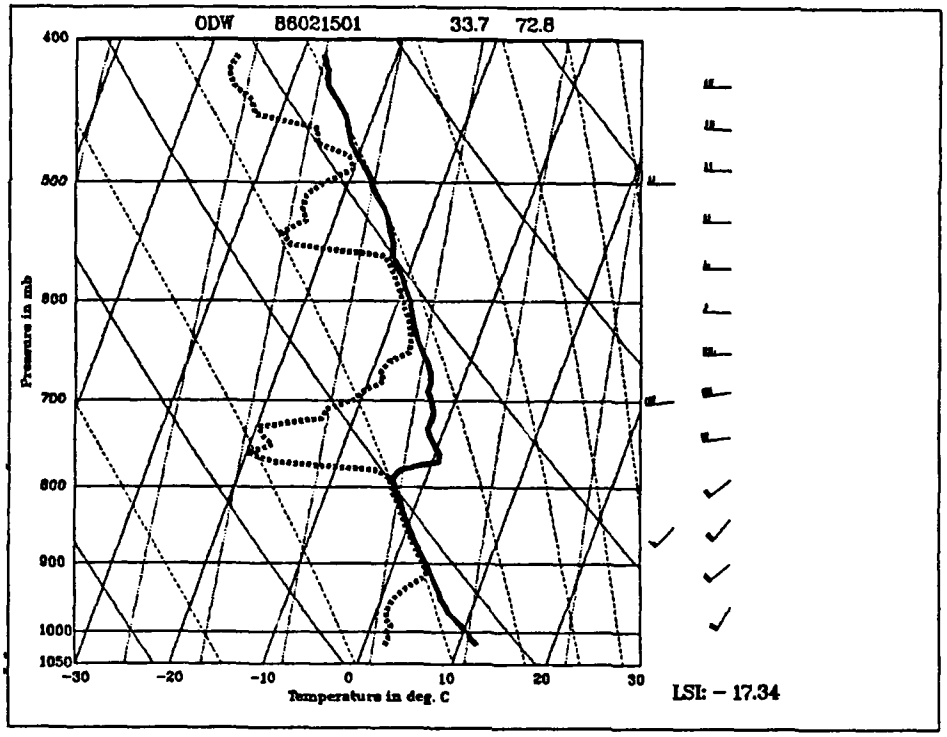
ODW 86021501 33.7 72.8
Pressure in mb
400
500
600
700
800
900
1000
1050
-30
-20
-10
0
10
20
30
Temperature in deg. C
LSI: - 17.34

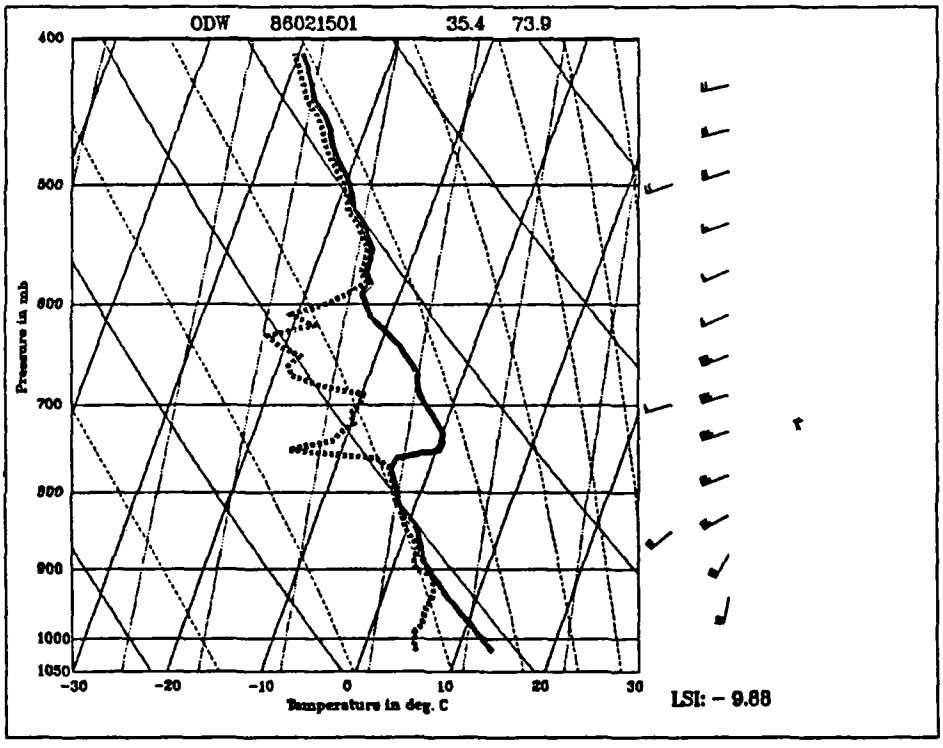
ODW 86021501 35.4 73.9
Pressure in mb
400
500
600
700
800
900
1000
1050
-30
-20
-10
0
10
20
30
Temperature in deg. C
LSI: - 9.88

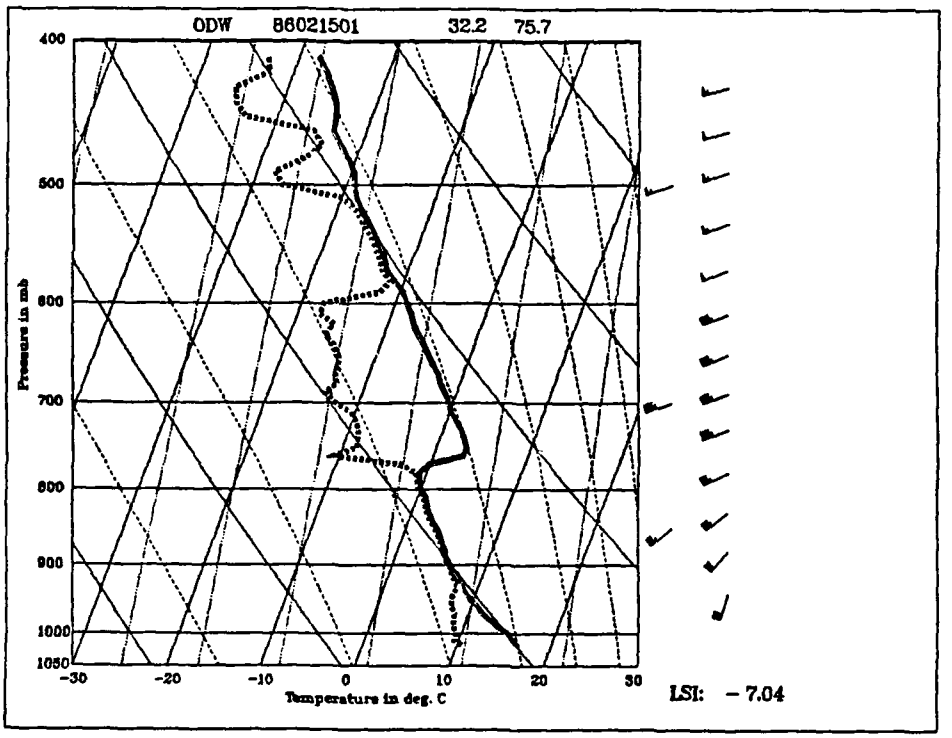
ODW 86021501 32.2 75.7
Pressure in mb
400
500
600
700
800
900
1000
1050
-30
-20
-10
0
10
20
30
Temperature in deg. C
LSI: -7.04

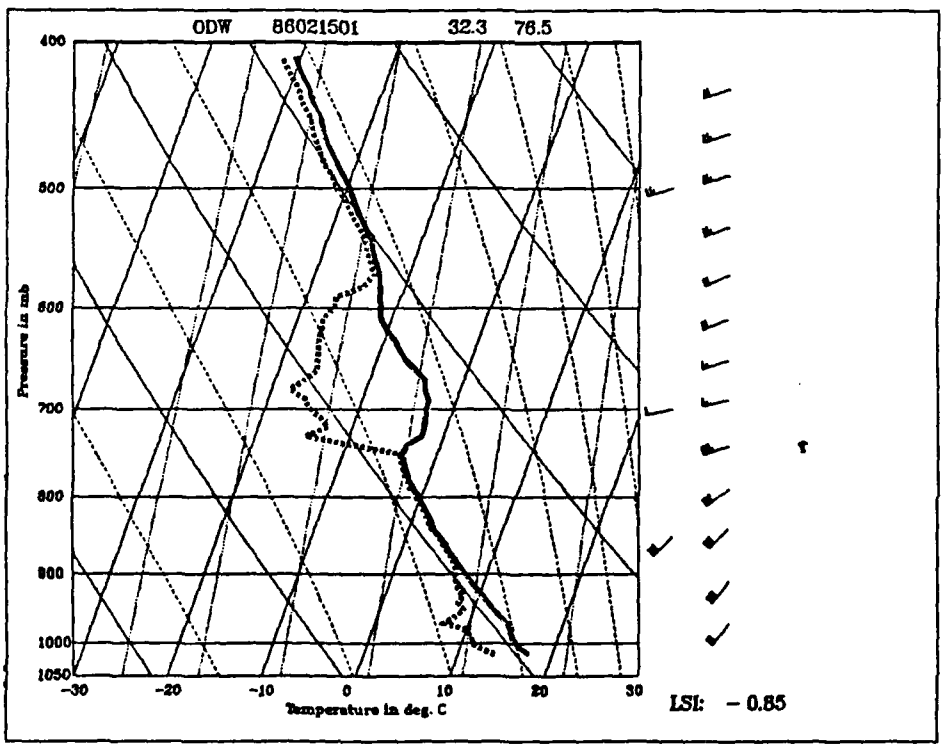
ODW 86021501 32.3 76.5
Pressure in mb
400
500
600
700
800
900
1000
1050
-30
-20
-10
0
10
20
30
Temperature in deg. C
LSI: -0.85

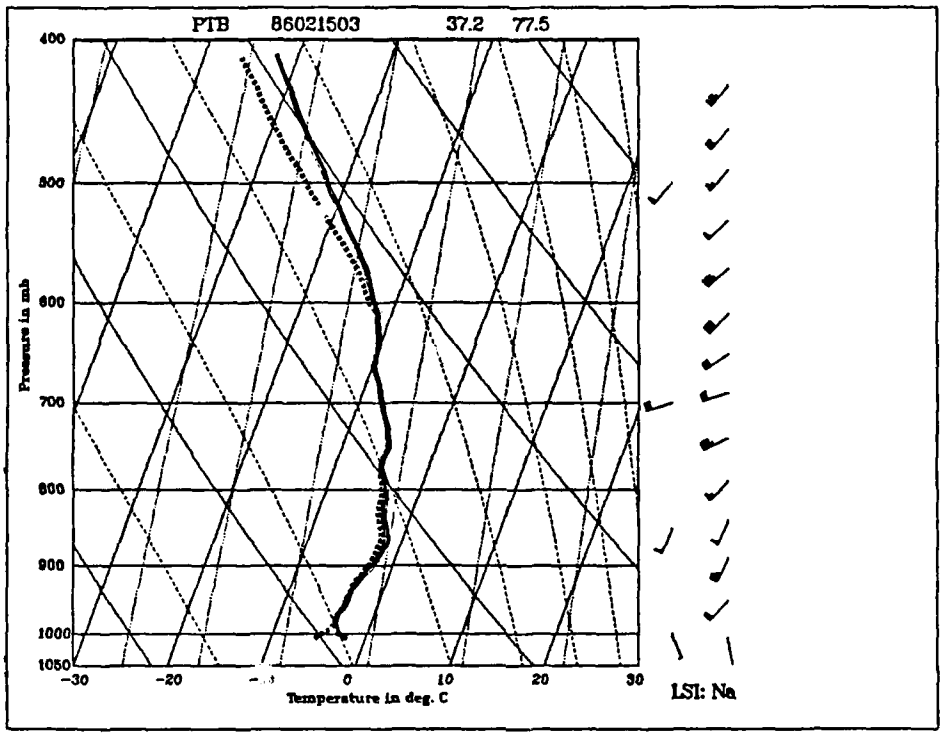
PTB 86021503 37.2 77.5
400
500
600
700
800
900
1000
1050
Pressure in mb
-30
-20
0
10
20
30
Temperature in deg. C
LSI: Na

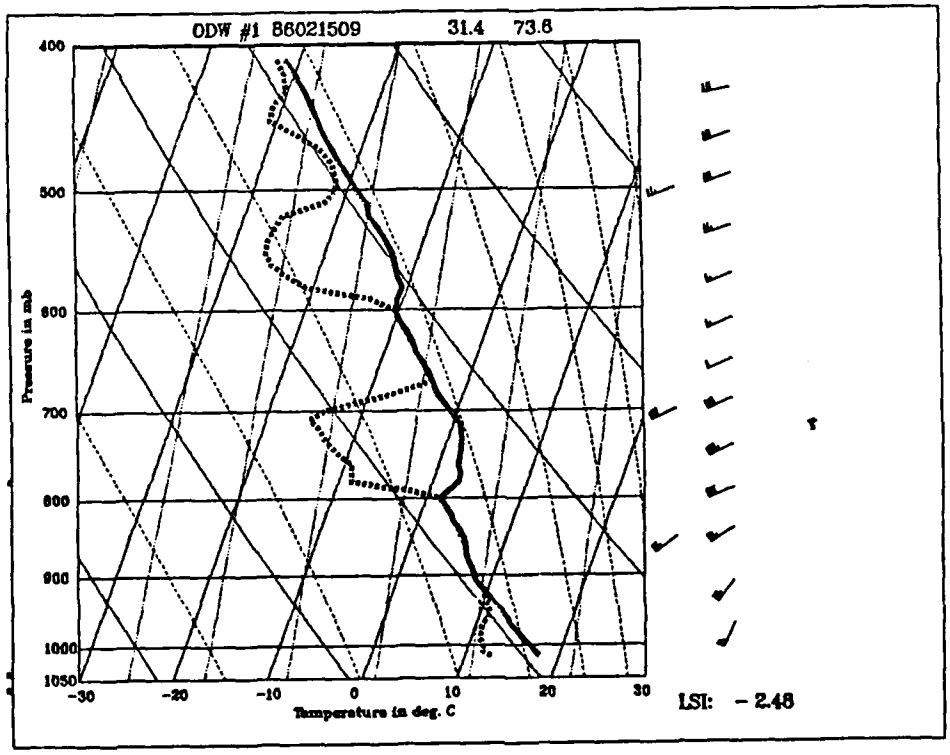
ODW #1 86021509 31.4 73.6
400
500
600
700
800
900
1000
1050
Pressure in mb
-30
-20
-10
0
10
20
30
Temperature in deg. C
LSI: - 2.48

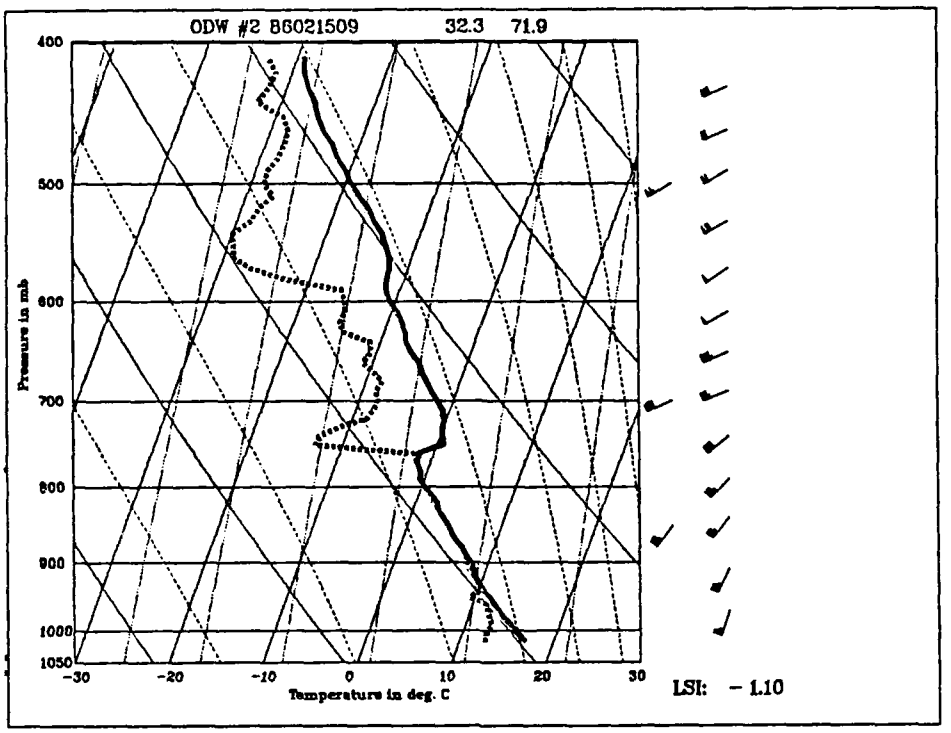
ODW #2 86021509 32.3 71.9
400
500
600
700
800
900
1000
1050
Pressure in mb
-30
-20
-10
0
10
20
30
Temperature in deg. C
LSI: - 1.10

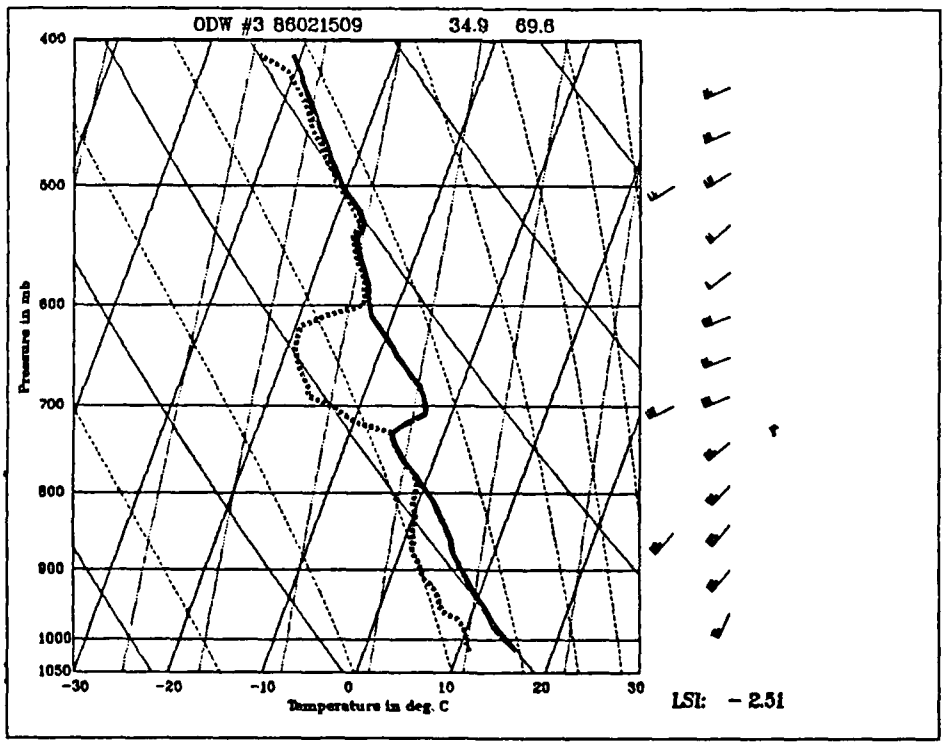
ODW #3 86021509 34.9 69.6
400
500
600
700
800
900
1000
1050
Pressure in mb
-30
-20
-10
0
10
20
30
Temperature in deg. C
LSI: - 2.51

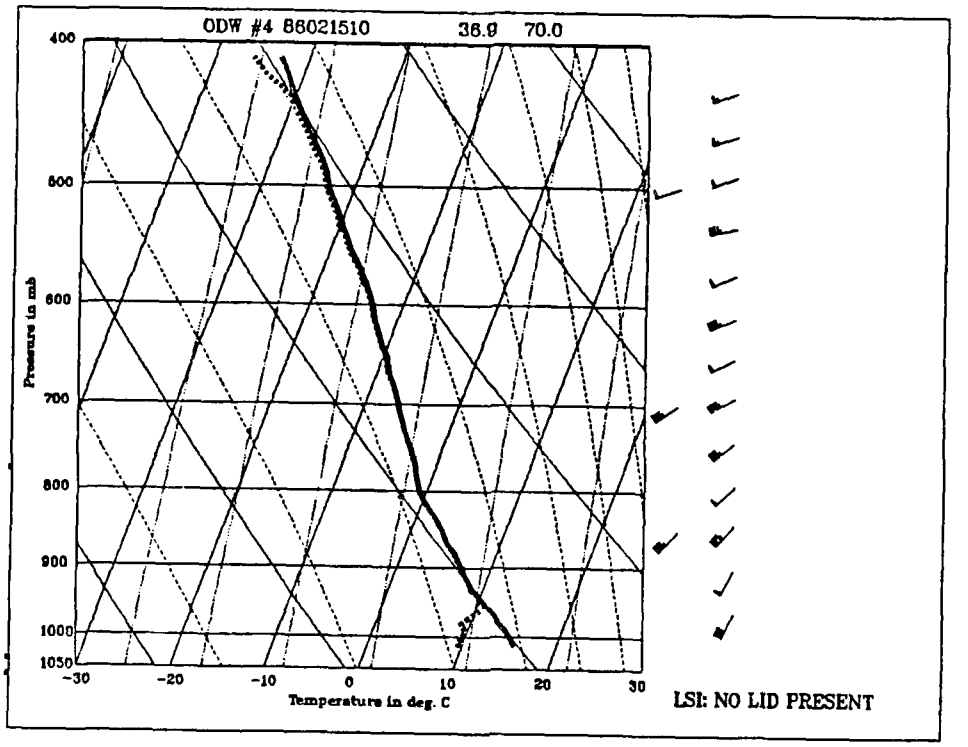
ODW #4 86021510 36.9 70.0
400
500
600
700
800
900
1000
1050
Pressure in mb
-30
-20
-10
0
10
20
30
Temperature in deg. C
LSI: NO LID PRESENT

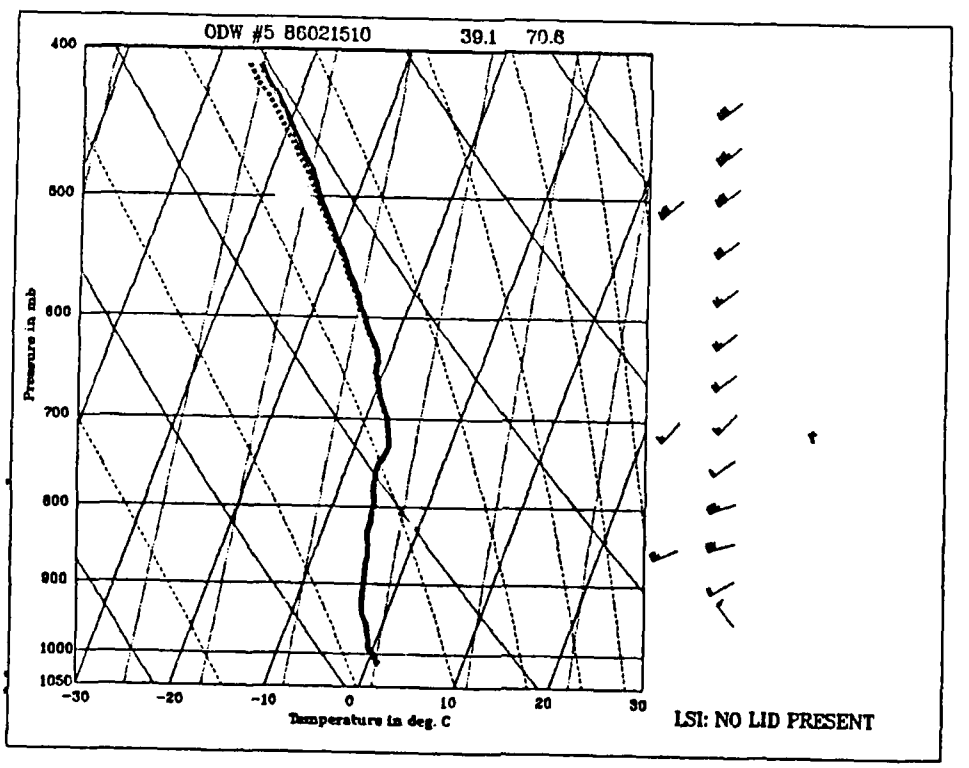
ODW #5 86021510 39.1 70.8
400
500
600
700
800
900
1000
1050
Pressure in mb
-30
-20
-10
0
10
20
30
Temperature in deg. C
LSI: NO LID PRESENT

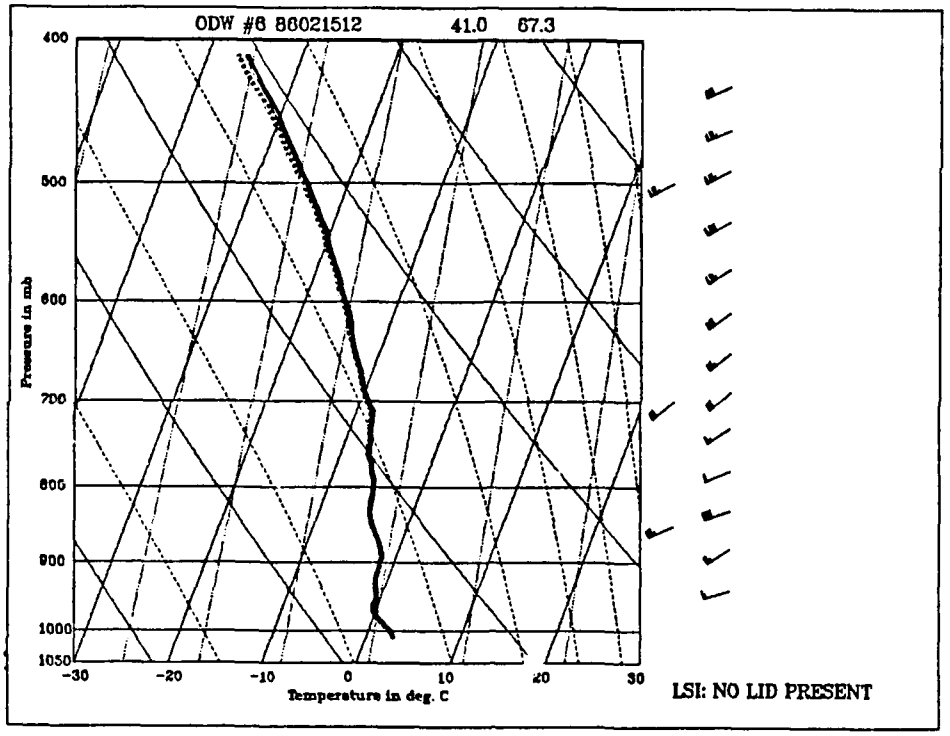
ODW #8 86021512 41.0 67.3
400
500
600
700
800
900
1000
1050
Pressure in mb
-30
-20
-10
0
10
20
30
Temperature in deg. C
LSI: NO LID PRESENT

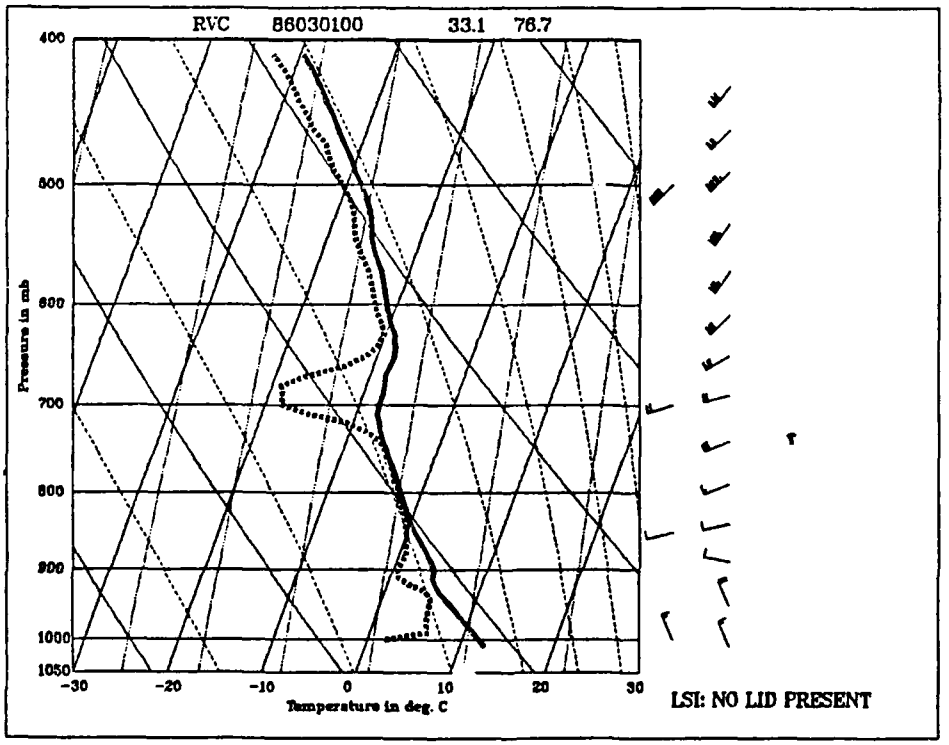
RVC 86030100 33.1 76.7
400
500
600
700
800
900
1000
1050
Pressure in mb
-30
-20
-10
0
10
20
30
Temperature in deg. C
LSI: NO LID PRESENT

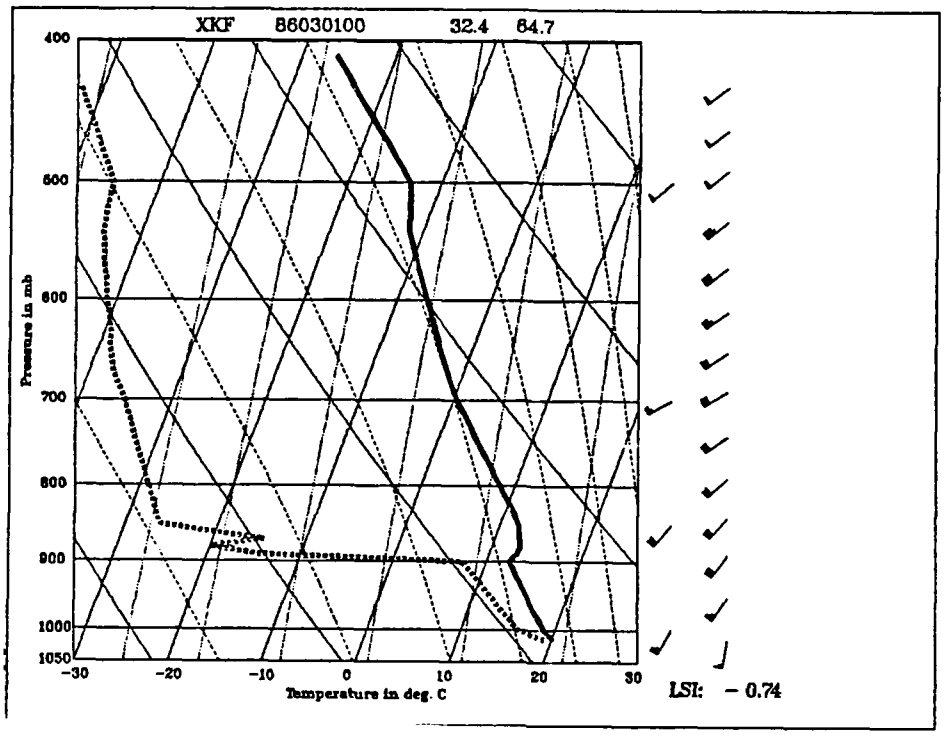
XKF 86030100 32.4 64.7
400
500
600
700
800
900
1000
1050
Pressure in mb
−30 −20 −10 0 10 20 30
Temperature in deg. C
LSI: − 0.74

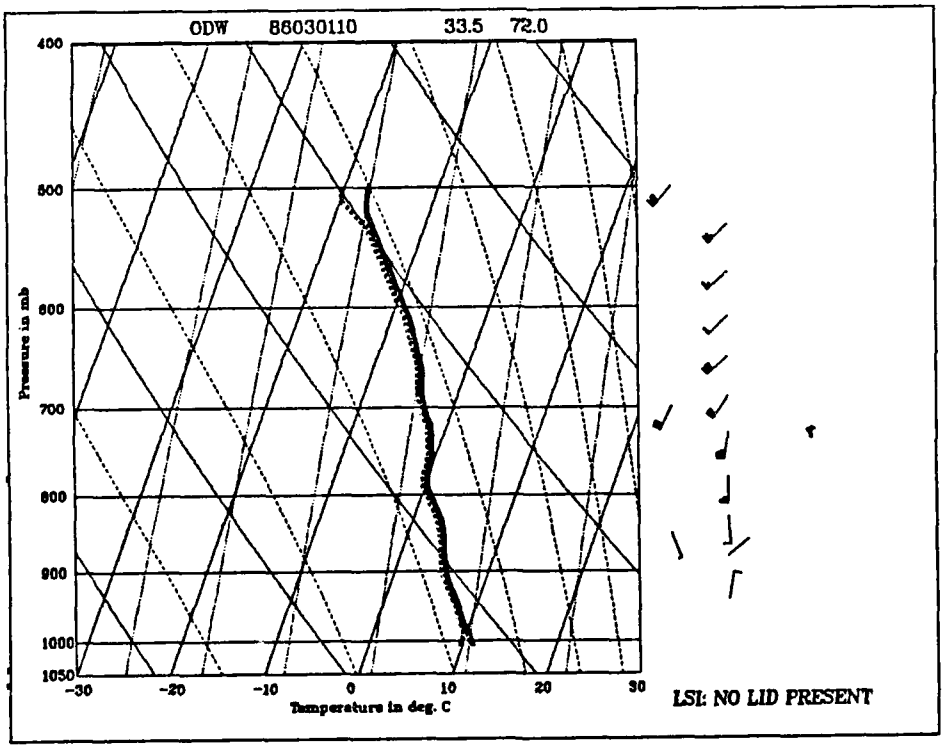
ODW 86030110 33.5 72.0
400
500
600
700
800
900
1000
1050
Pressure in mb
−30 −20 −10 0 10 20 30
Temperature in deg. C
LSI: NO LID PRESENT

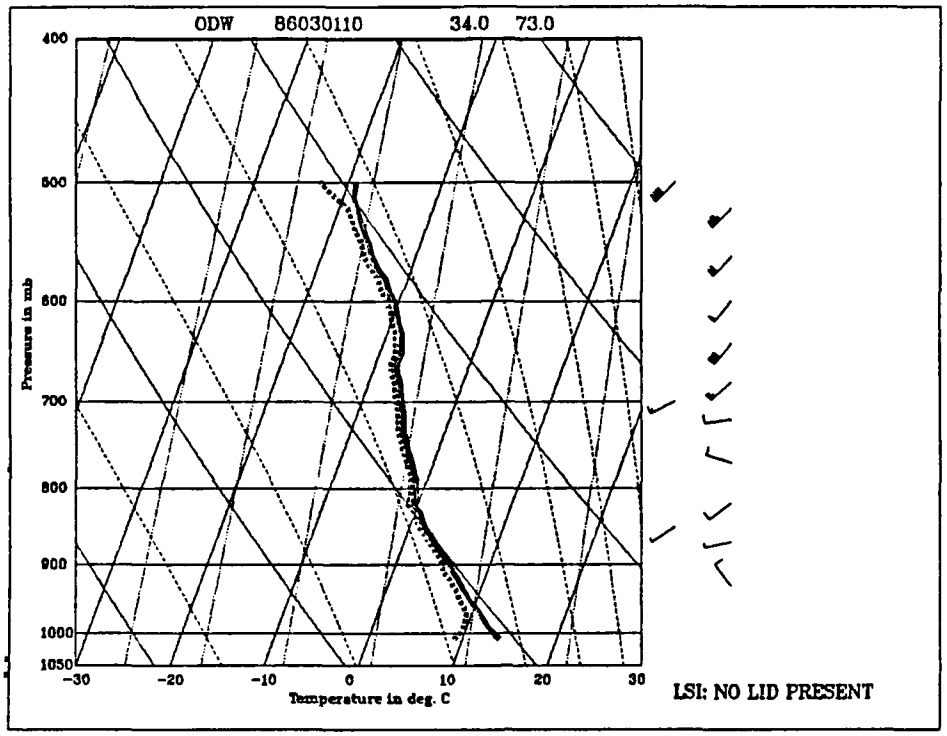
ODW 86030110 34.0 73.0
Pressure in mb
400
500
600
700
800
900
1000
1050
-30
-20
-10
0
10
20
30
Temperature in deg. C
LSI: NO LID PRESENT

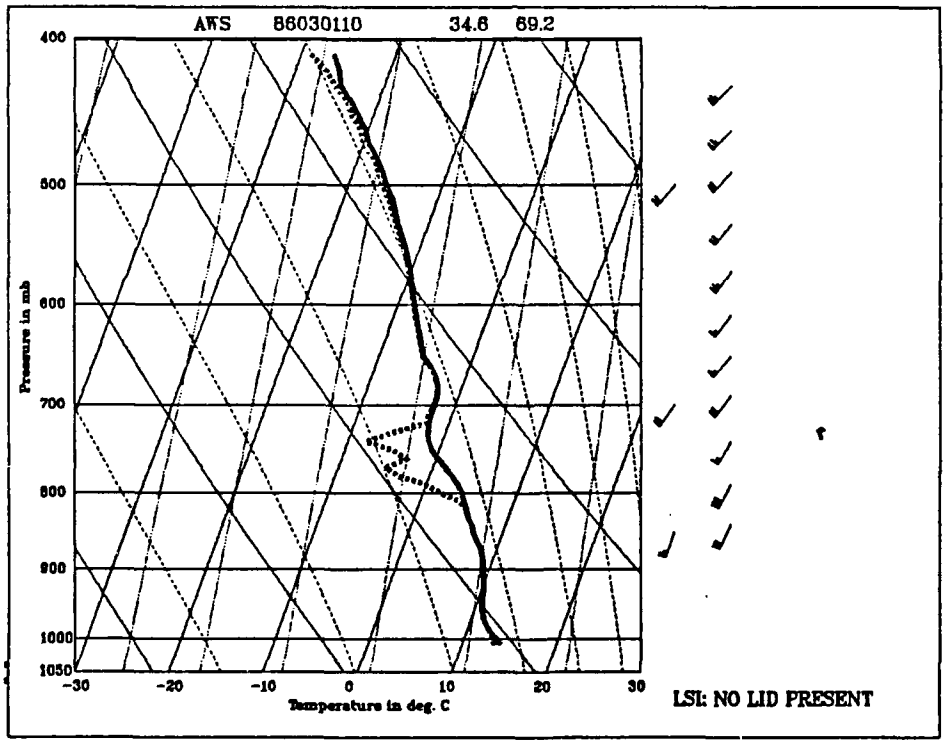
AWS 86030110 34.6 69.2
Pressure in mb
400
500
600
700
800
900
1000
1050
-30
-20
-10
0
10
20
30
Temperature in deg. C
LSI: NO LID PRESENT

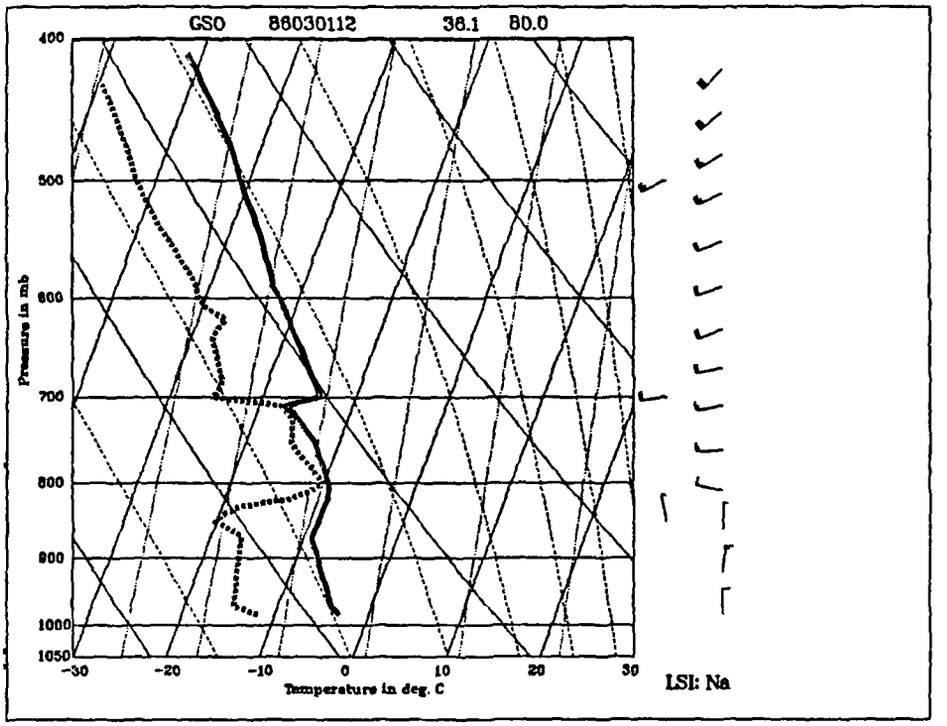
GSO 86030112 36.1 80.0
Pressure in mb
400
500
600
700
800
900
1000
1050
-30
-20
-10
0
10
20
30
Temperature in deg. C
LSI: Na

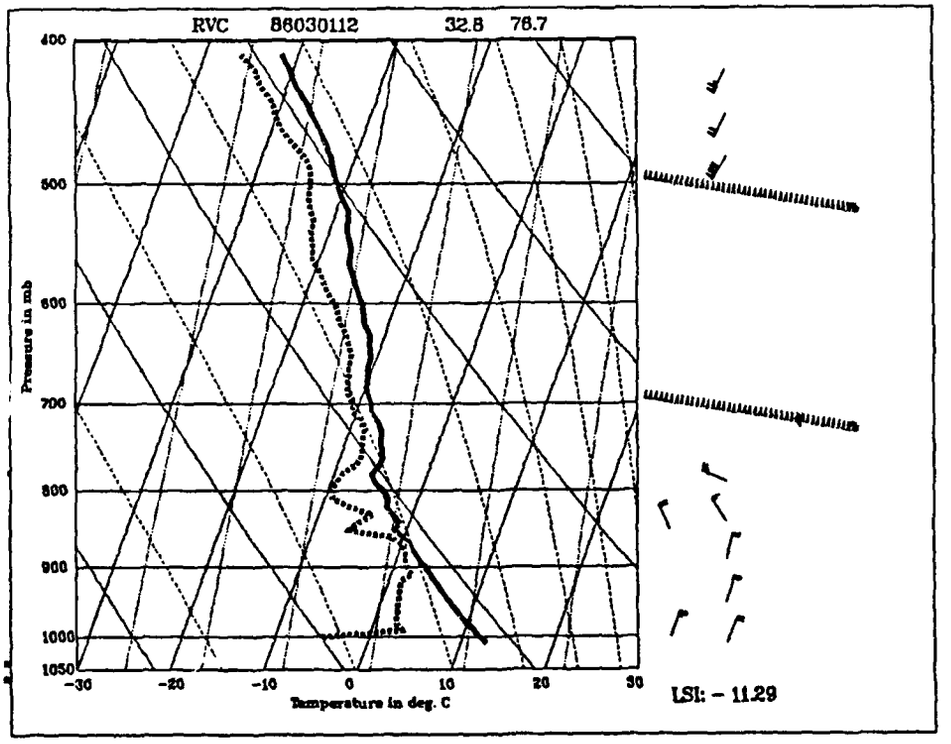
RVC 86030112 32.8 78.7
Pressure in mb
400
500
600
700
800
900
1000
1050
-30
-20
-10
0
10
20
30
Temperature in deg. C
LSI: - 11.29

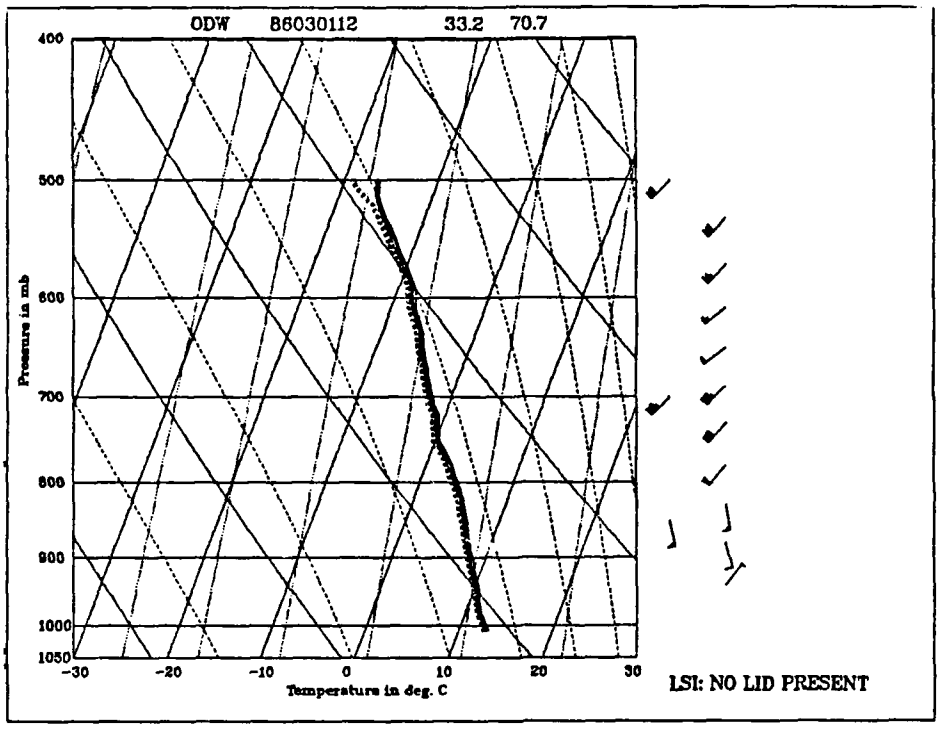
ODW 86030112 33.2 70.7
Pressure in mb
400
500
600
700
800
900
1000
1050
-30
-20
-10
0
10
20
30
Temperature in deg. C
LSI: NO LID PRESENT

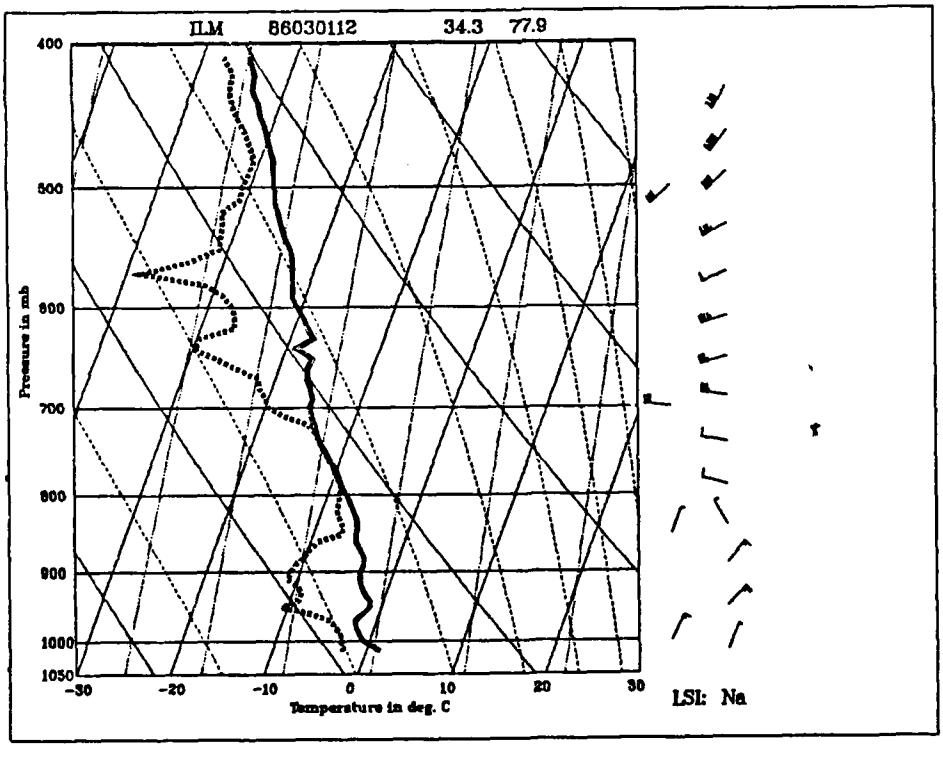
ILM 86030112 34.3 77.9
Pressure in mb
400
500
600
700
800
900
1000
1050
-30
-20
-10
0
10
20
30
Temperature in deg. C
LSI: Na

APPENDIX B. EVALUATION OF LSI FOR OTHER IOP'S.

An examination of dropwindsondes acquired during IOP's 2,4,5 and 9 has been conducted to determine the possible contribution of lid conditions to cyclogenesis. The discussion for each IOP will consist of a summary of the weather synopsis given in the **GALE Field Program Summary** (1986). Following the synopsis, an overview of the LSI values and the apparent correlation of lids and cyclogenesis will be discussed. Although individual soundings will not be included, the LSI values will be given in table form for each period.

A. IOP 2

1. Synopsis

The two cyclogenesis events that occurred during IOP2, were Miller (1946) type A. The first event at 00 UTC 27 January was offshore near 35°*N*,75°*W*. Over the next 12 h the storm movement was northward just offshore and nearly parallel to the coast. At 12 UTC 27 January, the storm crossed the coast and was located over Maine. At the same, time RV Endeavor reported lower pressures than expected. Coastal North Carolina stations were reporting rapidly falling pressures, with other indications of imminent offshore cyclogenesis present in the satellite imagery. A second cyclogenesis occurred near 35°*N*, 77°*W* between 18 UTC 27 January and 00 UTC 28 January. By 12 UTC 28 January, the second deepening cyclone center was located over Maine. The storms were both technically explosive cyclones, but did not produce heavy snow along the eastern seaboard. Each storm moved too rapidly northward to deposit any extensive amounts of snow.

2. LSI discussion

Lid Strength Index values in the vicinity of the first cyclogenesis (35°*N*, 75°*W*) were positive, which indicates unstable air. The 27 January soundings in Table 3 reflect the increase of lid strength with time after the first storm and before the second storm. Dropwindsondes taken at 21 UTC 27 January upstream of the second storm in the vicinity of 31°*N*, 76°*W* had LSI values near -15 K. Just after the second cyclogenetic event at 00 UTC 28 January, no lids were evident upstream of the cyclogenetic region even though dry air was available. After the passage of the second storm, the lid returned with increasing LSI values . One particularly interesting factor is the high winds in the middle of the troposphere after the first cyclogenesis event. Southwesterly winds in excess of

100 kt at 600 mb along the coast provided an ample supply of dry continental air. By 00 UTC 28 January, the second storm is located off New York and has strong winds. Two dropwindsondes near the center of the storm measured winds greater than 50 kt above 800 mb. The strong lids that existed early in the second cyclogenesis event, were rapidly removed with the deepening storm. However, rapid northward storm movement possibly prevented advection of moisture or the accumulation of CAPE in the moist air below the lids.

Table 3. LID STRENGTH INDEX (IOP 2): Over-ocean Lid Strength Index values for 27-28 January 1986. Note the negative LSI values in the region upstream of the second cyclogenesis near 35°*N*, 75°*W*.

Station	Time YYMMDDHH	Lat ° N	Long ° W	LSI (K)	Lid Height mb
AWS	86012701	31.80	73.90	4.3	940
AWS	86012701	37.00	71.80	3.8	710
AWS	86012703	39.50	68.10	no lid	n/a
AWS	86012703	40.90	67.30	- 2.4	800
ODW	86012704	35.40	73.30	no lid	n/a
ODW	86012704	35.80	71.60	no lid	n/a
AWS	86012710	30.10	76.80	-10.4	680
AWS	86012710	31.70	73.40	-8.4	700
AWS	86012721	31.50	76.50	-16.3	650
AWS	86012800	31.70	73.60	-7.6	700
AWS	86012800	37.00	71.70	no lid	n/a
AWS	86012800	39.30	70.40	no lid	n/a
AWS	86012801	41.10	67.00	no lid	n/a
ODW	86012801	34.70	73.60	no lid	650
ODW	86012801	34.80	73.60	no lid	n/a
ODW	86012801	36.20	71.20	-7.3	550
ODW	86012807	36.30	71.00	-14.0	620
ODW	86012809	37.20	72.40	-14.6	570
AWS	86012813	42.40	65.00	-16.7	650

B. IOP 4

1. Synopsis

During IOP 4, "warm, moist southerly flow at the surface preceded a mature cyclone tracking northeastward from the western Gulf of Mexico to west of the Appalachians." A lower tropospheric dry slot was propagating from west to east across the Carolinas and apparently was causing a "pronounced surface pressure fall-line". By 06 UTC 7 February a Miller (1946) type B cyclogenesis occurred near Cape Hatteras, North Carolina. The pressure fall was a relatively slow 0.5 mb/h for the 12 h period between 00 and 12 UTC 7 February. There appeared to be some connection between a low-level jet at 4 km and the storm. Movement of the storm was in the northeastward direction.

2. LSI discussion

Even though soundings were acquired for 7 February only (Table 4) some information is available for this IOP. All soundings were taken seaward of the storm, which remained close to the coast. The dry air in the middle and lower troposphere combined with high low-level temperatures (greater than 10° C) and resulted in positive values of LSI for dropwindsondes taken during this period. With these positive LSI values, even a weak lifting would result in convection. Even though a capping inversion is present, the warm surface layer reduced the total effects of the lid.

C. IOP 5

1. Synopsis

This observation period was dominated by several vorticity centers that resulted in different precipitation events. The first three centers produced precipitation coupled with weak surface perturbations. The third system passed through eastern North Carolina and Virginia at 21 UTC 10 February. This fourth system apparently produced a Miller (1946) type B cyclogenetic event as it passed off the coast near $36°N, 72°W$. The system moves to the northeast with nonexplosive development for the remainder of the IOP.

2. LSI discussion

Dropwindsondes were available only for the 10-11 February period. LSI values in Table 5 for these soundings are positive or near zero for all dropwindsondes. As in the previous IOP, high lower-level temperatures (in this case greater than $20°C$) appear to dominate the LSI terms. The absence of strong lid conditions appears to prevent the buildup of CAPE or advection of moisture by a conveyor belt as in the earlier discussion of IOP 6.

Table 4. LID STRENGTH INDEX (IOP 4): Over-ocean Lid Strength Index values for 7 February. Note LSI values in the region of cyclogenesis near 35°N, 75°W

Station	Time YYMMDDHH	Lat ° N	Long ° W	LSI (K)	Lid Height mb
ODW	86020701	33.60	72.70	no lid	n/a
ODW	86020701	34.50	71.40	-0.4	960
ODW	86020701	36.10	71.10	-8.4	850
ODW	86010709	33.70	72.80	4.84	850
ODW	86020709	34.60	71.40	5.2	940
ODW	86020709	36.20	71.20	-2.8	720
ODW	86020706	36.40	71.40	-3.5	720
AWS	86020710	30.40	77.00	1.7	940
AWS	86020710	31.20	73.70	-0.4	960
AWS	86020810	32.60	71.20	0.35	950
AWS	86020812	39.30	70.50	no lid	n/a
AWS	86020712	37.00	69.40	-7.1	810

As noted in the **GALE Field Program Summary,** (1986) "after the passage of the last storm there was very strong cold advection and unseasonably cold temperatures." On 13 February, a large vorticity maximum crossed the coast of North Carolina. No dropwindsondes were available for this period. Cyclogenesis near Bermuda appears to be a weak "polar low" type of event. The cold air advection over the ocean will influence the conditions for IOP 6 as shown in Chapter III.

D. IOP 9

1. Synopsis

The **GALE Field Program Summary** (1986) noted that rapid development occurred for an offshore system after 00 UTC 25 February. A weak frontal system developed into two separate low pressure centers as the result of strong PVA aloft in a Miller type B cyclogenesis. The centers merge and develop rapidly over the next 18 h. The **GALE Field Program Summary** noted that support was not particularily strong for storm growth, as "This weak cyclone developed rapidly to become a 973 mb low further offshore by 26/06Z. Although well offshore, this rapid development indicates that even relatively modest conditions can lead to significant oceanic storms."

Table 5. LID STRENGTH INDEX (IOP 5): Over-ocean Lid Strength Index values for 10-11 February. Note LSI values in the region of cyclogenesis near 32°N, 72°W

Station	Time YYMMDDHH	Lat ° N	Long ° W	LSI (K)	Lid Height mb
ODW	86021003	31.10	79.40	no lid	n/a
ODW	86021003	30.70	75.60	2.5	830
ODW	86021004	32.50	77.90	0.29	710
ODW	86021015	35.60	74.00	3.0	920
ODW	86021019	31.10	78.00	5.8	760
ODW	86021104	35.40	72.50	1.4	840
ODW	86021106	33.00	72.80	-2.9	940
ODW	86021106	33.00	74.30	no lid	n a
ODW	86021107	34.00	75.20	3.2	940
ODW	86021107	31.40	76.70	3.2	940
AWS	86021110	30.40	77.00	1.7	940
AWS	86021110	31.20	73.70	-0.1	940
AWS	86021112	32.60	71.20	0.2	960
AWS	86021112	34.60	69.40	1.2	940
AWS	86021112	37.10	69.60	no lid	n a

2. LSI discussion

The lid strength analysis is based on dropwindsondes for 25 February, no earlier dropwindsondes were available. Soundings for 26 February were acquired after 12 UTC 25 February when the storm had developed and left the region. One unique aspect is that the soundings are close to the shore in the western section of the developing low, and upwind of the system. LSI values show negative values close to shore (Table 6) with increasing values towards the low. The two sets of dropwindsondes acquired on 25 February, were from 00 to 04 UTC and from 10 to 12 UTC. Both sets were within the western center of the two developing lows discussed in the synopsis. A large dry air mass was located in the middle troposphere. The westerly winds at these levels provide evidence of the apparent continental origin of the dry air. The lid height increases from 930 mb near the coast to 700 mb near 33.7°*N*, 72.8°*W* at 04 UTC. This sounding is located

west of the NMC analyzed storm position. From this brief evaluation, lid conditions appear to be similar but weaker than those found in the Chapter III for the explosive development case.

Table 6. LID STRENGTH INDEX (IOP 9): Over-ocean Lid Strength Index values for 25 February. Note the LSI values in the region of cyclogenesis near 32.5°N, 72.5°W

Station	Time YYMMDDHH	Lat ° N	Long ° W	LSI (K)	Lid Height mb
ODW	86022500	31.00	79.70	-5.6	930
ODW	86022500	29.80	79.00	-5.4	930
ODW	86022500	30.70	77.90	1.4	890
ODW	86022500	31.50	76600	0.4	880
ODW	86022501	33.10	74.20	3.5	850
ODW	86022501	34.00	75.30	-1.9	710
ODW	86022510	33.20	76.30	-7.4	810
ODW	86022510	32.20	75.20	2.9	870
ODW	86022510	33.00	74.20	no lid	n a
ODW	86022512	33.70	72.80	no lid	n a
ODW	86022512	33.70	72.80	no lid	n a
ODW	86022512	34.50	71.50	-2.6	690
AWS	86022513	39.80	69.00	no lid	n a
AWS	86022513	41.10	67.00	no lid	n a
ODW	86022515	37.40	74.20	-13.5	860
ODW	86022515	38.30	73.00	-17.2	820
ODW	86022516	36.10	71.30	no lid	n a
ODW	86022516	34.50	71.40	0.9	810
ODW	86022516	33.70	72.90	1.8	810

LIST OF REFERENCES

Bullock, B.R., and D.R. Johnson, 1971: The generation of available potential energy by latent heat release in a mid-latitude cyclone. *Mon. Wea. Rev.*, **99**, 1-14.

Carlson,T.N., 1980: Airflow through midlattitude cyclones and the comma cloud pattern. *Mon. Wea. Rev.*, **108**, 1498-1509.

Carlson,T.N., R.A.Anthes, M.Schwartz, S.G.Benjamin, and D.G. Baldwin, 1980: Analysis and prediction of severe storms environment. *Bull. Amer. Meteor. Soc.*, **61**, 1018-1032.

Chang, C.B., D.J. Perkey, and C.W. Kreitzberg, 1984: Latent heat induced energy transformations during cyclogenesis. *Mon. Wea. Rev.*, **112**, 357-367.

Clark, J.D., 1983: The GOES user's guide. U.S. Department of Commerce National Oceanic and Atmospheric Administration, Washington D.C., 156 pp.

Danard, M.B., 1964: On the influence of released latent heat on cyclone development. *J. Appl. Meteor.*, **3**, 27-37.

Danard, M.B., 1966: On the conditions of latent heat to change in available potential energy. *J. Appl. Meteor.*, **5**, 81-84.

Gall, R.J., and D.R. Johnson, 1971: The generation of available potential energy by sensible heating: a case study. *Tellus*, **23**, 465-482.

Genesis of Atlantic Lows Experiment (GALE) Experimental Design, 1985: GALE Project Office, National Center of Atmospheric Research (NCAR), Boulder Colorado, 199 pp.

Genesis of Atlantic Lows Experiment (GALE) Field Program Summary, 1986: GALE Data Center, Drexel University, Department of Physics and Atmospheric Science, Philadelphia, Pennsylvania, 152 pp.

Graziano, T.M., and T.N. Carlson, 1987: A statistical evaluation of lid strength of deep convection. *Wea. and Fore.*, **2**, 127-139.

Hodur, R.M., 1982: Description and evaluation of NORAPS: The Navy Operational Regional Atmosphere Prediction System. *Mon. Wea. Rev.*, **110**, 1591-1602.

List, R.J., 1949: **Smithsonian Meteorological Tables, 6th ed.** Smithsonian Institution Press, 350 pp.

MacDonald,B.C., and E.R. Reiter, 1988: Explosive cyclogenesis over the eastern United States. *Mon. Wea. Rev.*, **116**, 1568-1586.

Miller, J.E., 1946: Cyclogenesis in the Atlantic Coastal region of the United States. *J.of Met.*, **3**, 31-44.

Petterssen, S., 1955: A general survey of factors influencing development at sea level. *J. of Meteor.*, **12**, 36-42.

Petterssen, S., G.E. Dunn and L.L. Means, 1955: Report of an experiment in forecasting of cyclone development. *J. of Meteor.*, **12**, 58-67.

Petterssen, S., D.L. Bradbury, and K. Pedersen, 1962: The Norwegian cyclone models in relation to heat and cold sourses. *Geofys. Publ.*, **24**, 243-280.

Petterssen, S., and S.J. Smebye, 1971: On development of extratropical cyclones. *Quart. J. Roy. Metero. Soc.*, **12**, 36-42.

Roebber, P.J., 1984: Statistical analysis and updated climatology of explosive cyclones. *Mon. Wea. Rev.*, **112**, 1577-1589.

Robertson, F.R. and P.J. Smith, 1983: The impact of model moist processes on the energies of extratropical cyclones. *Mon. Wea. Rev.*, **111**, 723-744.

Sanders, F., and J.R. Gyakum, 1980: Synoptic dynamic climatology of the "bomb". *Mon. Wea. Rev.*, **108**, 1598-1606.

Sanders F., 1986: Explosive cyclogenesis in the West-Central North Atlantic Ocean 1981-1984. Part I: Composite structure and mean behavior. *Mon. Wea. Rev.*, **114**, 1781-1794.

Uccellini, L.W., P.J. Kocin, R.A. Petterson, C.H. Wash, and K.F. Brill, 1984: The Presidents' Day Cyclone of 18-19 February 1979: Synoptic overview and analysis of the subtropical jet streak influencing the pre-cyclogenetic period. *Mon. Wea. Rev.*, **112**, 31-55.

Uccellini, L.W., D. Keyser, K.F. Brill, and C.H. Wash. 1985: The Presidents' Day Cyclone of 18-19 February 1979: Influence of upstream trough amplification and associated tropopause folding on rapid cyclogenesis. *Mon. Wea. Rev.*, **113**, 962-988.

Uccellini, L.W., R.A. Petersen, K.F. Brill, P.J. Kocin and J.J. Tuccillo. 1987: Synergistic interactions between an upper-level jet streak and diabatic processes that influence the development of a low-level jet and secondary coastal cyclone. *Mon. Wea. Rev.*, **115**, 2227-2261.

Vincent D.C., G.B. Pant, and H.E. Edmond Jr., 1977: Generation of available potential energy of and extratropical cyclone system. *Mon. Wea. Rev.*, **105**, 1252-1265.

INITIAL DISTRIBUTION LIST

		No. Copies
1.	Defense Technical Information Center Cameron Station Alexandria, VA 22304-6145	2
2.	Library, Code 0142 Naval Postgraduate School Monterey, CA 93943-5002	2
3.	Chairman (Code 63Rd) Department of Meteorology Naval Postgraduate School Monterey, CA 93943-5000	1
4.	Chairman (Code 68Co) Department of Oceanography Naval Postgraduate School Monterey, CA 93943-5000	1
5.	Professor Russell L. Elsberry (Code 63Es) Department of Meteorology Naval Postgraduate School Monterey, CA 93943-5000	2
6.	Professor Wendell A. Nuss (Code 63Nu) Department of Meteorology Naval Postgraduate School Monterey, CA 93943-5000	1
7.	Professor Kenneth L. Davidson (Code 63Ds) Department of Meteorology Naval Postgraduate School Monterey, CA 93943-5000	1
8.	LCDR Charles W. Green , USN Rt 6 Box 87 Martinsville, VA 24112	1
9.	Director, Naval Oceanography Division Naval Observatory 34th and Massachusetts Avenue NW Washington, DC 20390	1
10.	Commander Naval Oceanography Command NSTL Station Bay St. Louis, MS 39522	1

11. Commanding Officer — 1
Naval Oceanographic Office
NSTL Station
Bay St. Louis, MS 39522

12. Commanding Officer — 1
Fleet Numerical Oceanography Center
Monterey, CA 93943

13. Commanding Officer — 1
Naval Environmental Prediction Research Facility
Monterey, CA 93943

14. Chairman, Oceanography Department — 1
U. S. Naval Academy
Annapolis, MD 21402

15. Chief of Naval Research — 1
800 North Quincy Street
Arlington, VA 22217

16. Office of Naval Research (Code 420) — 1
Naval Ocean Research and Development Activity
800 North Quincy Street
Arlington, VA 22217